Long-term safety assessment for disposal of VTT's decommissioning wastes in Loviisa LILW repository

Master's thesis, 21.12.2019

Tekijä:

Juha Pitkäoja

Ohjaaja:

Jaana Kumpulainen
Olli Nummi (Fortum Power and Heat Oy)

JYVÄSKYLÄN YLIOPISTO
FYSIIKAN LAITOS

© 2019 Juha Pitkäoja
Julkaisu on tekijänoikeussäännösten alainen. Teosta voi lukea ja tulostaa henkilökohtaista käyttöä varten. Käyttö kaupallisiin tarkoituksiin on kielletty. This publication is copyrighted. You may download, display and print it for Your own personal use. Commercial use is prohibited.

Tiivistelmä

Pitkäoja, Juha
VTT:n käytöstäpoistojätteiden pitkäikaisturvallisuusanalyysi
Pro gradu -tutkielma
Fysiikan laitos, Jyväskylän yliopisto, 2019, 161 sivua

Teknologian tutkimuskeskus VTT Oy on aloittanut FiR 1 tutkimusreaktorin ja Otakaari 3 materiaalitutkimuslaboratorion käytöstäpoistoprojektin. Käytöstäpoiston yhteydessä syntyy ydinjätettä, jonka yksi mahdollinen loppusijoituspaikka on Fortum Power and Heat Oy:n omistama Loviisan voimalaitoksen loppusijoituslaitos. Tämän työn on tarkoitus osoittaa, että VTT:n käytöstäpoistojätteiden loppusijoitus Loviisaan ei aiheuta merkittävää kasvua Loviisan voimalaitoksen omista jätteistä tuleviin vuotuisiin säteilyannoksiin.

Pitkäaikaisturvallisuusanalyysi vaatii, että loppusijoitusjärjestelmän ja jätteiden kehitys tarkastelujakson aikana on mallinnettava matemaattisesti, ja tähän käytettiin Ecolego -mallinnusohjelmistoa. Jätteiden loppusijoitukseen on valittu kaksi mahdollista jätetilaa, jotka ovat huoltojätetila 2 (MWH2) ja käytöstäpoistojätetila 1 (DWH1).

Suurimmat annos- ja päästönopeudet saatiin DWH1-jätetilan referenssilaskentatapauksesta, joiden arvot olivat 0.713 µSv/a ja 0.00132. MWH2-jätetilan tulokset olivat matalammat. Kaikki tulokset olivat alle 2 % viranomaisten asettamista raja-arvoista. VTT:n käytöstäpoistojätteiden vaikutus verrattuna Loviisan voimalaitoksen jätteistä aiheutuviin annos- ja päästö nopeuksiin on pieni, joten pitkäaikaisturvallisuuden kannalta loppusijoittamiselle ei ole esteitä.

Tämän työn tarkoitus on myös tunnistaa epävarmuustekijöitä jätteiden lähtötiedoissa, jotka saattavat tarvita lisätutkimusta. Tällaisia epävarmuustekijöitä ovat muun muassa hiili-14:sta vapautuminen grafiittijätteestä, Otakaari 3 materiaalitutkimuslaboratorion aktiivisuusinventaari ja Fluentaalin ominaisuudet.

Avainsanat: ydinjäte, ydinreaktori, käytöstäpoisto, FiR 1, pitkäaikaisturvallisuus

Abstract

Pitkäoja, Juha
Long-term safety assessment for disposal of VTT's decommissioning wastes in Loviisa LILW repository
Master's thesis
Department of Physics, University of Jyväskylä, 2019, 161 pages.

VTT Technical Research Centre of Finland Ltd has initiated the decommissioning process of FiR 1 research reactor and Otakaari 3 material research laboratory. The processes generate nuclear waste and one possible disposal location of the waste is Loviisa LILW repository owned by Fortum Power and Heat Oy. The purpose of this work is to show that the disposal of VTT's decommissioning wastes into the Loviisa LILW repository does not cause a significant increase in the annual dose rate caused by the waste originating from Loviisa NPP.

The radionuclide release from VTT's decommissioning waste and their transport in the disposal system over the assessment period of 100 000 years have been modelled with Ecolego modelling software. Two waste caverns were considered as potential disposal caverns: maintenance waste hall 2 (MWH2) and decommissioning waste hall 1 (DWH1).

The highest annual dose rate and normalized release rate (ratio between releases into surface environment divided with respective regulatory constraints) were calculated from the reference case of DWH1 with the values of 0.713 µSv/a and 0.00132 respectively and the results for the reference case of MWH2 were lower. The results remained below 2 % of the constraints. Therefore, VTT's decommissioning wastes contribute only slightly to the doses and releases caused by Loviisa NPP's own waste, thus the disposal can be carried out safely from the perspective of the long-term safety.

One purpose of this work was also to identify uncertainties relating to the decommissioning wastes, possibly requiring additional research. Such uncertainties are the release of C-14 from graphite waste, the activity inventory of OK3 and the properties of Fluental.

Keywords: nuclear waste, nuclear reactor, decommissioning, FiR 1, long-term safety

Contents

Tiivistelmä **3**

Abstract **5**

1 Introduction **11**
1.1 Aims of the report . . . 11
1.2 Regulatory requirements . . . 12
1.3 Loviisa LILW repository . . . 14
1.4 Safety case for Loviisa LILW repository 2018 . . . 16

2 VTT's Decommissioning wastes **19**
2.1 FIR 1 decommissioning waste . . . 19
2.1.1 Irradiation ring . . . 22
2.1.2 Reflector . . . 23
2.1.3 FiR 1 activity inventory . . . 24
2.2 OK3 laboratory decommissioning waste . . . 26
2.2.1 Activated metal dust contamination . . . 26
2.2.2 Cs-137 contamination . . . 28
2.2.3 Alpha contamination . . . 29
2.2.4 OK3 activity inventory . . . 30
2.3 Clearance of waste from regulatory control . . . 32
2.4 Waste packages . . . 33
2.4.1 Classification of the waste and waste packages . . . 37
2.4.2 Long-term safety requirements for the waste packages . . . 37
2.5 Comparison with the waste from Loviisa NPP . . . 38

3 Evolution of the repository system **41**
3.1 Processes affecting the repository . . . 41
3.2 External processes . . . 42
3.2.1 Climate evolution . . . 42

3.2.2 Future human actions . . . 44
3.3 Surface environment . . . 44
3.4 Repository system . . . 46
3.4.1 Concrete barriers . . . 46
3.4.2 Groundwater flow . . . 47
3.4.3 Waste packages . . . 48
3.4.4 Gas generation . . . 49
3.4.5 Aluminium corrosion . . . 50
3.4.6 Steel corrosion . . . 52
3.4.7 Total gas generation . . . 53
3.4.8 Gas transport . . . 55

4 Radionuclide transport modelling 57
4.1 Modelling approach . . . 57
4.2 Concentration . . . 58
4.3 Solubility limited concentrations . . . 60
4.4 Diffusion . . . 61
4.5 Radionuclide release from the waste . . . 62
4.5.1 Modelling approach . . . 62
4.5.2 Releases from metals . . . 63
4.5.3 Releases from graphite . . . 66
4.5.4 Releases from aluminium, concrete, Fluental and other materials 68
4.6 Radionuclide transport in near-field . . . 69
4.6.1 Modelling of the concrete packages . . . 71
4.6.2 Modelling of the special concrete container . . . 72
4.6.3 Maintenance waste hall 2 (MWH2) . . . 72
4.6.4 Decommissioning waste hall 1 (DWH1) . . . 73
4.7 Radionuclide transport in bedrock . . . 75
4.8 Radionuclide transport in surface environment . . . 76
4.9 Dose assessment . . . 78

5 Modelling of scenarios and calculation cases 81
5.1 Scenarios . . . 81
5.2 Accelerated concrete degradation . . . 82
5.3 Large earthquake . . . 84

5.4 Calculation cases 85
5.4.1 Drilled well 85
5.4.2 High release rates 86
5.4.3 Smaller volume of MWH2 88
5.4.4 Alternate climate evolutions 88

6 Modelling results 89
6.1 Results from the base scenario 89
6.1.1 Release rates 90
6.1.2 Release constraint period 93
6.1.3 Dose assessment period 97
6.1.4 Probabilistic analysis 103
6.1.5 Uncertainty analysis 105
6.2 Results from deterministic calculation cases 108
6.2.1 Drilled well 108
6.2.2 High release rates 111
6.2.3 Smaller volume of MWH2 114
6.2.4 Alternate climate evolutions 115
6.3 Results from other scenarios 117
6.3.1 Accelerated concrete degradation 117
6.3.2 Large earthquake 119
6.4 Results summary 120

7 Chemical toxicity of VTT's decommissioning wastes 123
7.1 Regulatory requirements 123
7.2 Waste description 123
7.2.1 Aluminium 124
7.2.2 Fluental 125
7.2.3 Lead 126
7.2.4 Bismuth 126
7.3 The modelling of the chemical toxicity 127
7.4 Results from the base scenario 128
7.5 Results from drilled wells calculation case 131
7.6 Results summary 132

8 Confidence and Uncertainties **135**
8.1 Activity inventories . . . 135
8.2 External processes . . . 136
8.3 Surface environment . . . 136
8.4 Repository system . . . 136
8.5 Radionuclide release . . . 137
8.6 Radionuclide transport and dose assessment . . . 138
8.7 Chemical toxicity . . . 139

9 Conclusions **141**

References **143**

A Results from probabilistic analysis - figures **153**
A.1 Uncertainty analysis . . . 153

B Results from calculation cases - figures **157**
B.1 Drilled wells . . . 157

C Results from scenarios - figures **159**
C.1 Accelerated concrete degradation . . . 159
C.2 Large earthquake . . . 159

1 Introduction

1.1 Aims of the report

The purpose of this work is to show that disposing the FiR 1 and OK3 decommissioning waste to the Loviisa LILW repository does not cause a significant increase in the annual dose rate and normalized release rate, caused by the waste originating from Loviisa NPP.

This document concerns the long-term safety of the decommissioning wastes of FiR 1 (Finnish Research Reactor 1) and OK3 (Otakaari 3) material research laboratory, and their disposal to Loviisa LILW (low and intermediate level waste) repository.

FiR 1 is a 250 kW TRIGA Mark II open pool reactor which was commissioned in 1962. The reactor is owned by VTT Technical Research Centre of Finland Ltd, and was initially used for training and research, but later also for production of isotopes and radiotherapy. The reactor was permanently shut down in the summer of 2015. OK3 laboratory was used for studying the effects of neutron and ionizing radiation in metals and disposal of nuclear fuel. Currently the decommissioning planning is on-going and it is coordinated by VTT. The decommissioning includes multiple steps e.g. dismantling, packing and decontamination.

Earlier studies have already been conducted regarding the disposal of FiR 1 decommissioning waste into Loviisa LILW repository [1], [2]. The disposal into TVO's LILW repository has also been assessed [3]. This report is the most up to date study about the subject, and considers only the possibility of the disposal. However, no final decision about the disposal has been made.

The initial information about the decommissioning wastes of FiR 1 and OK3 have been provided by VTT in multiple references such as [4], [5] and [6]. Due to the fact that most of the reports related to the waste were made before this work, they may have missing, insufficient or uncertain information about certain subjects important to the long-term safety analysis. One aim of this work is also to identify uncertain factors in the reference material needing additional research.

The long-term safety of the Loviisa LILW repository has been addressed in the safety case for Loviisa LILW repository, which is a document portfolio. The 2018 safety case is briefly described in section 1.4. Two of the waste caverns are potential choices for the disposal, which are maintenance waste hall 2 (MWH2) and decommissioning waste hall 1 (DWH1). The repository and the differences between the waste halls are described in sections 1.4, 4.6.3 and 4.6.4, respectively.

The disposal into both waste caverns is modelled mathematically using Ecolego modelling software, which calculates the annual dose rate and normalized release rate (ratio between releases into surface environment divided with respective regulatory constraints) caused by the waste. Also, scenarios and calculation cases causing possibly higher results are also taken into account. Whichever waste cavern gives lower dose rate and release rate values is a better choice, but there are also other factors to be considered.

This document also briefly addresses the chemical toxicity of VTT's decommissioning wastes. The chemical toxicity of FiR 1 decommissioning wastes was addressed in [3], and is used as a basis in the analysis.

1.2 Regulatory requirements

The nuclear and radiation safety requirements must comply with the requirements concerning the long-term safety, suitability of the disposal method, engineered barriers and the disposal site. The fulfilment of the requirements must be proven through a safety case that must include an analyzation of the possible evolution scenarios of the disposal system, including the rare events. The analysis must be done via numerical calculation based on the evolution scenarios and complementary considerations.

This report adheres to the same requirements as all of the Loviisa LILW repository safety case reports and uses the same terminology. The final disposal of radioactive waste is governed and guided by the following regulations:

1. Nuclear Energy Act 990/1987 [7]
2. Nuclear Energy Decree 161/1988 [8]
3. STUK's Regulation Y/4/2018 [9]
4. STUK's Guide YVL D.5 [10]

These regulations are based on the international guidance and emphasize the protection of humans and environment from radioactive substances. The constraints for the radiation impacts and the releases of radioactive substances are listed in YVL D.5 [10].

The disposal of nuclear waste must be designed in a such way, that the annual dose rate to the most exposed group remains under 100 µSv/a, and the dose rate to other individuals is insignificantly low. These limits must be applied over the assessment period, during which the exposure of humans can be approximated with sufficient reliability, and which must extend over several thousands of years.

The assessment period in the safety case for Loviisa LILW repository is 100,000 years and consists of the dose assessment period which covers the first 10,000 years and remaining time period of 90,000 years is called release constraint period [11].

Radiation exposure of terrestrial and aquatic populations in the disposal site environment must be estimated. The estimated exposure must remain below the dose constraints known to cause significant detriment to any living populations. [9] The radiation exposure to other biota is also analysed during the dose assessment period.

After the assessment period the long-term quantities of radioactive materials released into the living environment from the disposed radioactive waste must remain below the nuclide specific constraints listed in table 1. The releases can be averaged over a period of 100 years at most. The release rate divided by the respective release constraint is referred to as normalized release rate. The sum of the nuclide specific normalized release rates must be less than one. [10]

The radiation exposure caused to people during the release constraint period must be estimated using stylized models of the surface environment which takes into account the alternative evolutions of the surface environment. [9] Stylised models are also applied using similar principles as when estimating the doses for the most exposed group. Exposure characteristics, human habits, nutritional needs and metabolism can assumed to be similar to the current ones [10]. The stylized models are not applied during permafrost and glacial periods, as the groundwater flow in the repository is minimal and practically no activity is released, or during submerged periods, as the activity is released into the sea.

According to [9], rare events must be also taken into account in the safety case. Rare event refers to an event that has a low probability of occurring but

Table 1. Nuclide specific constraints for radioactive releases into surface environment. The values are taken from [10]. *No values for Mo-93 and Ca-41 were provided in [10]. STUK recommends to use the same value for Mo-93 as Tc-99. The value of Zr-93 is used for Ca-41 due to the similarities in their dose coefficients.

Radionuclide	**Release constraint (GBq/a)**
Long-lived, alpha-emitting radium, thorium, protactinium, plutonium, americium and curium isotopes	0.03
Se-79, Nb-94, I-129 and Np-237	0.1
C-14, Cl-36 and Cs-135 and long-lived uranium isotopes	0.3
Sn-126	1
Tc-99, Mo-93*	3
Zr-93, Ca-41*	10
Ni-59	30
Pd-107	100

may compromise the long-term safety in case of occurrence. Rare events can be a consequence of e.g. future human actions or seismic activity. The rare events include at least rock movements, drilling of a medium-deep water and core drilling or boring hitting a disposed waste package [10]. In such case, the existence of the final disposal repository is assumed to be unknown and that the incident earliest may occur at least 200 years after the closure [10]. The probability, the importance of safety and the annual doses or activity releases arising in case of an occurrence of rare event must be estimated where practicable.

1.3 Loviisa LILW repository

Loviisa repository for low and intermediate level waste (LILW) is located at the Loviisa nuclear power plant (NPP) site at the depth of 110 m. The repository was constructed during 1992-1996 and it can be accessed through shafts and access tunnel. Currently the repository consists of three maintenance waste halls (MWH) and a solidified waste hall (SWH), and the rest of the caverns are not yet excavated. Figure 1 presents the layout of the repository. At the moment only MWH1 and MWH2 and SWH are licensed for disposal use. The repository is planned to be closed in 2068, after the NPP has been decommissioned. [12]

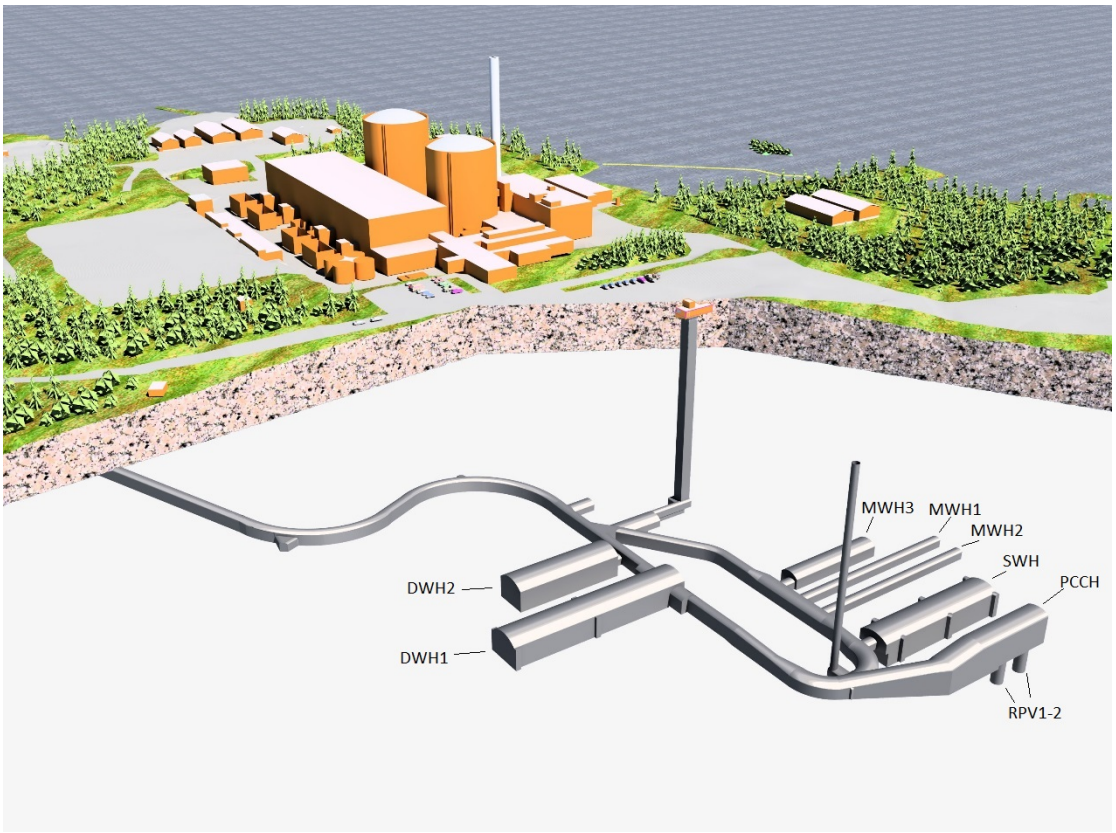

Figure 1. Stylized figure of the Loviisa LILW repository. The abbreviations are: MWH=maintenance waste hall, SWH=solidified waste hall, RPV=reactor pressure vessel silos, PCCH=primary circuit component hall, DWH=decommissioning waste hall. Figure by courtesy of Timo Kirkkomäki, Fortum.

1.4 Safety case for Loviisa LILW repository 2018

The safety case for Loviisa LILW repository is a report portfolio which demonstrates that the long-term safety requirements for the repository are met. The safety case considers the operational and decommissioning wastes arising from Loviisa nuclear power plant, consisting of two VVER-440 reactor units. The safety case portfolio consist of four primary and five supporting reports (see figure 2). The primary reports form the core of the safety case and are displayed in hierarchical order, meaning that the information in the description of the disposal system and design basis -report is used as a basis in the other primary reports [13].

The main report in the bottom of the figure is a summary of the other reports. The report performance assessment and the formulation of scenarios studies the evolution of the disposal system without taking the radionuclides into account [14], and the analysis of releases and doses -report assesses the fate of the radionuclides and their impacts [15]. The supporting reports supplement the primary reports and address certain topics in more detail. For example, the performance assessment and the formulation of scenarios -report contains the summary of the gas generation and transport -report. This report is structured and written in a similar fashion to the Analysis of releases and doses -report.

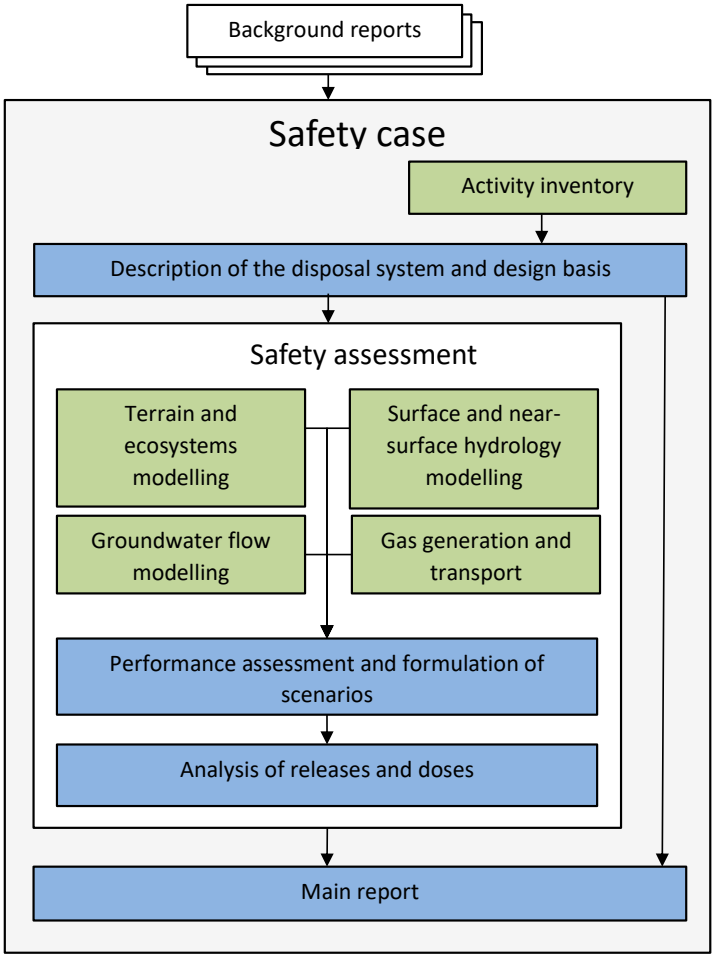

Figure 2. A flow chart indicating the information flow between the safety case reports. The main reports are shown in blue and supporting reports in green. The figure is taken from [11].

2 VTT's Decommissioning wastes

2.1 FIR 1 decommissioning waste

The waste amounts and their activity inventory are provided by VTT in their decommissioning planning report. [4]. The waste masses and volumes are estimated from the 3D MCNP (Monte Carlo N-Particle) model based on original construction drawings. A general presentation of the modelling domain is presented in figure 3. The inventory given in [4] lists at least 131 different components and materials, for which the mass, volume and activity have been calculated. Only a few selected components require closer examination due to their high activity. Such components are irradiation ring and reflector, which are covered in subsections 2.1.1 and 0respectively. Fluental mentioned in tables 2 and 4 is a special material used as a neutron moderator. Fluental contains 69 w-% AlF3, 30 w-% metallic aluminium and 1 w-% LiF [5].

Table 2 lists the masses and volumes of waste materials to be dismantled. Some decommissioning waste was generated when the BNCT (boron neutron capture therapy) station was built, and the list of the dismantled materials are listed in table 3. Table 4 summarizes the amounts of different waste materials in the FiR 1 decommissioning waste, including the data given in tables 2 and 3. The estimated volumes correspond to the intact components prior to dismantling and packaging.

The total estimated mass of the decommissioning waste is 94 tons and its volume is 38 m^3. The large items will be cut into smaller parts and packaged separately during the dismantling. This makes the large items easier to handle and reduces the amount of waste that needs to be disposed of.

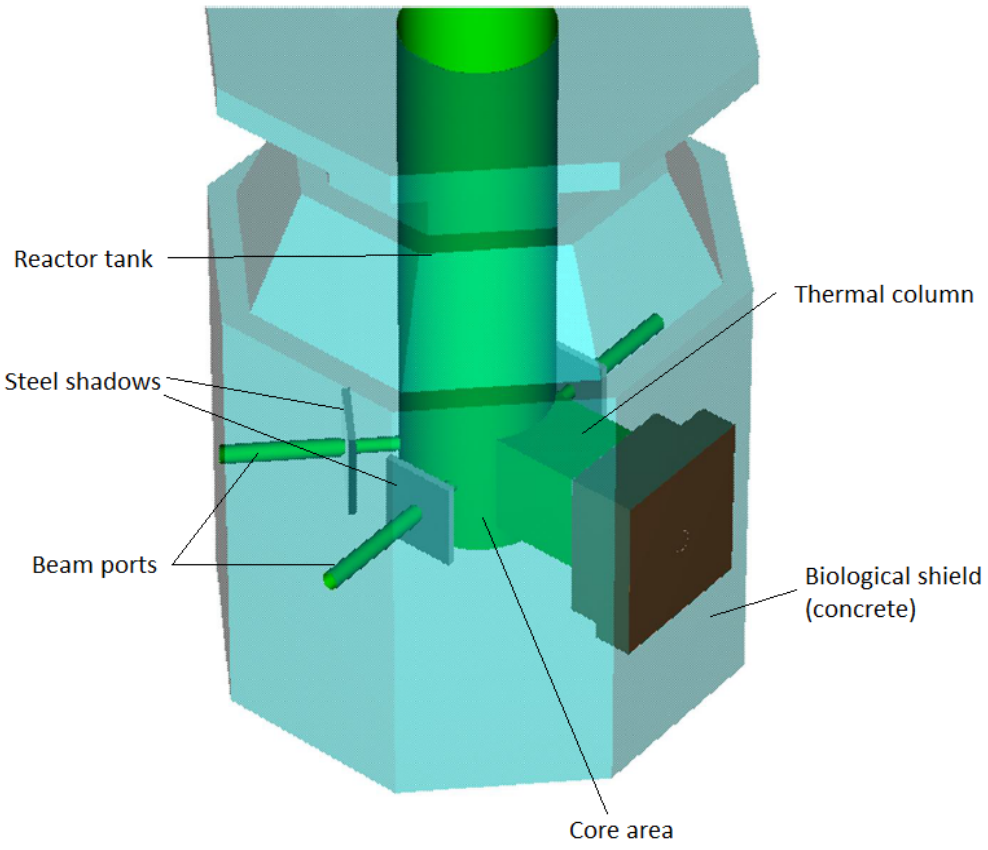

Figure 3. A general view of the MCNP modelling domain. The beam ports have been used for material research during first decades of operation. The thermal column was used production of thermal neutrons. In 1995 the thermal column was replaced with an epithermal BNCT station. The figure is taken from [4]

Table 2. List of materials to be dismantled during FiR 1 decommissioning. The volumes correspond to intact and unpacked volumes of the components prior to decommissioning. The table is taken from [4].

Material	**Density (kg/m^3)**	**Volume (m^3)**	**Mass (t)**
Fluental	2990	0.45	1.33
7 % Li-enriched plastic	1080	0.0087	0.0094
Li-Nat RX215 plastic	1050	0.35	0.36
3.5 % Li-enriched RX215 plastic	1000	0.026	0.026
Stainless steel	7900	0.013	0.095
Boral	2530	0.0034	0.0087
$AlMg_3$ (US type)	2660	0.074	0.20
Aluminium in tank and tubes (Finnish type)	2660	0.63	1.68
Li carbonate plastic	1650	0.97	1.60
Lead	11180	0.24	2.70
Bismuth	9800	0.079	0.78
Boronated concrete	2300	0.066	0.15
AGOT graphite	1700	0.33	0.55
Wood	650	0.15	0.10
17-4 PH steel	7780	0.0037	0.029
Steel in shadows	7900	0.43	3.41
Concrete in biological shield	2440	25	61
Bitumen around the tank	1050	0.126	0.132
Total		**29.0**	**74.2**

Table 3. Materials of the thermal column already dismantled in 1995. The volumes correspond to intact volumes of the components prior to decommissioning. The table is taken from [4].

Material	**Density (kg/m^3)**	**Volume (m^3)**	**Mass (t)**
Al in thermal column (Finnish type)	2660	0.14	0.36
Boral	2530	0.038	0.10
AGOT graphite	1700	2.28	3.88
Heavy-aggregate concrete	3500	3.79	13.3
Total		**6.2**	**17.6**

Table 4. Summary of the amounts of different waste materials in the FiR 1 decommissioning waste. The table is edited from table 2.

Material type	**Volume (m^3)**	**Mass (t)**
Concrete	25	61
Steel	0.45	3.54
Graphite	2.61	4.45
Aluminium	0.84	2.23
Fluental	0.45	1.33
Other	8.4	21.80
Total	**37.75**	**94.35**

2.1.1 Irradiation ring

The original irradiation ring was experiencing some problems in the early years of reactor operation, and a new one was manufactured by Tampella. However, the problems were solved, and the new ring was never installed.

The material specifications of the original irradiation ring are unknown, which causes uncertainty in the activity inventory. The two irradiation rings are assumed to be identical, and the material specifications are based on a mechanical CAD-model (computer-aided-design) [16], which was made for the new irradiation ring. The new irradiation ring is presented in figure 4.

Based on the CAD-model of the new irradiation ring, the original irradiation ring was approximated to contain 6.69 kg steel parts and 51.54 kg aluminium parts, but the mass of aluminium is overestimated. Cobalt impurities of the steel parts are unknown, but it was conservatively assumed that they contain 0.09 w% of cobalt. [4].

The actual mass of the original irradiation ring in the reactor is 90 kg, which approximately 30 kg heavier than calculated. The calculation based on the new irradiation ring does not perfectly reflect the original one. The original irradiation ring also made of steel and aluminium, but the proportions of unknown. Removal of aluminium parts from the irradiation ring was discussed, but it is not known how easy this process is, or is it even possible.

The irradiation ring is the most active component in the waste inventory, so from radiation protection point of view the removal of aluminium is controversial. According to [6] the dose rate from the irradiation ring was estimated to be 43 mSv/h without cover from the distance of one meter. The most important parameters of

Figure 4. FiR 1irradiation ring. The figure is taken from [4].

the irradiation ring are presented in table 5. The modelling of the irradiation ring assumes that it is made on stainless steel and contains no aluminium.

Table 5. The most important parameters of the irradiation ring. The dimensions are taken from the original CAD drawing of the component [17] and the activities are calculated with the information provided in [4]

Parameter	**Value**	**Activity in 2015**
Outer diameter	71 cm	C-14: $3.48 \cdot 10^{9}$ Bq
Inner diameter	51 cm	Co-60: $5.04 \cdot 10^{11}$ Bq
Height	36 cm	Ni-59: $5.74 \cdot 10^{9}$ Bq
Mass	90 kg	Ni-63: $5.86 \cdot 10^{11}$ Bq
		Total: $1.10 \cdot 10^{12}$ Bq

2.1.2 Reflector

The core reflector is made of graphite, which is sealed inside an aluminium casing. The casing is only few millimetres thick, and should be kept intact during the decommissioning process due to radiation protection. The reactor core and reflector assembly are shown in figure 5. The reflector will be disposed of in one piece, so the graphite and aluminium will not be separated. The graphite material contains considerable amounts of long-lived mobile nuclides such as C-14 and Cl-36.

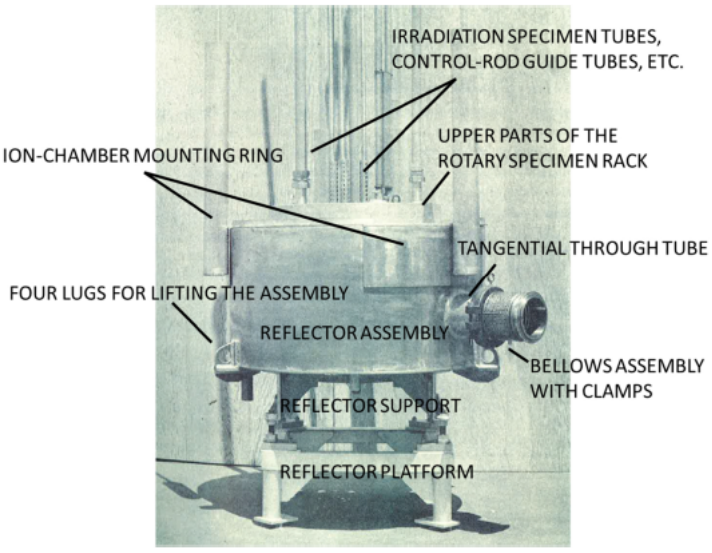

Figure 5. Picture of the reactor core and reflector assembly. The figure is taken from [4]

2.1.3 FiR 1 activity inventory

The aim of the activity report has been to provide conservative activity inventory, so that the actual inventory is lower than the calculated one with a high certainty. The radionuclide inventories were calculated in two parts. MCNP5-computer code and 3D geometry was used to calculate the neutron fluence rate distributions. The neutron source is based on MCNP criticality calculations. Installation of the BNCT station was taken into account by changing the geometry and materials. For operational history and the radioactive decay, the ORIGEN-S computer code was used. [4]

Table 6 lists all of the known radionuclides in the FiR 1 decommissioning waste, estimated with ORIGEN-S. [4] More detailed activities will be determined during the decommissioning. Radionuclides with half-lives less than five years are not included in the analysis. These nuclides are not interesting from the perspective of the long term safety because they will decay during the operational phase of the repository.

It is assumed that all of the activity given in table 6 is assumed to be disposed into Loviisa LILW repository. The possible clearance of wastes from regulatory control does not have a considerable effect on the total inventory, but reduces the amount of waste. Loviisa LILW repository will be closed in 2068, and the activity of decommissioning waste will decay prior to the closure. The activities of the short-lived-nuclides will be lower than at the shut-down of the reactor in 2015. Such

Table 6. Radionuclide activities (Bq) in the FiR 1 decommissioning waste at the end of 2015. The radionuclides with half-life less than 5 years have been excluded. Materials denoted as 'other' contain miscellaneous decommissioning wastes and spent ion-exchange resins. The activities are taken from [4] and the table was put together in [3]. The half-lives are taken from [15].

Nuclide	T_1 (a)	Graphite	Steel	Aluminium	Fluental	Concrete	Other	Total
Ag-108m	$4.38{\cdot}10^{2}$						$5.1{\cdot}10^{6}$	$\mathbf{5.1{\cdot}10^{6}}$
Ar-39	$2.69{\cdot}10^{2}$					$8.6{\cdot}10^{8}$	$9.9{\cdot}10^{4}$	$\mathbf{8.6{\cdot}10^{8}}$
Ba-133	$1.05{\cdot}10^{1}$	$1.4{\cdot}10^{8}$				$6.1{\cdot}10^{7}$		$\mathbf{2.0{\cdot}10^{8}}$
C-14	$5.70{\cdot}10^{3}$	$7.4{\cdot}10^{9}$	$3.8{\cdot}10^{9}$		$1.3{\cdot}10^{5}$	$3.3{\cdot}10^{8}$	$8.0{\cdot}10^{4}$	$\mathbf{1.2{\cdot}10^{10}}$
Ca-41	$1.00{\cdot}10^{5}$					$5.6{\cdot}10^{8}$	$6.4{\cdot}10^{4}$	$\mathbf{5.6{\cdot}10^{8}}$
Cl-36	$3.01{\cdot}10^{5}$	$6.0{\cdot}10^{8}$				$1.5{\cdot}10^{7}$	$1.7{\cdot}10^{3}$	$\mathbf{6.1{\cdot}10^{8}}$
Co-60	5.27	$2.2{\cdot}10^{10}$	$5.5{\cdot}10^{11}$	$3.1{\cdot}10^{6}$		$5.1{\cdot}10^{8}$	$1.8{\cdot}10^{7}$	$\mathbf{5.8{\cdot}10^{11}}$
Cs-137	$3.01{\cdot}10^{1}$						$8.2{\cdot}10^{7}$	$\mathbf{8.2{\cdot}10^{7}}$
Eu-152	$1.35{\cdot}10^{1}$	$2.6{\cdot}10^{10}$				$1.7{\cdot}10^{10}$	$2.0{\cdot}10^{6}$	$\mathbf{4.3{\cdot}10^{10}}$
Eu-154	8.60	$2.2{\cdot}10^{9}$				$5.3{\cdot}10^{8}$	$6.1{\cdot}10^{4}$	$\mathbf{2.7{\cdot}10^{9}}$
H-3	$1.23{\cdot}10^{1}$	$4.0{\cdot}10^{11}$			$1.3{\cdot}10^{12}$	$8.4{\cdot}10^{10}$	$4.3{\cdot}10^{11}$	$\mathbf{2.2{\cdot}10^{12}}$
Ni-59	$7.60{\cdot}10^{4}$		$6.3{\cdot}10^{9}$	$2.7{\cdot}10^{6}$		$2.1{\cdot}10^{6}$	$3.9{\cdot}10^{4}$	$\mathbf{6.3{\cdot}10^{9}}$
Ni-63	$1.01{\cdot}10^{2}$		$6.4{\cdot}10^{11}$	$2.8{\cdot}10^{8}$		$2.1{\cdot}10^{8}$	$4.1{\cdot}10^{6}$	$\mathbf{6.4{\cdot}10^{11}}$
Total		$\mathbf{4.6{\cdot}10^{11}}$	$\mathbf{1.2{\cdot}10^{12}}$	$\mathbf{2.8{\cdot}10^{8}}$	$\mathbf{1.30{\cdot}10^{12}}$	$\mathbf{1.0{\cdot}10^{11}}$	$\mathbf{4.3{\cdot}10^{11}}$	$\mathbf{3.5{\cdot}10^{12}}$

nuclides are Co-60, Eu-154, Eu-152 and Ba-133. The nuclide inventory at the time of closure are presented in table 7. Nuclides like H-3, Ar-39 and some of C-14 are gaseous, and may release from the decommissioning waste during handling and storage. It is challenging to estimate such releases, so it is conservatively assumed that such releases will not happen.

Table 7. Radionuclide activities (Bq) in the FiR 1 decommissioning waste in 2068, which is the time of closure of Loviisa LILW repository. The values are of the table are calculated from table 6.

Nuclide	T_1 (a)	Graphite	Steel	Aluminium	Fluental	Concrete	Other	Total (Bq)
Ag-108m	$4.38{\cdot}10^{2}$						$4.69{\cdot}10^{6}$	$\mathbf{4.69{\cdot}10^{6}}$
Ar-39	$2.69{\cdot}10^{2}$					$7.50{\cdot}10^{8}$	$8.64{\cdot}10^{4}$	$\mathbf{7.50{\cdot}10^{8}}$
Ba-133	$1.05{\cdot}10^{1}$	$4.23{\cdot}10^{6}$				$1.84{\cdot}10^{6}$		$\mathbf{6.08{\cdot}10^{6}}$
C-14	$5.70{\cdot}10^{3}$	$7.35{\cdot}10^{9}$	$3.78{\cdot}10^{9}$		$1.29{\cdot}10^{5}$	$3.28{\cdot}10^{8}$	$7.95{\cdot}10^{4}$	$\mathbf{1.15{\cdot}10^{10}}$
Ca-41	$1.00{\cdot}10^{5}$					$5.60{\cdot}10^{8}$	$6.40{\cdot}10^{4}$	$\mathbf{5.60{\cdot}10^{8}}$
Cl-36	$3.01{\cdot}10^{5}$	$6.00{\cdot}10^{8}$				$1.50{\cdot}10^{7}$	$1.70{\cdot}10^{3}$	$\mathbf{6.15{\cdot}10^{8}}$
Co-60	5.27	$2.07{\cdot}10^{7}$	$5.16{\cdot}10^{8}$	$2.91{\cdot}10^{3}$		$4.79{\cdot}10^{5}$	$1.69{\cdot}10^{4}$	$\mathbf{5.37{\cdot}10^{8}}$
Cs-137	$3.01{\cdot}10^{1}$						$2.42{\cdot}10^{7}$	$\mathbf{2.42{\cdot}10^{7}}$
Eu-152	$1.35{\cdot}10^{1}$	$1.71{\cdot}10^{9}$				$1.12{\cdot}10^{9}$	$1.32{\cdot}10^{5}$	$\mathbf{2.83{\cdot}10^{9}}$
Eu-154	8.60	$3.07{\cdot}10^{7}$				$7.40{\cdot}10^{6}$	$8.51{\cdot}10^{2}$	$\mathbf{3.81{\cdot}10^{7}}$
H-3	$1.23{\cdot}10^{1}$	$2.02{\cdot}10^{10}$			$6.56{\cdot}10^{10}$	$4.24{\cdot}10^{9}$	$2.17{\cdot}10^{10}$	$\mathbf{1.12{\cdot}10^{11}}$
Ni-59	$7.60{\cdot}10^{4}$		$6.30{\cdot}10^{9}$	$2.70{\cdot}10^{6}$		$2.10{\cdot}10^{6}$	$3.90{\cdot}10^{4}$	$\mathbf{6.30{\cdot}10^{9}}$
Ni-63	$1.01{\cdot}10^{2}$		$4.45{\cdot}10^{11}$	$1.95{\cdot}10^{8}$		$1.46{\cdot}10^{8}$	$2.85{\cdot}10^{6}$	$\mathbf{4.45{\cdot}10^{11}}$
Total		$\mathbf{2.99{\cdot}10^{10}}$	$\mathbf{4.55{\cdot}10^{11}}$	$\mathbf{1.97{\cdot}10^{8}}$	$\mathbf{6.56{\cdot}10^{10}}$	$\mathbf{7.17{\cdot}10^{9}}$	$\mathbf{2.17{\cdot}10^{10}}$	$\mathbf{5.80{\cdot}10^{11}}$

2.2 OK3 laboratory decommissioning waste

The material research laboratory contains activated metal waste and mixed contaminated waste. The activated metal waste consists of samples irradiated in reactors for research purpose, and they are usually returned to their respective owners. Fortum owns most of the metal samples. Three sources of contamination have been identified. Most of the rooms in the laboratory are contaminated by dust and chips from handling of metal samples. In addition, some rooms have contamination from an incident with a Cs-137 generator and contamination from the handling of uranium and plutonium sources.

2.2.1 Activated metal dust contamination

Most of the contamination originates from activated steel samples, which were handled in laboratory. The laboratory contains heavy machinery which were used to drill and cut large metal samples to smaller pieces, in order to study them. The machining of metal samples creates fine dust, some of which has spread around the laboratory. The metal dust gets stuck in hard to reach places easily and can be almost impossible to remove. Some of the metal particles can be so small that they cannot be seen with the naked eye, but can be easily detected with a radiation

detector. The dust from metal samples has contaminated e.g. some parts of the laboratory floor which had cracks on it, computers and other machines through their ventilation.

The contaminated wastewater of the laboratory is stored in the basement before flushing it to the main sewerage system. There has been problems with the pipelines over the years, which has caused certain rooms in the basement to be flooded multiple times with contaminated water. The wastewater contains the same isotopes found in the metal samples. Since some parts of the laboratory have been contaminated, the structures must be taken apart which increases the total waste amount. Some of the machines in the laboratory must be decontaminated, in order to release them regulatory control or to reduce their waste classification. Machines released from regulatory control can be reused or recycled. table 8 contains a rough estimation of the different waste materials in the decommissioning waste of OK3.

Table 8. Summary of the amounts of different waste materials and their activity in the OK3 decommissioning waste in 2018. The waste amounts were approximated in [18].

Waste type	**Mass (kg)**	**Volume (m^3)**	**Activity (GBq)**
Activated metal samples	300	0.055	1700
Contaminated concrete	11000	5	0.3
Contaminated machines	3500	5	0.03
Operational waste	2500	10	0.03
Contaminated pipes (sewer and air conditioning)	2000	3	0.015
Other	2000	3	0.015
Total	21300	26.055	1700.39

At the moment at least 10 000 activated metal samples with varying dimensions are stored at the laboratory [18]. The activated metal samples have been collected for many years from different clients all over the Europe. Most of the samples originate from Loviisa NPP's pressure vessel.

Many of the samples will be moved to VTT's new laboratory before their return to clients or transfer to storage or disposal. There a number of samples that cannot be returned to the owners for various reasons. The activity of the samples, which are guaranteed to be disposed to Loviisa LILW repository is less than the total activity of the activated metal samples in table 8. A possibility that all of the samples will be disposed to the Loviisa LILW repository has to be taken into account, which increases the activity of the metal samples to be disposed to 1.7 TBq.

The total activity was calculated by measuring the dose rate from the samples storage and assuming that all of the activity is contained in a Co-60 point source [18]. The nuclide vector describing the radionuclides found in the metal samples is described in [19]. However, the nuclide vector cannot be used to describe the nuclide composition of a single waste unit e.g. metal sample because the laboratory contains many different types of steel which all have different elemental compositions. Also the irradiation and decay times vary from sample to sample. Thus, the nuclide vector can only be used to describe the decommissioning waste of the lab as a whole. The nuclide vector is presented in table 9.

Table 9. An approximated nuclide vector for the metal samples in the laboratory sample storage in 2018. [19]

Nuclide	**Percentage (%)**
C-14	0.57
Fe-55	10.87
Co-60	17.38
Ni-59	0.73
Ni-63	70.41
Mo-93	0.0015
Nb-94	0.0016
Ag-108m	0.0093

2.2.2 Cs-137 contamination

In 1986 an experiment with a Cs-137-Ba-137m generator (total activity inventory of 370 MBq) was done in the laboratory. The experiment was conducted in order to study the flow of water in the pipeline of the pilot hall of the laboratory. Due to an unfortunate mishap, some Cs-137 was spread into the flow test pipeline and the concrete well. Samples were taken from the contaminated water and they were analysed. According to the results the activity concentration of water was 2.0 Bq/ml.

The total volume of the well is 12 m^3, so activity of the water in the well was 22.2 MBq in 1986 (or 10.6 MBq in 2018). The contaminated water was removed by pumping it into a tank. The floor around the place, where the elution was done, was also contaminated by droplets of the contaminated water. The concrete floor was decontaminated scrubbing it with a steel wool and removing some parts of the floor with a hammer and a chisel.

The pipeline and the well were decontaminated by flushing, but some of the Cs-137 still remains. The waste from the decontamination work was sent to Loviisa NPP. The contamination level of the well was measured a few years after the incident and the activity in the well was estimated to be 5.6 MBq. The activity level was lower than earlier because some of the contamination was absorbed into the concrete structures. The remaining contamination in the well was painted over with a dovecote in order the prevent it from spreading any further. [20] However, the efficiency of the decontamination is hard to estimate

A highly conservative approximation of the total Cs-137 activity in the laboratory was 50 MBq in 2018, which takes into account the possibility of undocumented cases where Cs-137 has been handled in the laboratory. [18]

2.2.3 Alpha contamination

In addition to the metal dust and Cs-137 contamination, alpha activity has been detected in the laboratory. The alpha contamination originates from the experiments used to develop the nuclear safeguard measurements. The experiments are described in [21].

The total masses of the uranium and plutonium used in the experiments are 400 mg and 35 mg respectively. The uranium samples had different levels of enrichment and the highest percentage was 3 %. The radionuclide proportions of the samples are presented in table 10. A highly conservative assumption is that 10 % of the mass of the samples are spread into the laboratory as contamination and that the enrichment percentage of all the uranium handled in the laboratory is 3 %. [18]

Since the only information about the alpha contamination is the masses of the samples and the compositions of the isotopes, the specific activity a (Bq/kg) of each isotope can be calculated, which is given by

$$a = \frac{A}{m}, \tag{1}$$

where m(kg)is the mass of the isotope and A (Bq) is the activity of the isotope. The activity is simply

$$A = \frac{N \ln 2}{T_{1/2}}, \tag{2}$$

where $T_{1/2}$ (a) is the half-life of the isotope and N is the number of atoms [22].

The mass in equation (1) can be written as

$$m = M\frac{N}{N_A}, \tag{3}$$

where N_A (1/mol) is the Avogadro's constant, M (mol/g) is the molar mass. Combining equations (1), (2) and (3) gives the final form to the specific activity

$$a = \frac{N_A \ln 2}{MT_{1/2}}. \tag{4}$$

The activity of each isotope can be calculated by multiplying its mass with the specific activity. The values are listed in table 10. All uranium isotopes and Pu-242 can be left out of the analysis due to the fact that their activities fall below the exemption values.

Table 10. Radionuclide proportions and activities of the plutonium and uranium samples handled in the laboratory in 2018 [18]. The exemption values are taken from [23].

Nuclide	**wt% (%)**	**Specific activity (GBq/g)**	**Activity (kBq)**	**Exemption value (kBq)**
Pu-238	0.19	634.1	4217.0	10
Pu-239	86.56	2.3	6959.0	10
Pu-240	10.71	8.4	3150.9	1
Pu-241	1.94	3832.9	260253.4	100
Pu-242	0.60	0.15	3.0	10
U-234	0.0057	0.23	0.52	10
U-235	3	$8.0{\cdot}10^{-5}$	0.096	10
U-238	96.9943	$1.2{\cdot}10^{-5}$	0.48	10

2.2.4 OK3 activity inventory

Since the decommissioning plan of the laboratory is still preliminary, the list of waste materials and activities etc. is very scarce. The activity inventory was calculated with all the available information in sections 2.2.1, 2.2.2 and 2.2.3. The radionuclide composition of the waste given in table 11 was calculated by multiplying the total activities with the percentages of the nuclide vector given in 9. The activity inventory of the laboratory in 2018 is presented in table 11.

It is assumed that all of the activity is disposed into Loviisa LILW repository. The possible clearance of wastes from regulatory control have little effect on the total inventory. The activities of the short-lived-nuclides will be much lower at time

Table 11. Nuclide-wise activities (Bq) in the OK3 laboratory decommissioning waste at the end of 2018. The radionuclides with half-life less than 5 years have been excluded.

Nuclide	T_1 (a)	**Activated metal samples**	**Cont. floor concrete**	**Cont. machines**	**Operational waste**	**Cont. pipes**	**Other**	**Alpha cont.**	**Total**
Ag-108m	$4.38{\cdot}10^{2}$	$1.60{\cdot}10^{8}$	$7.32{\cdot}10^{4}$	$7.32{\cdot}10^{3}$	$7.32{\cdot}10^{3}$	$3.66{\cdot}10^{3}$	$3.66{\cdot}10^{3}$		$1.60{\cdot}10^{8}$
C-14	$5.70{\cdot}10^{3}$	$9.78{\cdot}10^{9}$	$7.00{\cdot}10^{5}$	$7.00{\cdot}10^{4}$	$7.00{\cdot}10^{4}$	$3.50{\cdot}10^{4}$	$3.50{\cdot}10^{4}$		$9.78{\cdot}10^{9}$
Co-60	5.27	$3.00{\cdot}10^{11}$	$4.29{\cdot}10^{7}$	$4.29{\cdot}10^{6}$	$4.29{\cdot}10^{6}$	$2.14{\cdot}10^{6}$	$2.14{\cdot}10^{6}$		$3.00{\cdot}10^{11}$
Cs-137	$3.01{\cdot}10^{1}$					$5.00{\cdot}10^{7}$			$5.00{\cdot}10^{7}$
Mo-93	$4.00{\cdot}10^{3}$	$2.54{\cdot}10^{7}$	$1.80{\cdot}10^{3}$	$1.80{\cdot}10^{2}$	$1.80{\cdot}10^{2}$	$9.00{\cdot}10^{1}$	$9.00{\cdot}10^{1}$		$2.54{\cdot}10^{7}$
Nb-94	$2.03{\cdot}10^{4}$	$2.76{\cdot}10^{7}$	$1.50{\cdot}10^{3}$	$1.50{\cdot}10^{2}$	$1.50{\cdot}10^{2}$	$7.50{\cdot}10^{1}$	$7.50{\cdot}10^{1}$		$2.76{\cdot}10^{7}$
Ni-59	$7.60{\cdot}10^{4}$	$1.26{\cdot}10^{10}$	$9.09{\cdot}10^{5}$	$9.09{\cdot}10^{4}$	$9.09{\cdot}10^{4}$	$4.55{\cdot}10^{4}$	$4.55{\cdot}10^{4}$		$1.26{\cdot}10^{10}$
Ni-63	$1.01{\cdot}10^{2}$	$1.22{\cdot}10^{12}$	$9.60{\cdot}10^{7}$	$9.60{\cdot}10^{6}$	$9.60{\cdot}10^{6}$	$4.80{\cdot}10^{6}$	$4.80{\cdot}10^{6}$		$1.22{\cdot}10^{12}$
Pu-238	$8.77{\cdot}10^{1}$							$4.22{\cdot}10^{6}$	$4.22{\cdot}10^{6}$
Pu-239	$2.41{\cdot}10^{4}$							$6.96{\cdot}10^{6}$	$6.96{\cdot}10^{6}$
Pu-240	$6.56{\cdot}10^{3}$							$3.15{\cdot}10^{6}$	$3.15{\cdot}10^{6}$
Pu-241	$1.40{\cdot}10^{1}$							$2.60{\cdot}10^{8}$	$2.60{\cdot}10^{8}$
Total		$1.54{\cdot}10^{12}$	$1.41{\cdot}10^{8}$	$1.41{\cdot}10^{7}$	$1.41{\cdot}10^{7}$	$5.70{\cdot}10^{7}$	$7.03{\cdot}10^{6}$	$2.75{\cdot}10^{8}$	$1.54{\cdot}10^{12}$

the closure of the repository than in 2018. The short-lived isotopes in the activity inventory are Co-60, Cs-137 and Pu-241. In 2068 only 0.14 % of Co-60, 31.6 % of Cs-137, 8.41 % of Pu-241 remain and total activity has been reduced to 58 % of its original activity in 2018. The activity inventory at the time of closure is presented in table 12.

Table 12. Nuclide-wise activities (Bq) in the OK3 laboratory decommissioning waste in 2068. The radionuclides with half-life less than 5 years have been excluded.

Nuclide	T_1 (a)	Activated metal samples	Cont. floor concrete	Cont. machines	Operational waste	Cont. pipes	Other	Alpha cont.	Total
Ag-108m	$4.38{\cdot}10^{2}$	$1.48{\cdot}10^{8}$	$6.76{\cdot}10^{4}$	$6.76{\cdot}10^{3}$	$6.76{\cdot}10^{3}$	$3.38{\cdot}10^{3}$	$3.38{\cdot}10^{3}$		$1.48{\cdot}10^{8}$
C-14	$5.70{\cdot}10^{3}$	$9.72{\cdot}10^{9}$	$6.95{\cdot}10^{5}$	$6.95{\cdot}10^{4}$	$6.95{\cdot}10^{4}$	$3.48{\cdot}10^{4}$	$3.48{\cdot}10^{4}$		$9.72{\cdot}10^{9}$
Co-60	5.27	$4.18{\cdot}10^{8}$	$5.97{\cdot}10^{4}$	$5.97{\cdot}10^{3}$	$5.97{\cdot}10^{3}$	$2.99{\cdot}10^{3}$	$2.99{\cdot}10^{3}$		$4.18{\cdot}10^{8}$
Cs-137	$3.01{\cdot}10^{1}$					$1.58{\cdot}10^{7}$			$1.58{\cdot}10^{7}$
Mo-93	$4.00{\cdot}10^{3}$	$2.52{\cdot}10^{7}$	$1.78{\cdot}10^{3}$	$1.78{\cdot}10^{2}$	$1.78{\cdot}10^{2}$	$8.92{\cdot}10^{1}$	$8.92{\cdot}10^{1}$		$2.52{\cdot}10^{7}$
Nb-94	$2.03{\cdot}10^{4}$	$2.76{\cdot}10^{7}$	$1.50{\cdot}10^{3}$	$1.50{\cdot}10^{2}$	$1.50{\cdot}10^{2}$	$7.49{\cdot}10^{1}$	$7.49{\cdot}10^{1}$		$2.76{\cdot}10^{7}$
Ni-59	$7.60{\cdot}10^{4}$	$1.26{\cdot}10^{10}$	$9.09{\cdot}10^{5}$	$9.09{\cdot}10^{4}$	$9.09{\cdot}10^{4}$	$4.54{\cdot}10^{4}$	$4.54{\cdot}10^{4}$		$1.26{\cdot}10^{10}$
Ni-63	$1.01{\cdot}10^{2}$	$8.63{\cdot}10^{11}$	$6.81{\cdot}10^{7}$	$6.81{\cdot}10^{6}$	$6.81{\cdot}10^{6}$	$3.41{\cdot}10^{6}$	$3.41{\cdot}10^{6}$		$8.63{\cdot}10^{11}$
Pu-238	$8.77{\cdot}10^{1}$							$2.84{\cdot}10^{6}$	$2.84{\cdot}10^{6}$
Pu-239	$2.41{\cdot}10^{4}$							$6.95{\cdot}10^{6}$	$6.95{\cdot}10^{6}$
Pu-240	$2.41{\cdot}10^{4}$							$3.15{\cdot}10^{6}$	$3.15{\cdot}10^{6}$
Pu-241	$1.40{\cdot}10^{1}$							$2.19{\cdot}10^{7}$	$2.19{\cdot}10^{7}$
Total		$8.85{\cdot}10^{11}$	$6.98{\cdot}10^{7}$	$6.98{\cdot}10^{6}$	$6.98{\cdot}10^{6}$	$1.93{\cdot}10^{7}$	$3.49{\cdot}10^{6}$	$3.42{\cdot}10^{7}$	$8.86{\cdot}10^{11}$

2.3 Clearance of waste from regulatory control

The clearance of waste from regulatory control is defined in [24]. General and case-specific clearance options for FiR 1 decommissioning waste were considered in [25]. An estimation of the amounts of wastes to be cleared was made based on the scarce inventory data (especially concerning chemically toxic waste materials like lead and bismuth).

The clearance does not considerably affect the total nuclide inventory of FiR 1 decommissioning waste, because the waste that can be cleared has relatively low activity. This reduces the total mass and volume of the wastes to be disposed, and some waste material types may be possible to be cleared. Such materials include e.g. wood and lead.

All movables (meaning all furniture, equipment etc.) must be removed from the laboratory before the decommissioning of OK3 can be initialized. The contamination levels will be measured and decontamination will be carried out if necessary. As many of the items will be cleared from regulatory control as possible, in order to reduce the amount waste to be disposed. Due to the high activity of the samples handled in the lab, lead bricks have been used as a radiation protection in the lab.

Some lead bricks have been contaminated with metal dust from the samples, and

this makes them hard to decontaminate. Lead is such a soft material compared to steel, and small metal particles can easily get stuck in them. Even if the contamination cannot be removed completely, it is possible to achieve a lower waste classification for the lead bricks, which increases them probability of them being cleared from regulatory control.

However, metal recycling companies in Finland require that the metal waste must be completely contamination free. The lead bricks which cannot be decontaminated will be send to the waste treatment plant owned by Cyclife Sweden. The processes used at the waste treatment can separate the contamination from dry waste [26]. However, several tons of contaminated lead is required before the company is willing to process them. One possibility is to combine the contaminated lead into one shipment with Fortum's own lead waste, if not enough lead waste is not generated in the decommissioning process.

The masses and volumes given in table 8 are conservative estimations, but at the moment more detailed list of the waste materials has not been made. The decontamination work done in the laboratory has a considerable effect on the amount of waste to be disposed. However, this report it is assumed that no materials are cleared, and that all the waste will be disposed.

2.4 Waste packages

The dismantling and packaging of decommissioning waste was originally described in [27], but the updated version is [28]. The design and selection of the packages has been mainly based on the compatibility with the waste packages used by Fortum. [28] The waste handling and packaging is done at the work site. The selection of waste package depends on the of the waste (including the external dose during handling), storage, transport and dimensions of the waste. So far a packaging plan has not been made for OK3 decommissioning waste, but a preliminary estimation of the packages needed for the disposal has been made. The waste packages and their dimensions are presented in table 13.

With the information that has been provided by VTT about the decommissioning waste of OK3, it seems that most of the wastes will be packaged in waste drums. The waste drums must be packaged in such way, that they can be handled with the methods used at the Loviisa NPP. Waste drum is the main waste package type used at Loviisa NPP and they are favoured due to their weight and ease of handling. The

Table 13. Dimensions of the waste packages. Translated and edited from table 4 in [28] The values in the table are inner dimensions. *The steel box consists of two 1 mm plates which are 8 mm apart. The gap between the plates contains air.

Type	Wall thickness (mm)	Length/ diameter (mm)	Width (mm)	Height (mm)	Mass (kg)	Material
200 l drum	1	570		880	20	Steel
Steel box*	1	1500	950	750	280	Steel
Concrete box	120	1900	1300	1300	3800	Reinforced concrete
Special concrete container	105	1300	-	1300	3100	Concrete

maximum weight of a waste drum is 500 kg. [28]

The metal samples require a special concrete container, as a waste drum is not a practicable choice due to radiation protection and the mass versus volume ratio of the metal samples and the dimensions of the waste drum. The special concrete container chosen for OK3 metal samples is originally designed for highly active filters. The container is cylindrical and has five tubes for the filters in the middle. The length of one tube is 830 mm and the diameter is 220 mm. The diameter of the container is 1300 mm which leaves enough concrete around the tubes to reduce the dose rate acceptable levels. The volume of one container is large enough to hold all the metal samples, but the surface dose rate of such container would be too high. It is recommended to use at least three containers but more can be used if necessary. The steel boxes are mainly used to make the handling of the waste easier at the worksite and they cannot be considered as an release barrier due to the thin wall thickness. All the steel boxes will be packaged inside the concrete packages at the worksite.

The irradiation ring and core reflector will be packaged into concrete waste packages. The irradiation ring will be removed from the reactor, using a crane with a radiation shield that covers the irradiation ring. The radiation shield must be used due to the high activity of the irradiation ring. The irradiation ring will be lifted into a concrete waste package along with the radiation shield. The radiation shield reduces the dose rate during handling and transportation. There will be empty space left in the package, so smaller components or concrete can be added. Maximum waste mass for a concrete package is 6000 kg [28]. The core reflector will also be packaged with a radiation shield, but the shield is not as heavy as the one packaged

with the irradiation ring. The number of packages, their mass and volume for the decommissioning wastes are listed in table 14 and 15. The package/waste specific activities of the VTT's decommissioning waste are listed in table 16.

Table 14. The number of packages needed for the FiR 1 decommissioning waste.

Waste package	**Total mass (kg)**	**Total volume (m^3)**	**Number of packages**
Waste drums	4800	7	33
Concrete packages	16000	71	22
Total	20800	78	55

Table 15. The number waste packages needed for the OK3 decommissioning waste. Edited from table 8.

Waste type	**Total mass (kg)**	**Total volume (m^3)**	**Number of packages**
Activated metal samples	9600	0.055	3 (special concrete containers)
Contaminated concrete	12300	10	50 (waste drums)
Contaminated machines	4100	5	25 (waste drums)
Operational waste	3800	10	50 (waste drums)
Contaminated pipes	2400	3	15 (waste drums)
Other	2400	3	15 (waste drums)
Total	34600	31.055	158

Table 16. The waste/package specific activities of VTT's decommissioning wastes in 2068.

Nuclide	**Activated metal samples (Bq)**	**Irradiation ring (Bq)**	**Reflector and thermal column (Bq)**	**FiR1 steel components (Bq)**	**Other (Bq)**		**Total (Bq)**
Package	**Special concrete container**	**Concrete package**	**Concrete package**	**Concrete package**	**Concrete package**	**Waste drums**	
Ag-108m	$1.48{\cdot}10^{8}$					$4.78{\cdot}10^{6}$	$1.53{\cdot}10^{8}$
Ar-39					$7.50{\cdot}10^{8}$	$8.64{\cdot}10^{4}$	$7.50{\cdot}10^{8}$
Ba-133			$4.23{\cdot}10^{6}$		$1.84{\cdot}10^{6}$		$6.07{\cdot}10^{6}$
C-14 inorg			$2.57{\cdot}10^{9}$				$2.57{\cdot}10^{9}$
C-14 org	$9.72{\cdot}10^{9}$	$3.46{\cdot}10^{9}$	$4.78{\cdot}10^{9}$	$3.22{\cdot}10^{8}$	$3.28{\cdot}10^{8}$	$9.83{\cdot}10^{5}$	$1.86{\cdot}10^{10}$
Ca-41					$5.60{\cdot}10^{8}$	$6.40{\cdot}10^{4}$	$5.60{\cdot}10^{8}$
Cl-36			$6.00{\cdot}10^{8}$		$1.50{\cdot}10^{7}$	$1.70{\cdot}10^{3}$	$6.15{\cdot}10^{8}$
Co-60	$4.18{\cdot}10^{8}$	$4.74{\cdot}10^{8}$	$2.07{\cdot}10^{7}$	$4.25{\cdot}10^{7}$	$4.79{\cdot}10^{5}$	$9.74{\cdot}10^{4}$	$9.55{\cdot}10^{8}$
Cs-137						$4.00{\cdot}10^{7}$	$4.00{\cdot}10^{7}$
Eu-152			$1.71{\cdot}10^{9}$		$1.12{\cdot}10^{9}$	$1.32{\cdot}10^{5}$	$2.83{\cdot}10^{9}$
Eu-154			$3.07{\cdot}10^{7}$		$7.40{\cdot}10^{6}$	$8.51{\cdot}10^{2}$	$3.81{\cdot}10^{7}$
H-3			$2.02{\cdot}10^{10}$		$6.98{\cdot}10^{10}$	$2.17{\cdot}10^{10}$	$1.12{\cdot}10^{11}$
Mo-93	$2.52{\cdot}10^{7}$					$2.31{\cdot}10^{3}$	$2.52{\cdot}10^{7}$
Nb-94	$2.76{\cdot}10^{7}$					$1.95{\cdot}10^{3}$	$2.76{\cdot}10^{7}$
Ni-59	$1.26{\cdot}10^{10}$	$5.74{\cdot}10^{9}$		$5.61{\cdot}10^{8}$	$2.10{\cdot}10^{6}$	$3.92{\cdot}10^{6}$	$1.89{\cdot}10^{10}$
Ni-63	$8.63{\cdot}10^{11}$	$4.07{\cdot}10^{11}$		$3.79{\cdot}10^{10}$	$1.46{\cdot}10^{8}$	$9.14{\cdot}10^{7}$	$1.31{\cdot}10^{12}$
Pu-238						$2.84{\cdot}10^{6}$	$2.84{\cdot}10^{6}$
Pu-239						$6.95{\cdot}10^{6}$	$6.95{\cdot}10^{6}$
Pu-240						$3.15{\cdot}10^{6}$	$3.15{\cdot}10^{6}$
Pu-241						$2.19{\cdot}10^{7}$	$2.19{\cdot}10^{7}$
Total (Bq)	$8.86{\cdot}10^{11}$	$4.17{\cdot}10^{11}$	$2.99{\cdot}10^{10}$	$3.88{\cdot}10^{10}$	$7.28{\cdot}10^{10}$	$2.19{\cdot}10^{10}$	$1.47{\cdot}10^{12}$

2.4.1 Classification of the waste and waste packages

Nuclear waste is classified as long-lived, if its activity concentration after 500 years is over 100 MBq/kg in one waste package or above 10 MBq/kg in one emplacement room [10]. If neither of these requirements is not met, the waste is considered to be short-lived. The irradiation ring and the activated metal samples exceed the value of 100 MBq/kg, thus they are classified as long-lived nuclear waste. The classification affects only the package requirements, which was already taken into account when the packages were chosen.

2.4.2 Long-term safety requirements for the waste packages

The requirements for the long-term safety of waste packages are set by STUK [10]. The engineered barriers must be designed such that they adequately limit, retard and impede the release of radioactive waste into the surrounding bedrock in the underground waste repository The release must be retarded in relation to the half-life of the radionuclides in the waste such that nuclides have decayed enough before major releases can happen. For long-lived nuclear waste the major releases must be retarded for at least several thousands of years, and for short-lived nuclear waste at least several hundreds of years. The engineered barriers should not be made of materials that are unfavourable to the long-term safety or whose characteristics may change in the underground waste repository in a way, that the release of radionuclides increase.

Based on the inventory estimates, almost all of the decommissioning wastes are classified as short-lived nuclear waste, with the exception of the irradiation ring and activated metal samples. The waste packages will be categorized based on their activity inventory and other characteristics. Each waste package shall meet the disposal room specific criteria, referred to STUK's Guide YVL D.5 [10].

2.5 Comparison with the waste from Loviisa NPP

The activity inventories of the wastes of Loviisa NPP and decommissioning wastes of VTT must be compared due to the fact, that a limit has been set for the total activity, that the Loviisa LILW repository can hold. The Loviisa LILW depository contains multiple waste halls, and two of them stand out as the possible place for VTT's decommissioning wastes, which are MWH2 and DWH1. The overall activities of FiR 1 and OK3 decommissioning waste compared to the activity inventory of DWH1 and MWH2 is presented in figure 6.

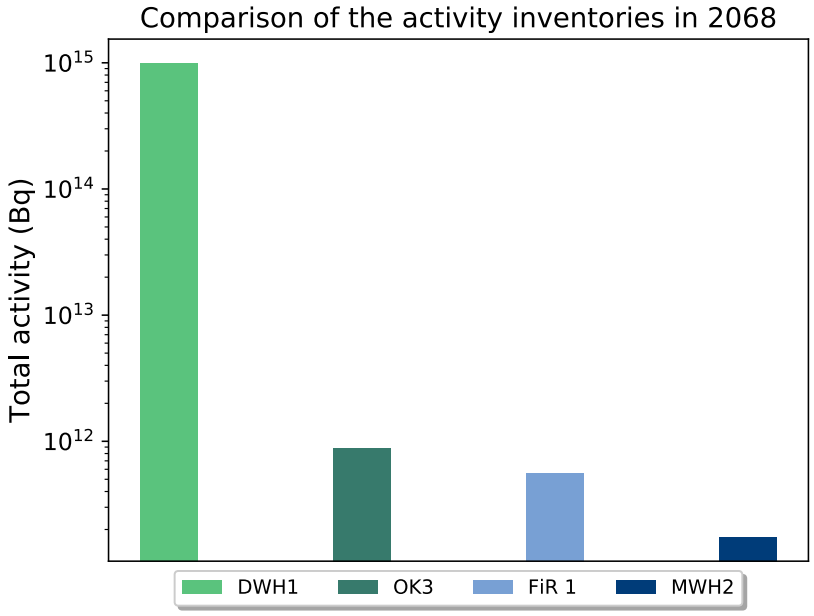

Figure 6. Comparison of activity inventories in 2068 between the activity inventories of two waste halls and the decommissioning wastes of FiR1 and OK3. The activities of DWH1 and MWH2 are taken from [29]

The activity of VTT's decommissioning wastes is extremely low compared to the activity inventory of DWH1, but higher compared to MWH2. The activity inventory of DWH1 is high due to the fact, that it is assumed to contain the decommissioning wastes of Loviisa NPP, which is much more active compared to the operational waste stored in MWH2. The total activity of FiR 1 waste is over 300 % of the activity inventory of MWH2 due to the high activity of Ni-63 in the irradiation ring. The activity inventory of OK3 is about 500 % of the total activity of MWH2, and the biggest contributor is also Ni-63. The total activity itself does not describe the

dangerousness of the waste from the perspective of the long-term safety, as the more important factor is the composition of radionuclides.

3 Evolution of the repository system

3.1 Processes affecting the repository

The 2018 safety case addresses the evolution of the disposal system over the assessment period of 100,000 years. The disposal system form a complex system whose evolution is affected by multiple processes and factors e.g. climate evolution, future human actions, evolution of the waste packages etc. A flow chart in figure 8 presents schematically how the different assessment activities affect one another. The common legend of the flow chart is presented in figure 7. This report covers only the processes considered to be most important from the perspective of the long-term safety of VTT's decommissioning wastes. The evolution of the repository is explained in-depth in [14].

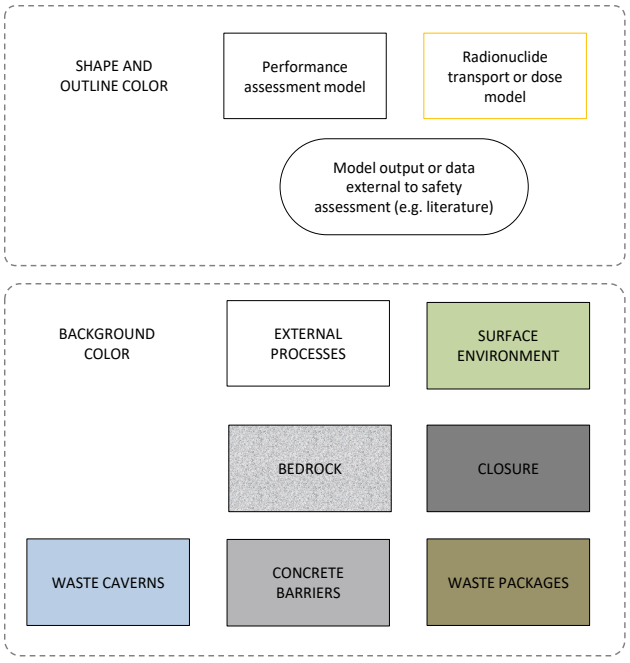

Figure 7. A common legend for the modelling flow charts. The figure is taken from [15].

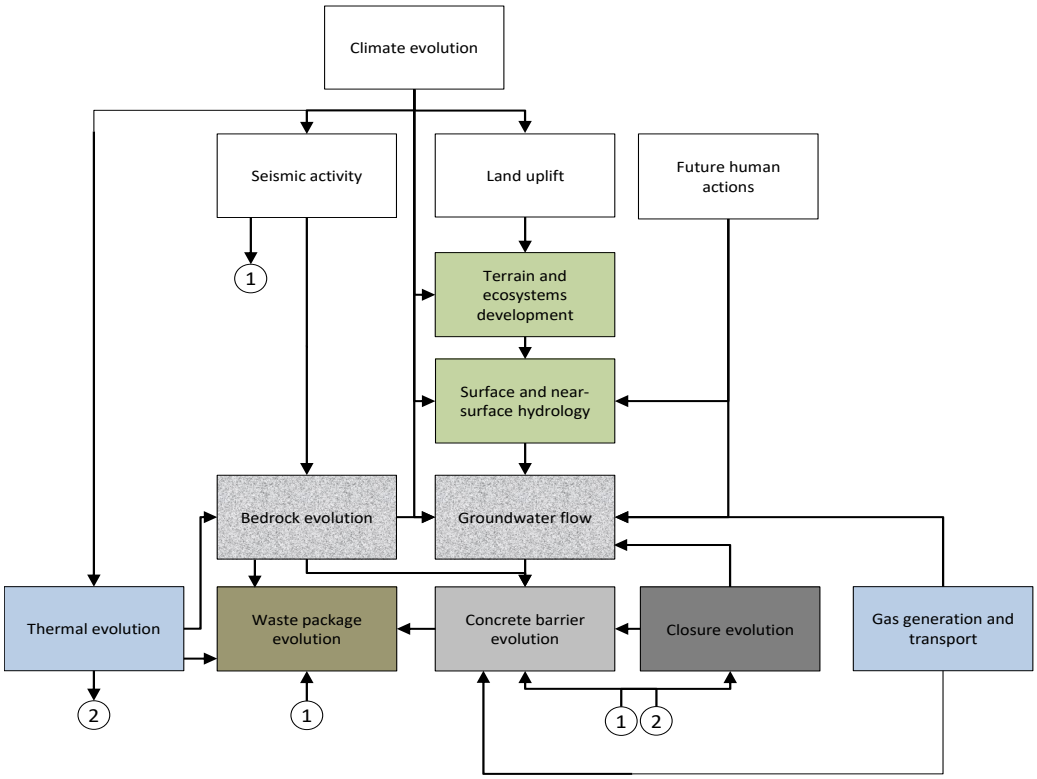

Figure 8. A flow chart describing the processes affecting the repository. The figure is taken from [14]. The common legend of the figure is presented in 7.

3.2 External processes

3.2.1 Climate evolution

Climate is a term that is used to describe long-term weather conditions in a specific region. Internal and external forcing mechanisms are constantly causing changes in the climate, which is called climate change. Internal forcing mechanisms are completely natural and are contained within the system itself e.g. distribution of plant and animals. External forcing mechanisms include both natural (e.g. volcano eruptions) and unnatural mechanisms (carbon emissions caused by humans). The main factors taken into account in the alternate climate evolutions are climate forcing, climate evolution, permafrost formation, glaciation and sea level change. [14] In the base scenario (see table 23) for the definition of the term) it is assumed that two glacial and permafrost periods exist during the assessment period.

The climate evolution modelling done by Posiva is based on four Representative Concentration Pathways (RPCs), which were introduced in [30]. The RCPs present different futures in terms of the greenhouse gas concentration in the atmosphere. Totally four RCPs were formed, which are RCP2.6, RCP4.5, RCP6 and RCP8.5.

SKB modelled the evolution of climate near the SFR LILW repository, located in the city of Forsmark in Sweden. SFR is located approximately 450 km away from Loviisa LILW repository, which means that the climate evolution may be similar. The SKB's climate evolution is described in [31]. Based on Posiva's and SKB's work, three of the RCPs were selected to be considered in the 2018 safety case for Loviisa LILW repository, which are presented in figure 9.

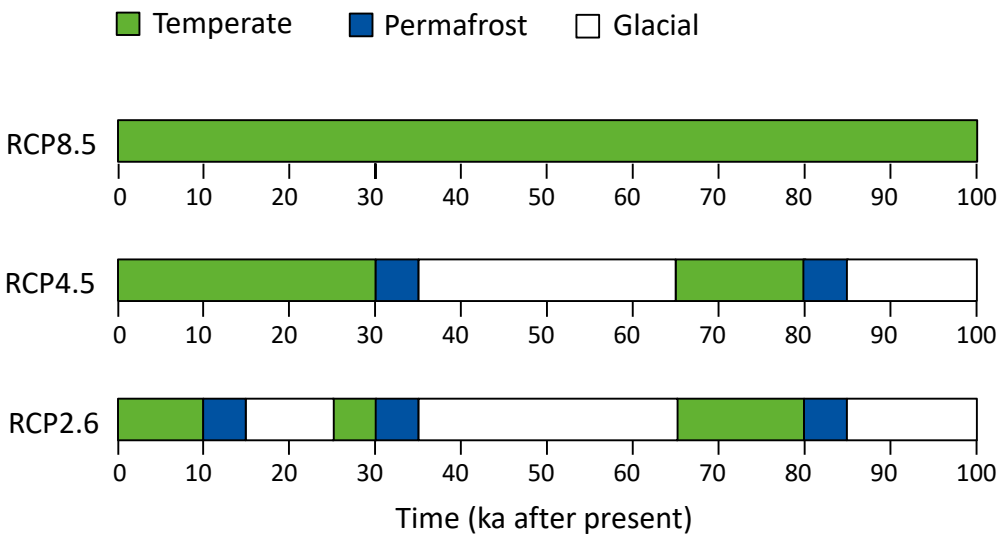

Figure 9. Summary of future climate evolutions. Style of this figure is based on figure in [32]. The permafrost between 10,000 and 15,000 years is not assumed to reach repository depth but assumed to reach repository during other permafrost periods. The figure is taken from [14].

3.2.2 Future human actions

Future human actions are possible actions caused by humans which may have an effect on the repository system. These actions are assumed to be carried out without the knowledge of the location of the repository, its purpose or consequences of the actions. Several future human actions potentially affecting the repository are listed in [14], but the most important ones consider drilling for different purposes e.g. to construct a well, drilling for geothermal heat or drilling for scientific or exploratory purposes. The drilling may damage the waste packages or the concrete basin in DWH1.

3.3 Surface environment

The terrain and ecosystem modelling has been carried out, in order to identify locations and properties of terrestrial ecotypes and water bodies. The results gained from the modelling are used in surface and near-surface hydrology modelling and radionuclide transport in surface environment. The radionuclide transport utilizes so called biosphere objects. The biosphere objects basically places chosen from the modelling area, which are the most probable locations of activity discharge. The evolution of the surface environment around the disposal site and areas surrounding the site is explained in detail in Terrain and ecosystems -report [33].

The modelling of the surface environment assumes that the climate evolution follows the RCP4.5 climate evolution. Figure 10 presents a small section of the modelling area, and also the evolution of the Hästholmen island in 2000 AD (anno domini) and 10,000 AD. The terrain and the ecosystems have been modelled only for 50,000 years for both low and high sea levels variants, since according to RCP4.5 the onset of glaciation is suggested to start after 45,000 AD. Only the low sea level variant of the RCP4.5 climate evolution has been implemented into the biosphere objects, as in the high sea level variant the area is submerged during the dose assessment period, which means that all the activity is released directly into sea bay. The landscape evolution in the low sea level variant is presented in different phases in figure 11. The common legend used in the map is presented in figure 12.

The modelling of the biosphere objects has been limited to 12,000 AD due to the fact, that after that the shoreline has moved far enough from the location of the disposal site, in order to consider it static. The landscape is considered to be

static in the modelling until next glacial period. [33] The area to the west of the Hästholmen island (object 1, Figure 10) is expected to receive the highest release of radionuclides, which makes it the most contaminated biosphere object.

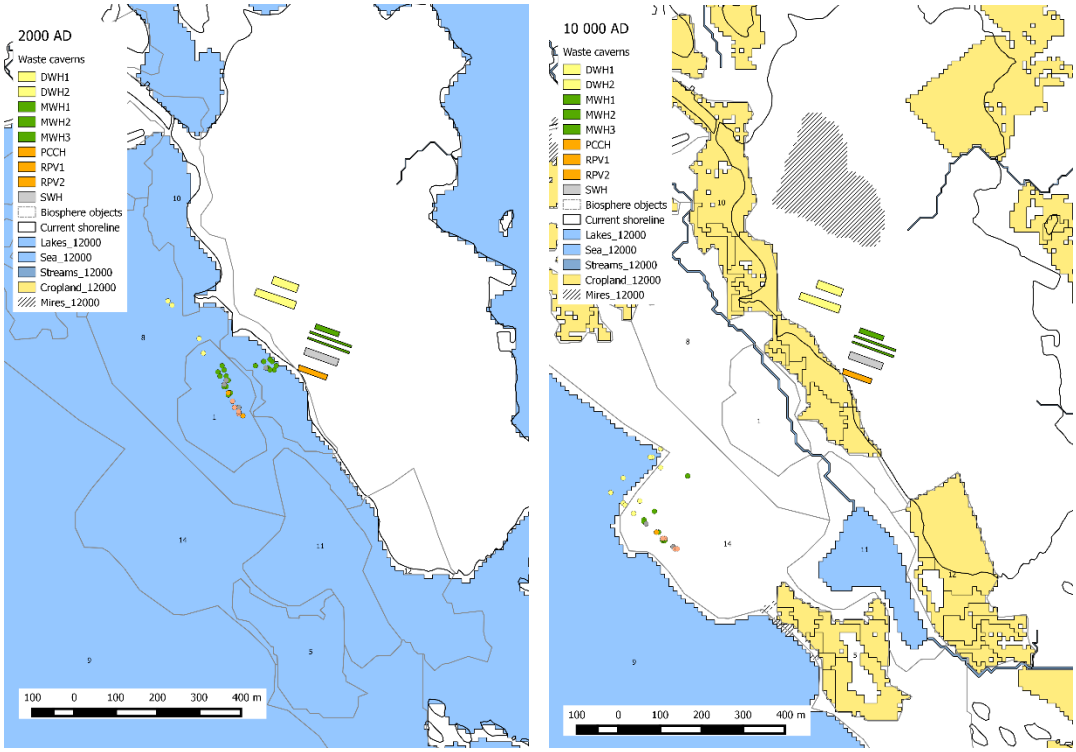

Figure 10. Locations of the waste caverns (rectangles) and their corresponding places (circles) of activity discharge at the Hästholmen island at times 2000 AD and 10,000 AD. The colours of the waste caverns correspond to colours of the discharge locations and the numbers refer to biosphere object. The figure is taken from [33].

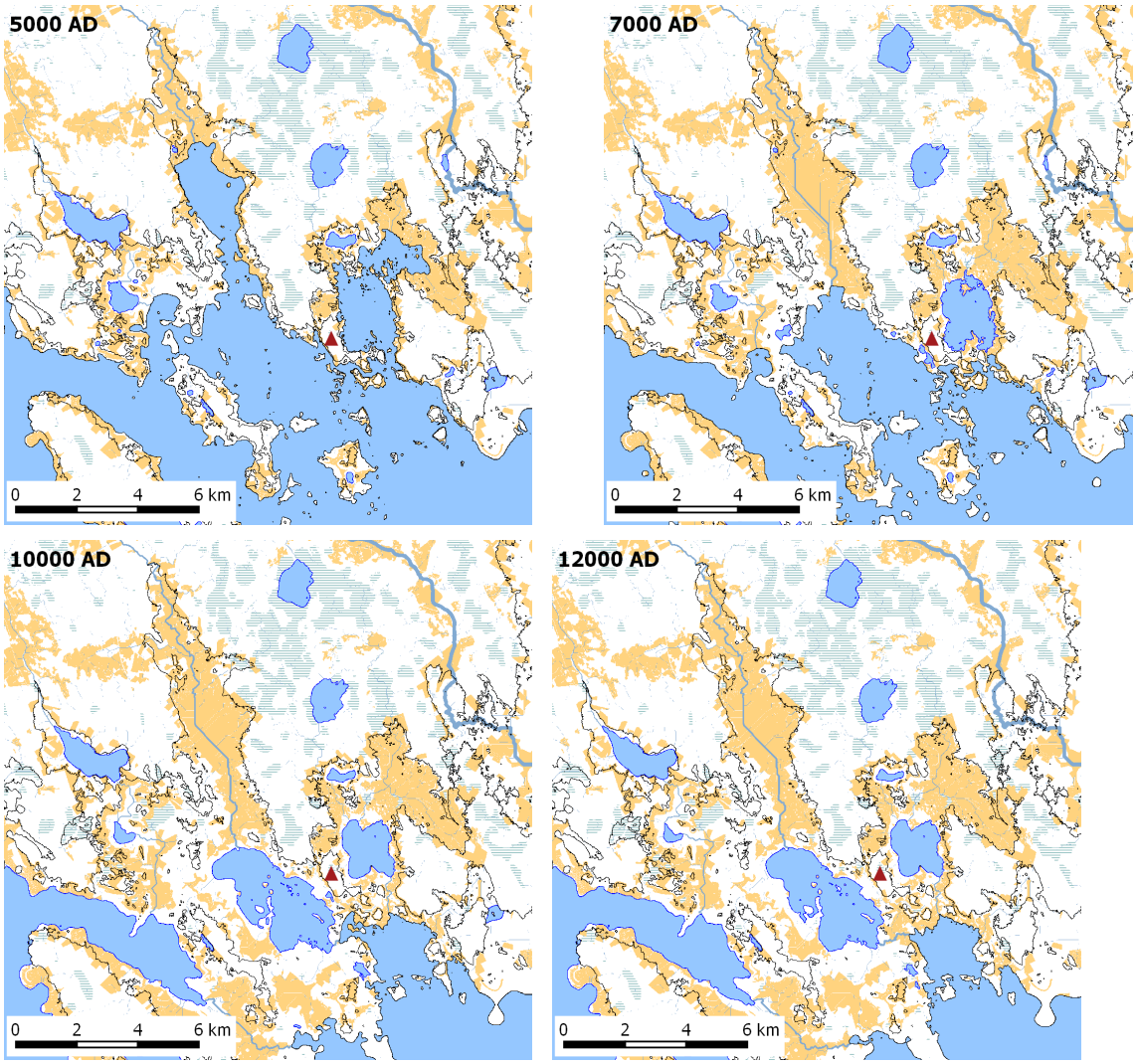

Figure 11. Landscape evolution until 10,000 years AP. The common legend of the map is presented in 12. The figure is taken from [33].

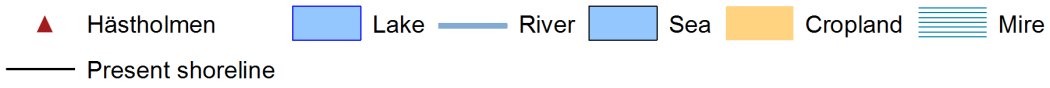

Figure 12. A common legend for the maps. The figure is taken from [33].

3.4 Repository system

3.4.1 Concrete barriers

The concrete degradation is chemical and mechanical process which causes concrete to lose its mechanical strength. As the concrete barriers degrade, their ability to

limit and retard radionuclide transport decreases. Concrete leaching was identified to be the most dominating one of the chemical degradation processes. Leaching of concrete contains multiple phases, and in the end it depletes all the portlandite (CH) from the concrete, after all of the calcium silicate hydrate gel (C-S-H) have been depleted. The process decreases the pH of concrete gradually. A one-dimensional shrinking core model was used to model the leaching of the concrete barriers, which is described in detail in the Performance assessment and formulation of scenarios -report [14]. The three most important processes impacting the leaching are diffusive transport through the leached zone of concrete, advective transport through the concrete barrier and concentration of leachable substances adjacent to the concrete barrier. The processes are schematically presented in figure 13.

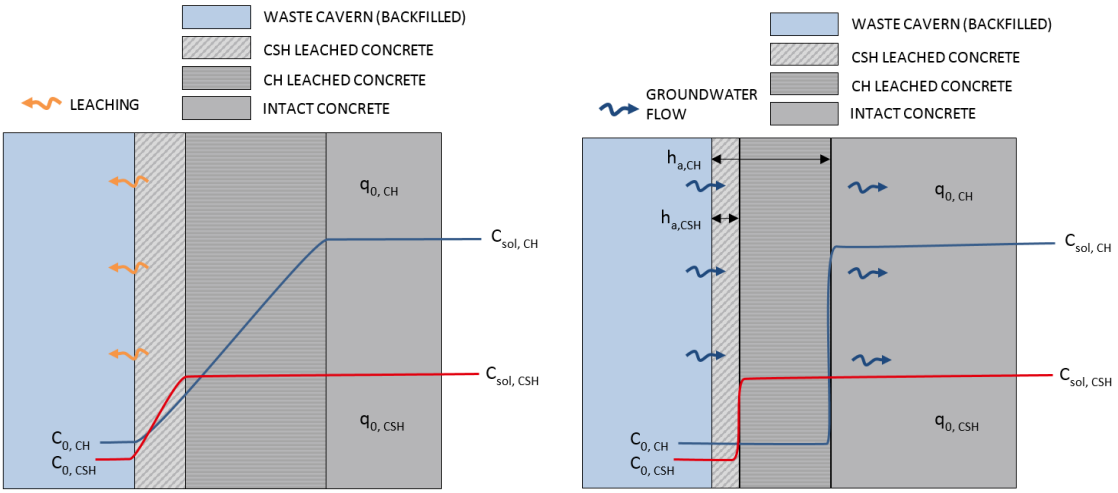

Figure 13. An illustration of diffusion (left) and advection(right) controlled leaching in concrete. The figure is taken from [11].

3.4.2 Groundwater flow

Groundwater flow is an important factor, as it is used to estimate the evolution of the concrete barriers and the modelling of radionuclide transport in near-field and in the bedrock. After the closure the repository will be filled by gradually inflowing groundwater, but this phase has not been modelled explicitly due to its low duration. The groundwater flow of the repository was modelled using Comsol Multiphysics 5.3 modelling software with Subsurface Flow -module. The modelling is explained in detail in Groundwater flow modelling -report [34]. The time development of

the groundwater flow rates of MWH2 and DWH1 are presented in figure 14. The uncertainty of the groundwater flow rate were estimated using sensitive analysis [34].

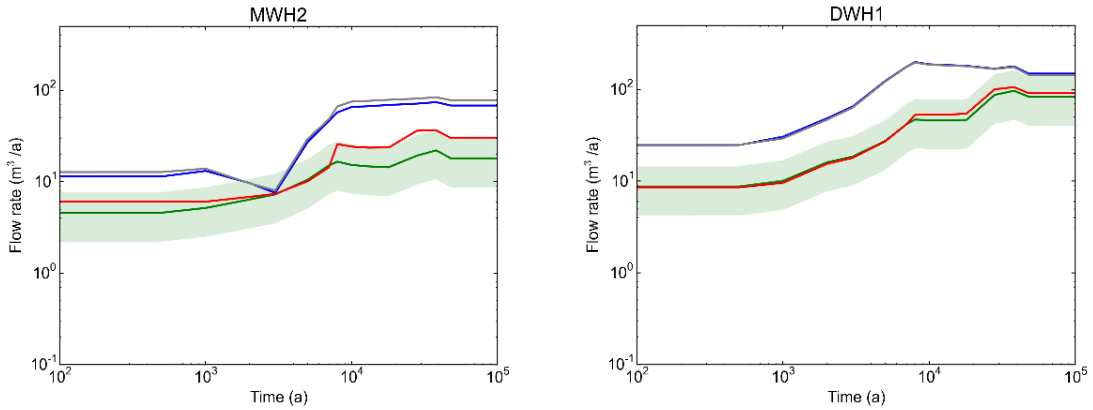

Figure 14. Groundwater flow through MWH2 and DWH1. The green shaded area indicates the range between 5th and 95th percentiles. The figure is edited from [14].

3.4.3 Waste packages

The evolution of the concrete waste packages depends on the concrete degradation process, especially by leaching and fracturing. The leaching is governed by the pH level of the surrounding water around the concrete. Alkaline conditions (high pH-value, low amounts of chloride and sulphate) slows down the degradation of concrete. The purpose of the concrete basin in DWH1 is to make sure, that the chemical conditions stay alkalic as long as possible and also provide mechanical protection. The degradation of concrete packages initiates only after the concrete basin becomes depleted of portlandite. [11]

The performance of the concrete containers is mainly characterized by their ability to limit the release of radionuclides by diffusion and their ability to provide alkaline conditions. The calculation of effective diffusion coefficient is based on the leaching depth and diffusion coefficient for different layers. After all of the calcium silicate hydrate gel (C-S-H) have been leached from the concrete, it is assumed to degrade mechanically and the value of the diffusion coefficient is set to $1{\cdot}10^{-9}$ m^2/s, which is the same value as the diffusion coefficient of free water. [14] The time evolution of the diffusion coefficient of the 120 mm concrete container is presented in figure 15.

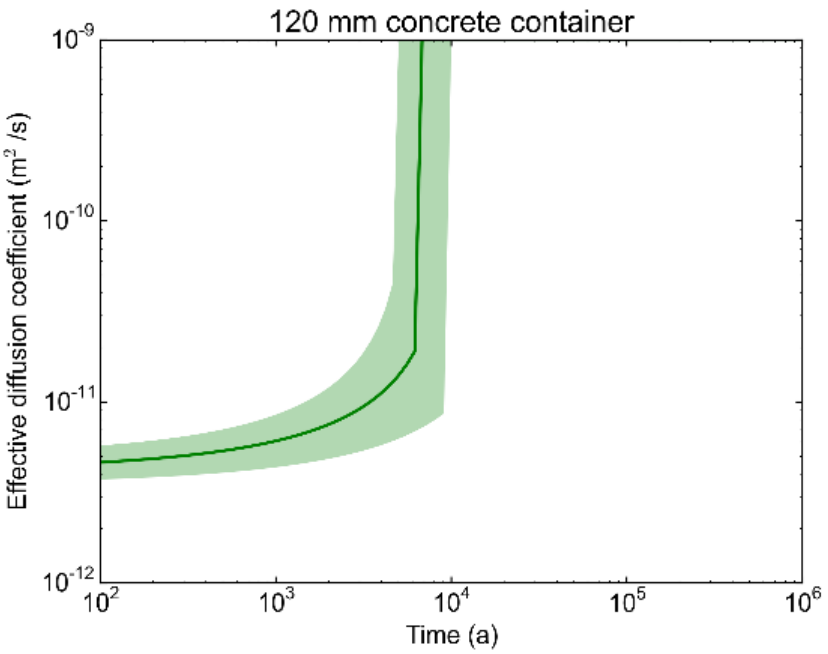

Figure 15. Evolution of diffusion coefficient of the 120 mm concrete container in the reference evolution. The solid line represents the reference value and the green shaded area the estimated uncertainty. The figure is taken from [15].

There is no concrete basin in MWH2 because it is originally designed to hold only waste drums which have low activity. The chemical conditions of MWH2 are assumed to be neutral which increases the concrete degradation rate. If concrete packages were to be disposed in MWH2, the degradation would start immediately with higher rate than in DWH1. The concrete packages degrade in 9620 years in MWH2 and in 48720 years in DWH1. The waste drums used in the packaging are not considered as release barrier instead the activity in them is assumed to release immediately upon contact with water.

3.4.4 Gas generation

The degradation of some waste materials and waste packages produce gases. The most important gas generation source in VTT's decommissioning wastes is the corrosion of metals. Other mechanisms are decomposition of organic materials and radiolysis. [35] Of these, the corrosion of aluminium has potential impact on the gas generation. The conditions in the maintenance waste hall 2 are assumed to be in the neutral pH regime, due to low amount of cement and microbiological activity [3].

The amount of organic waste in the FiR 1 decommissioning waste is low, so very little decomposition occurs. The radiolysis was addressed in appendix A of [36], and was concluded to be insignificant. The total gas generation due to radiolysis is 0.235 m^3/a in one of the disposed reactor pressure vessel, which is insignificant compared to the gas generation from metal corrosion.

Aerobic corrosion and anaerobic organic decay deplete the oxygen from the repository after the closure. It is assumed that the period of aerobic corrosion is relatively short, thus its effects are left out of the analysis. The analysis focuses more on the corrosion under anaerobic conditions. The amount of gas generated varies between different metal types. The most abundant metals in the decommissioning wastes of FiR 1 and OK3 are discussed in the subsections below.

3.4.5 Aluminium corrosion

According to [5] and [37], aluminium corrodes in the following chemical reactions:

$$2\mathrm{Al\,(s)} + 2\mathrm{OH^-} + 4\mathrm{H_2O} \rightarrow 2\mathrm{Al\,(OH)_2^-} + 4\mathrm{H_2(g)}, \tag{5}$$

$$2\mathrm{Al\,(s)} + 2\mathrm{OH^-} + 2\mathrm{H_2O} \rightarrow 2\mathrm{AlO_2^-} + 3\mathrm{H_2(g)}. \tag{6}$$

Multiple values for aluminium corrosion rate exist for different safety assessments. Such values are 24.5 µm/a [38], 10 µm/a [39] and according to reference [5] the value is usually 1000 µm/a and even 10000 µm/a.

Multiple values between 24.5 µm/a and 10000 µm/a makes the degree of uncertainty of the aluminium corrosion rate high. Aluminium corrosion rates up to 1000 µm/a have been measured in acidic and alkaline conditions [40], which is a conservative value used in the Loviisa LILW safety case [36], thus the same value is also used in this report for consistency.

The corrosion rate of aluminium depends on the chemical conditions of disposal hall. In MWH2 the pH is assumed to be close to neutral would decrease the corrosion rate and thus also the gas generation. If all of the aluminium were to be disposed into DWH1, the corrosion rate would be much higher due to the alkaline conditions.

Fluental also contributes to the gas generation due to its composition. According to the composition of Fluental, it contains 0.63 tons of aluminium, which means that the total amount of aluminium in FiR 1 decommissioning waste is 2.86 tons. It is as-

sumed that all of the aluminium is available for gas generation. The decommissioning waste of OK3 may contain small amounts of aluminium.

The volume of the hydrogen gas generated in reaction (6) can be calculated by setting the concentrations of aluminium C_{Al}(mol/kg) and hydrogen gas C_{H_2}(mol/kg) equal to each other

$$C_{Al} = C_{H_2}, \tag{7}$$

Concentration can expressed as the relation of density and molar mass ρ/M or as the amount of moles in volume n/V, thus

$$\frac{1}{2}\frac{\rho_{Al}}{M_{Al}} = \frac{1}{3}\frac{n_{H_2}}{V_{H_2}}, \tag{8}$$

where the numbers 2 and 3 are the stochastic coefficients. Ideal gas is a simplified model of gas which assumes that the collisions of atoms and molecules in the gas are elastic, and that there are no electrostatistical forces between them. The ideal gas equation can be written as

$$pV = nRT, \tag{9}$$

where R (J/Kmol) is the universal gas constant. [41] Combining equations (8) and (9) and solving for volume V (m^3) gives the following expression

$$V = \frac{3}{2}\frac{\rho_{Al}V_{H_2}}{M_{Al}}\frac{RT}{p}. \tag{10}$$

Taking a time derivative gives the change in volume over time, or how much gas is generated over time

$$\dot{V} = \frac{3}{2}\frac{\rho_{Al}Av_{corr}}{M_{Al}}\frac{RT}{p}, \tag{11}$$

where v_{corr} (µm/a) is the corrosion rate of aluminium, A (m^2) is the corroding area. Since STP conditions are assumed, RT/p can be replaced with the molar volume of an ideal gas V_g [41]. The final form of the equation is

$$V_H = \frac{3V_gA\rho_{Al}}{2M_{Al}}v_{corr}. \tag{12}$$

To be consistent with the safety case reports, an assumption of the 1 mm thick

plate and same the values of density and molar masses are used. For aluminium the values are 2700 kg/m^3 and 26.98 g/mol respectively. [36]

3.4.6 Steel corrosion

Steel is a mix made from iron, carbon and other metals, which all contribute to the gas generation. Upon contact with water, iron corrodes in the following chemical reaction

$$\mathrm{Fe} + 2\mathrm{H_2O} \rightarrow \mathrm{Fe(OH)_2} + \mathrm{H_2}, \tag{13}$$

where the main corrosion product $\mathrm{Fe(OH)_2}$ is called iron(II)hydroxide. Iron(II)hydroxide may also undergo the Schikorr reaction to produce magnetite $\mathrm{Fe_3O_4}$

$$3\mathrm{Fe(OH)_2} \rightarrow \mathrm{Fe_3O_4} + 2\mathrm{H_2O} + \mathrm{H_2}, \tag{14}$$

[42]. The Schikorr reaction is unlikely to occur due to the alkaline state inside the concrete packages because excess alkalinity has been shown to inhibit the formation of magnetite [43]. Combining reactions (13) and (14) gives the following net reaction

$$3\mathrm{Fe} + 4\mathrm{H_2O} \rightarrow \mathrm{Fe_3O_4} + 4\mathrm{H_2}. \tag{15}$$

The gas generation rate for steel derived similarly as for aluminium but the stochastic coefficients are different

$$V_H = \frac{4V_g A \rho_{Steel}}{3M_{Iron}} v_{corr}. \tag{16}$$

The values used for density and molar mass are 7850 kg/m^3 and 55.85 g/mol respectively [36]. If the Schikorr reaction does not occur then the hydrogen gas is generated according to (13), and the constant 4/3 is changed to 1 due to the stochastic coefficients. The larger constant increases the gas generation rate which makes the assumption of the Schikorr reaction more conservative.

It is assumed that all of the stainless steel is made of iron. Stainless steel contains approximately 18 % Cr and 10 % Ni so the chemical reactions producing hydrogen gas should be more complex than above. However, it is assumed that the corrosion rates for all components in stainless steel are equal. This means that calculating the generation rates for each element and summing them gives the same result, as if the

stainless steel was made of iron. [36]

Steel corrosion rate values depends on the type of steel and on the various external conditions e.g. pH. A literature review was originally performed in [44], and the results were later update in [45]. The most recent corrosion rate values for carbon steel and stainless steel are listed in table 17.

Table 17. Steel corrosion rates in anaerobic conditions used in the safety case. The table is taken from [36].

	Corrosion rate (µm/a)			
	Alkaline conditions		**Neutral conditions**	
	Realistic	Conservative	Realistic	Conservative
Carbon steel	0.05	0.5	0.5	5
Stainless steel	0.005	0.05	0.1	1

The previous literature reviews were based on both the experimental results and literature reviews by other radioactive waste management organisations. It is challenging to combine literature and experimental results and estimate the degree of conservatism, as the value varies between the recommendations by different organisations.

3.4.7 Total gas generation

The gas generation rate equations require the area of the corroding surface, but calculating the area of every single component is not feasible, thus an approximation for the area is needed. The geometry of the irradiation ring is known and its corroding area can be calculated (section 4.6.2). However, the masses of FiR 1 components, OK3 components and aluminium waste are assumed to be contained in a plate with a thickness of 1 mm. The area of the plate can be calculated, when the thickness of the plate, the density and the mass of waste are known.

The gas generation rates and the total gas yields for the aluminium and steel are presented in tables 18 and 19. The total gas yields are calculated by multiplying the gas generation rates with the corresponding corrosion end time i.e. the when the components have corroded completely and disappeared. The gas generation rates and the total gas yields for the different waste caverns are listed in table 20. The values in table 18 and table 19 are much smaller than those in table 20, so it can be concluded that the gas generation does not have considerable impact on the safety for the disposal. However, due to the fact that the gas generation rate of aluminium

is much higher and faster compared to the other gas generation rates and it does not give the whole picture about the gas generation.

Table 18. Summary of the gas generation rates and the total gas yields for FiR 1 and OK3 decommissioning wastes, when they are disposed in MWH2. The highest overall value indicates the highest gas generation rate of all the components excluding aluminium.

Waste	**Gas generation rate**	**Total gas yield**
Irradiation ring	$\begin{cases} 4.68 \cdot 10^{-6}\ m^3\mathrm{a}^{-1},\ t \leq 9620\ a \\ 9.37{\cdot}10^{-5}\ \mathrm{m}^3\mathrm{a}^{-1},\ 9620\ \leq t \leq 14139\ a \end{cases}$	0.47 m^3
FiR 1 components	$\begin{cases} 8.29 \cdot 10^{-4}\ m^3\mathrm{a}^{-1},\ t \leq 9620\ a \\ 1.66\ {\cdot}10^{-2}\ m^3\mathrm{a}^{-1}, 9620 \leq\ t\ \leq 9640\ a \end{cases}$	8.31 m^3
Aluminium waste	3167.98 $m^3\mathrm{a}^{-1}$, $t = 1\ a$	3167.98 m^3
OK3 components	$\begin{cases} 1.16 \cdot 10^{-2}\ m^3\mathrm{a}^{-1},\ t \leq 9620\ a \\ 2.31\ {\cdot}10^{-1}\ m^3\mathrm{a}^{-1}, 9620 \leq\ t\ \leq 9640\ a \end{cases}$	115.75 m^3
Total	**Highest value 1st year:** 3167.98 m^3a^{-1} **Highest value overall:** $2.31 \cdot 10^{-1}\ m^3a^{-1}$	3292.51 m^3

Table 19. Summary of the gas generation rates and the total gas yields for FiR 1 and OK3 decommissioning wastes when they are disposed in DWH1. The highest overall value indicates the highest gas generation rate of all the components excluding aluminium.

Waste	**Gas generation rate**	**Total gas yield**
Irradiation ring	$\begin{cases} 4.68 \cdot 10^{-6}\ m^3\mathrm{a}^{-1},\ t \leq 48720\ a \\ 9.37\ {\cdot}10^{-5}\ \mathrm{m}^3\mathrm{a}^{-1}, 48720 \leq\ t \leq 51284\ a \end{cases}$	0.47 m^3
FiR 1 components	$8.29 \cdot 10^{-4}\ m^3\mathrm{a}^{-1}$, $t \leq 10000\ a$	8.29 m^3
Aluminium waste	3167.98 $m^3\mathrm{a}^{-1}$, $t = 1\ a$	3167.98 m^3
OK3 components	$1.16 \cdot 10^{-2}\ m^3\mathrm{a}^{-1}$, $t \leq 10000\ a$	115.53 m^3
Total	**Highest value 1st year: 3167.98** m^3 **Highest value overall:** $1.16 \cdot 10^{-2}$ m^3	**3292.27** m^3

Table 20. Maximum gas generation rates in Loviisa LILW repository. The table is taken from [36].

Waste cavern	Maximum gas generation rate (m^3/a) Realistic	Conservative	Total gas yield (m^3)
RPV1	9.87E-01	9.87	$2.39 \cdot 10^5$
RPV2	9.87E-01	9.87	$2.39 \cdot 10^5$
PCCH	$7.45 \cdot 10^1$	$7.45 \cdot 10^2$	$1.16 \cdot 10^6$
DWH1	$1.28 \cdot 10^2$	$6.76 \cdot 10^2$	$2.71 \cdot 10^6$
DWH2	$2.64 \cdot 10^2$	$1.31 \cdot 10^3$	$4.08 \cdot 10^5$
MWH1	$4.42 \cdot 10^2$	$2.36 \cdot 10^3$	$3.96 \cdot 10^5$
MWH2	$4.61 \cdot 10^2$	$2.47 \cdot 10^3$	$4.89 \cdot 10^5$
MWH3	$3.46 \cdot 10^2$	$1.81 \cdot 10^3$	$3.59 \cdot 10^5$
SWH	$3.18 \cdot 10^1$	$1.21 \cdot 10^2$	$1.72 \cdot 10^6$

3.4.8 Gas transport

There are two ways for the gas to escape from waste caverns. The gas may dissolve in water and flow to the surface or it may flow through the bedrock or closure structures. The gas generation is considered in the disposing due to the possible overpressurisation of the waste caverns and the waste packages. [36] Due to the fact that the gas generation from VTT's decommissioning wastes does not create significant overpressurisation, the gas generation is not considered to be a problem. The gas transportation in Loviisa LILW repository is explained in detail in the Gas generation and transport -report [36].

4 Radionuclide transport modelling

4.1 Modelling approach

The modelling approach used for the modelling of VTT's decommissioning wastes is similar to the one described in the Analysis of releases and doses -report [15]. The modelling is based on a compartment model, which is a mathematical model, describing the transport of material or energy between different compartments. The system is divided into homogenous compartments which are connected to each other with transfer functions. The modelling consists of five distinct modelling activities, which are: radionuclide release from waste, radionuclide transport in the near-field, radionuclide transport through bedrock, radionuclide transport in the surface environment and dose assessment. A flow chart in figure 16 presents how the modelling activities relate to the modelling chain.

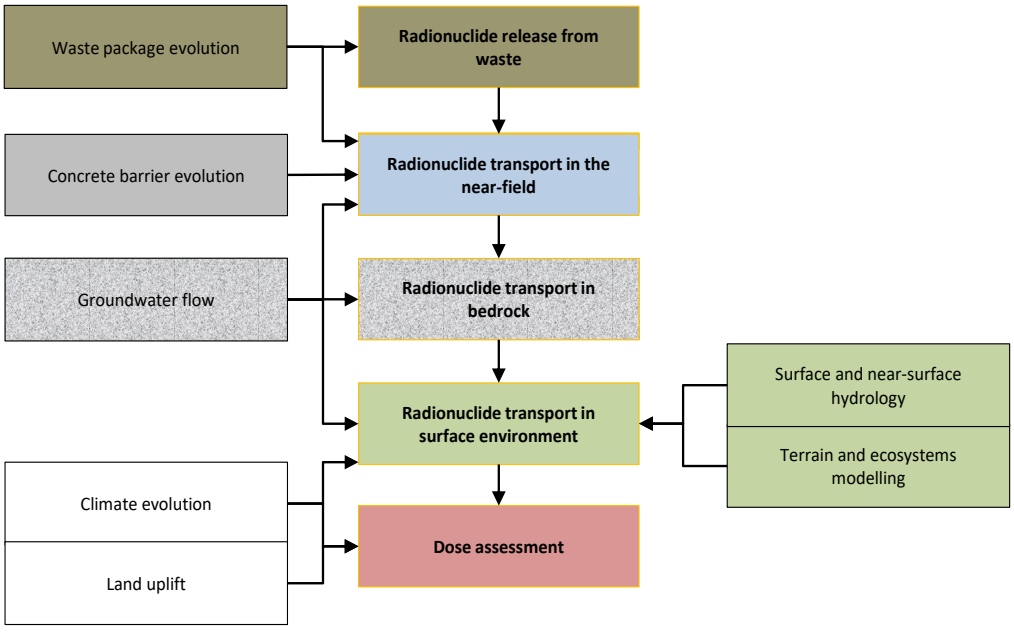

Figure 16. The modelling chain used in the analysis of releases and doses. The information flow is indicated by arrows. The figure is taken from [15].

The modelling is done with Ecolego, which is a software designed for compartment

transport modelling and for performing deterministic or probabilistic simulations. [46] The accuracy of the discretized model can be increased by adding more compartments, but this would make the model more complex and increase the model running time. Ecolego has a built-in feature for radioactive decay and decay chains which makes it ideal for modelling radionuclide transport.

The radionuclide releases are calculated with a system of differential equations. The equations describe the transportation (transfer) of radionuclides between the compartments

$$\frac{dN_i}{dt} = -\sum_{j \neq i} \sum_{k} \lambda_{i \to j,k} N_i + \sum_{j \neq i} \sum_{k} \lambda_{i \to j,k} N_j + S_i - \lambda_{i,s} N_i - \lambda N_i, \tag{17}$$

where the index j indicates the index of compartments in the model, k indicates the transfer processes between the compartments, $\lambda_{j \to i,k}$ is the transfer coefficient between two compartments and N is the activity of the specific radionuclide in the compartment. The source S_i indicates the release of radionuclides from waste or from the decay of the parent nuclide. It is required by [10] that the parameters used in the modelling, assumptions etc. are mentioned in the document and are easy to find (traceability). The parameters used in the 2018 safety case are not explicitly mentioned or explained, but are referenced instead.

4.2 Concentration

Radionuclides are generally transported dissolved in water, but some of them can be sorbed onto solid surfaces e.g. concrete and rock. The radionuclide concentrations in solids and water can be calculated using the element specific distribution coefficient and the total amount of radionuclides in the compartment. The ratio of activity concentrations in the soil and in the pore water is determined the distribution coefficient

$$Kd = \frac{C_s}{C_p}, \tag{18}$$

where C_s (Bq/kg) is the activity concentration in the solid and C_p (Bq/m^3) is the activity concentration in the water. The total activity N (Bq) in the compartment

is given by

$$N = C_p \varphi V + C_s m, \tag{19}$$

where φ (m^3/m^3) is the saturation coefficient of the compartment, V (m^3) is the volume of the compartment and m (kg) is the dry mass of the compartment. The saturation coefficient φ is a dimensionless variable that indicates the fraction of the whole compartment that is filled with water. The retardation factor in the solid is defined as

$$R_s = 1 + \frac{Kd\rho_s}{\varphi}, \tag{20}$$

where ρ_s(kg/m^3) is the average solid bulk density. Combining equations (18), (19) and (20), and solving for the concentrations gives the following expressions

$$C_p = \frac{N}{\varphi V + Kdm} = \frac{N}{\varphi V R_s}, \tag{21}$$

$$C_s = \frac{\mathrm{NKd}}{\varphi V + Kdm} = \frac{\mathrm{NKd}}{\varphi V R_s}. \tag{22}$$

Sometimes the compartments can consist only of water thus the saturation value is φ=1. The water compartments may also contain suspended solids which are assumed not to affect the saturation of the compartment. In such case radionuclides reside either in water itself or in suspended solids. The Kd (m^3/kg) value for such case is calculated similarly (equation (4-2)), but the total activity is

$$C_w V + C_{ss} \rho_{ss} V = N, \tag{23}$$

where C^{ss} (Bq/kg) is the radionuclide concentration in the suspended solid and ρ_{ss} (kg/m^3) is the density of the suspended solid. The retardation factor R_w is defined as

$$R_w = 1 + Kd\rho_{ss}. \tag{24}$$

The radionuclide concentrations can be solved similarly:

$$C_w = \frac{N}{V + Kd\rho_{ss} V} = \frac{N}{V R_w}, \tag{25}$$

$$C_{ss} = \frac{NKd}{V + Kd\rho_{ss}V} = \frac{NKd}{VR_w}. \tag{26}$$

If a water compartment contains no suspended solids, the concentration is simply

$$C = \frac{N}{V}. \tag{27}$$

4.3 Solubility limited concentrations

A solution becomes fully saturated when additional solute cannot be dissolved anymore. Different elements and substances have a specific solubility limit, which also applied to radionuclides, as the chemical properties of radioactive and non-radioactive atoms of the same element are the same. The solubility of the radionuclides is limited by the stable nuclides. The solubility limit C_w (Bq/m^3) is modelled by limiting the radionuclide concentration in water to a certain radionuclide specific limit in a compartment:

$$C_w = min(\frac{N}{V}, (N_A C_{sol} \lambda), \tag{28}$$

where N_A (1/mol) is the Avogadro's constant, C_{sol} (mol/m^3) is the radionuclide specific solubility limit and λ(1/s) is the radionuclide specific decay constant. In the modelling it is assumed that any excess nuclides in compartment reside in precipitated form until the water is no longer fully saturated. In equation (28) the function *min* indicates that the expression which gives the smaller value is used in the calculation. Each radionuclide has a solubility limit, but also the stable nuclides contribute to the concentration. The contribution of stable nuclide, with exceptions of nickel and calcium has not been implemented into the model. Radionuclides can actually exceed the limit in the model, thus the radionuclide concentrations in water are overestimated.

The solubility limit of Ca-41 in alkaline conditions $C_{sol,Ca-41}$ (mol/m^3) was calculated by scaling the solubility limit of stable calcium $C_{sol,Ca}$(mol/m^3)

$$C_{sol,Ca-41} = \frac{n_{Ca-41}}{n_{Ca,tot}} C_{sol,Ca} \tag{29}$$

where n_{Ca-41}(mol) and $n_{Ca,tot}$(mol) are the amounts of Ca-41 and stable calcium in moles. The fraction actually is time dependent due to radioactive decay of Ca-41.

The half-life of Ca-41 is approximately 100,000 years, which means that the activity has decayed to half of its original value at the end of the assessment period. However, radioactive decay is not the only process removing Ca-41 from the repository, thus the equation can be considered a reasonable approximation. The new solubility limit considers DWH1 due to the large amount of concrete present in the waste cavern. The total amount of calcium, based on the concrete mass (2,100,000 kg) in DWH1 is $5.26 \cdot 10^7$ mol, and the total amount of Ca-41 in FiR 1 decommissioning wastes is 0.00423 mol. The solubility limit of calcium used in the safety case is 18 mol/m^3 [15]. Based on these values, the new solubility limit of Ca-41 in alkaline conditions is $1.45 \cdot 10^{-9}$ mol/m^3. The new Ca-41 solubility limit does not apply for MWH2. The 2018 safety case applies similar limit for nickel, due to the large amount of stable nickel present in the pressure vessels of Loviisa NPP, but such limit has not been implemented in this model.

4.4 Diffusion

Diffusion is a process which describes the spreading of molecules due to concentration gradients. Diffusion plays key role in the modelling of radionuclide release and transport, and can be described mathematically by Fick's laws of diffusion. Fick's first law in three dimensions can be written as

$$J = -D\nabla C, \tag{30}$$

where J (particles/m^{2}s) is the particle flux D(m^2/s) is the diffusion coefficient of the material and C is the concentration of particles. [47]

For the modelling of radionuclide release and transport a simplified form of Fick's first law is used. Multiplying equation (30) with an area A and removing the y and z dependencies gives the equation used in the compartment modelling

$$I = -D_e A \frac{\partial C_p}{\partial x}, \tag{31}$$

where I (Bq/s) is the amount of activity that diffuses through the area A (m^2), D_e(m^2/s) is the effective diffusion coefficient and C_p(Bq/m^3) is the activity concentration in porewater and x(m) is the spatial coordinate. [15] In a compartment model the diffusion is modelled with two transfer equations (diffusion in and diffusion out) such that both equations only take into account the concentration of the source

compartment.

In the modelling of radionuclide release and transport the diffusion usually is modelled as a steady state going through a wall of certain thickness with a certain diffusion coefficient e.g. through the walls of the concrete boxes. The equation for the source compartment is

$$\frac{dN_i}{dt} = -\frac{D_e A}{d} C_{p,i}, \tag{32}$$

where d(m) is the thickness of the wall, A(m^2) is the area of the wall. The thickness of the wall is assumed to be half of the relevant thickness of the source compartment and half the thickness of the target compartment.

4.5 Radionuclide release from the waste

4.5.1 Modelling approach

The activity can exist as a contamination on the surface of the waste or it can be induced in the waste material. This is the main factor that determines how the activity is released. The activity due to contamination is assumed to be released immediately because the activity exists on the surface of waste which causes it to be released easily. The three main features, events and processes considered in the modelling are: metal corrosion, radionuclide release and radioactive decay and ingrowth. Figure 17 contains a flow chart that indicates the inputs needed to calculate the source term. The needed inputs are activity inventory and its partitioning, metal corrosion rates, the thickness of activated metal parts and the pH level inside the waste containers. The radionuclide release rates are used as input for the near-field modelling.

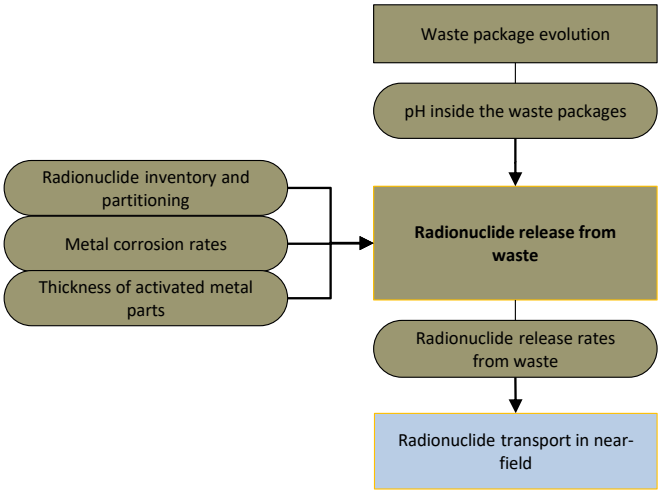

Figure 17. The flow chart for the radionuclide release from waste. The figure is taken from [15].

4.5.2 Releases from metals

The activity is gradually released from activated metal components due to corrosion, which can be written mathematically as

$$S_i = C_i \frac{dV}{dt}, \tag{33}$$

where $C_i = N_{i,0}/V_0$ is the radionuclide specific activity concentration. In the activity concentration $N_{i,0}$ is the activity and V_0 is the volume of the component. The time derivative of volume dV/dt) indicate the rate of change in the volume of the component due to corrosion, and it depends on the geometry of the component.

The active metal components in FiR 1 and OK3 decommissioning wastes are assumed to be like a plate with a thickness of 1 mm. With such assumption the corroding surface area can be assumed to remain constant. Thus the change in volume can be written the following way

$$\frac{dV}{dt} = A\frac{dx}{dt} = -2Av_{corr}, \tag{34}$$

where A is the corroding surface area, x is the thickness and v_{corr} is the uniform corrosion rate. The factor of two indicate that the corrosion is occurring on both

sides of plate. The final form of the equation is

$$S_i = 2v_{corr}\frac{N_{i,0}}{x}, \tag{35}$$

The irradiation ring resembles a cylinder (see figure 4) with the area of $A = 2\pi hR$, where h is the height of the cylinder and R is the outer radius of the cylinder. The volume of the irradiation ring is

$$V = \int_r^R 2\pi hR'dR' = \pi h(R^2 - r^2), \tag{36}$$

where r is the outer radius of the irradiation ring. Assuming that h is constant, the time dependent change in the volume is

$$\frac{dV}{dt} = \pi h(2R\frac{dR}{dt} - 2r\frac{dr}{dt}) = -2\pi h(R + r)v_{corr}. \tag{37}$$

The irradiation ring corrodes with an uniform rate v_{corr} from inside and outside. Assuming that the centre of the irradiation ring is the origin, changes the sign of dR/dt to negative because the corrosion rate vector points in the negative direction. The sum of the radii is constant due to the uniform corrosion rate thus they can be replaced with initial radii R_0 and r_0

$$\frac{dV}{dt} = -2\pi h(R_0 + r_0)v_{corr}, \tag{38}$$

$$S_i = \frac{2v_{corr}}{R_0 - r_0}N_{i,0}, \tag{39}$$

which is practically the same equation as (35). Due to the fact that the edges of the irradiation ring contain holes, the cylindrical geometry does not perfectly apply. The holes increase the corrosion area, as the irradiation ring also corrodes from the inside. If the thickness of the irradiation ring is assumed to be 1 cm, the corrosion area increases and the shape starts to resemble a twisted plate.

The estimation of the corrosion area due to holes is unnecessary complex, so assuming that the thickness is much smaller than it actually is increases the corrosion area. One factor limiting the radionuclides releases from activated steel is the corrosion time i.e. when the component corrodes completely. An equation for the corrosion time can be derived by considering when the volume of the component goes to zero. The volume of the activated steel components as a function of time is

governed by the following equation

$$V = V_0 + \frac{dV}{dt}t, \tag{40}$$

where V_0 is the initial volume of the component and dV/dt is the change in volume. The corrosion time can be calculated by setting the equation equal to zero and solving for t.

$$t_{corr} = -\frac{V_0}{\frac{dV}{dt}}. \tag{41}$$

The expression dV/dt depends on the geometry of the component. However, the corrosion rate is not constant over the time of assessment and is dependent on the chemical conditions of the waste hall. Inside the concrete boxes the chemical conditions are alkaline, until the concrete box dissolves completely (or how long the alkaline conditions last) which happens in 9620 years in MWH2 (see table 18). The corrosion rate for stainless steel in MWH2 is

$$v_{corr} = \begin{cases} -0.005\ mm/a, t \leq 9620\ a \\ -0.01\ mm/a, t > 9620\ a \end{cases} \tag{42}$$

Equation (40) can be easily be used, if one already knows that the component will corrode faster than the concrete box. However, the complete equation for the corrosion can written by combining the equations given in this subsection, which gives the following expression

$$V = \begin{cases} V_0 + \frac{\mathrm{dV}}{\mathrm{dt}}t,\ t \leq 9620\ a \\ V_0 - V_{9620} + \frac{\mathrm{dV}}{\mathrm{dt}}(t - 9620\ a),\ t > 9620\ a \end{cases} \tag{43}$$

where V_{9620} is the volume of gas generated in 9620 years. The equation applies for all steel components inside concrete packages disposed in MWH2. A similar equation can be written for the activated metal components in DWH1, but 48720 a is used instead of 9620 a. DWH1 has a concrete basin over the waste packages which extends the duration of the alkaline conditions. The corrosion end times for the components are listed in table 21.

The corrosion end times for FiR 1 components and OK3 samples are the same because it is only dependent on the thickness of the plate used in the approximation. If two plates are made of the same material, have the same thickness but different

Table 21. Corrosion end times for metal waste contained in FiR 1 and OK3 decommissioning wastes.

Waste	Corrosion end time MWH2 (a)	Corrosion end time DWH1 (a)
Irradiation ring	14139	51284
FiR 1 components	9640	10000
OK3 samples	9640	10000
Aluminium waste	1	1

area, the corrosion end time will be same. When the thickness of the plate is small compared to the area it can be assumed that there is no corrosion on the edges of the plate, only from above and below. This makes the area of the plate insignificant because all of the area is available for the corrosion immediately. The area of the plate is significant when considering the gas generation rate. The corrosion end time for the aluminium is simply one year because the thickness of the plate is 1 mm and the aluminium corrosion rate is 1 mm/a.

4.5.3 Releases from graphite

Naturally occurring graphite from Precambrian era have been observed, which is a geologic time that ended 600 million years ago. [48] This indicates that the long-term durability of graphite is very high. The long-term stability of graphite was discussed in [3], and it was concluded that could be stable at least 100 000 years after the closure of the repository. The FiR 1 graphite waste contains long-lived radionuclides C-14 and Cl-36, of which C-14 originates from nitrogen contained in the pores of the graphite and Cl-36 from chlorine gas used in the manufacturing process. The chlorine gas was used to enhance the properties of the graphite as a neutron reflector. According to an experimental model discussed in [49], the C-14 in the graphite can be divided into three parts (see figure 18) under cementitious (alkaline) disposal conditions. The values of the fractions depend on the origin of the graphite.

Under alkaline conditions C-14 can be released either in organic form or inorganic form or as a gas phase. The precipitation and sorption slows down the movement of inorganic C-14, but the organic and gaseous C-14 move through the repository without any significant resistance. [3]

According to [50] about 1 % of the C-14 releases as the gas phase. In [51] the release rates for inorganic and organic C-14 are 65 % and 35 % respectively and the release to gas phase is less than 0.1 %. It can be concluded that the release to the

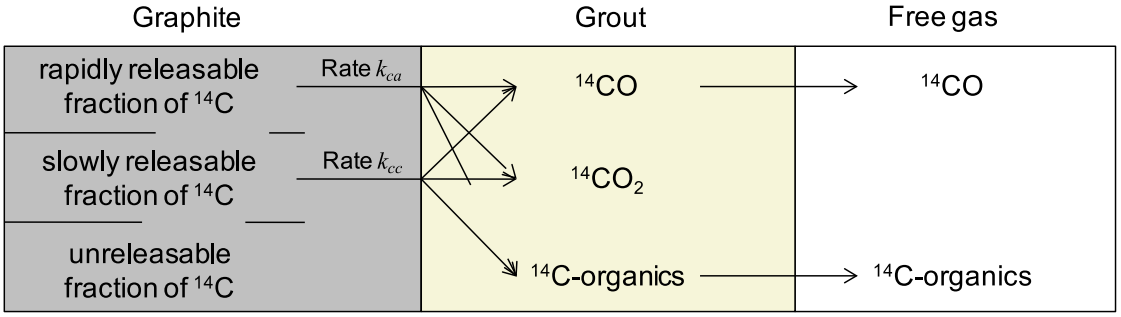

Figure 18. The release of C-14 from graphite in alkaline conditions. The figure is taken from [49].

gas phase is insignificant. The release of C-14 from TRIGA irradiated graphite was studied in Romania with leaching tests. [52]

The ratios of organic and inorganic C-14 under alkaline and anaerobic conditions were found to be 65 % and 35 % respectively [52], which is the same result as in [51]. However, the portion of gaseous release is not explicitly stated in [52]. Since the ratios of the organic and inorganic C-14 are rounded to one digit, it implies that the release to the gas phase is insignificant. However, the preceding information is highly dependent on the type of graphite and the disposal conditions. Thus, the report [52] can be considered to be the best source because the graphite originates from a similar reactor to FiR 1.

The timescales of the experiments are much shorter than the actual time scale considered in the disposal, thus the experimental model does not apply perfectly. However, it gives a decent approximation about the release of the rapidly releasable C-14, but not for slowly releasable fraction.

The release rate and the fractions in are based on results from multiple experiments and have not been scaled based on external geometric surface area due to uncertainties of the C-14 distribution in the samples and its release mechanism. The release rate of the slowly releasable C-14 is assumed not to depend on the chemical conditions (alkalic or neutral) of the waste halls. The suggested values for the release rates and fractions are presented in table 22.

Due to the short time scale of the rapidly releasable C-14 from graphite, an immediate release upon contact with water is assumed. The slowly releasable C-14 is assumed to be released linearly with the rate of 0.01 1/a. The probabilistic analysis carried out with Ecolego requires that the parameters are assumed to obey some kind statistical distribution. The lower and upper boundary values of the release rate

Table 22. The fractions of C-14 and release rate of graphite waste. The values are taken from [50].

Parameter	Lower bound	Reference value	Upper bound
Fraction of slowly releasable C-14	0.01	0.05	0.3
Fraction of rapidly releasable C-14	0	0.0002	0.002
Release rate of slowly releasable fraction	0.001 1/a	0.01 1/a	0.1 1/a
Fraction of organic C-14	-	0.65	-
Fraction of inorganic C-14	-	0.35	-

and fractions are assumed to correspond to the 5th and 95th percentiles in lognormal distribution.

The activity of Cl-36 can exist in two forms in irradiated graphite, which are called labile and less-labile form. The less-labile fraction of Cl-36 is bonded to carbon atoms with a covalent bond which makes it less mobile than earlier has been assumed. [53] Radionuclide releases from irradiated graphite repository conditions has been researched in [54] with similar results. The release rate of labile fraction is governed by diffusion and the porosity of the graphite. Non-labile fraction of Cl-36 releases much more slowly.

High reactor operating temperature causes Cl-36 from the graphite to be released in the reactor which reduces the amount of Cl-36 in the graphite and its release rate. The labile fraction of Cl-36 can be even up to 90 % of the initial activity inventory. Due to the high fraction and the low operating temperature of the FiR 1 reactor, it is assumed that all of the Cl-36 is in the labile form. The release of chlorine from the FiR 1 graphite has been studied in [3], and according to results almost all Cl-36 diffuse from the graphite during the first 30 years. In this document the Cl-36 is assumed to be released immediately upon contact with water, because 30 years is a short compared to the time scale used in the model.

4.5.4 Releases from aluminium, concrete, Fluental and other materials

The modelling process of certain materials like aluminium, concrete and Fluental is simplified. Aluminium is a reactive material that generates gas during corrosion. Most of the aluminium is disposed in waste drums which are not considered an engineered barrier that slows down the release of radionuclides. The corrosion rate of aluminium is assumed to be 1000 µm/a in alkaline conditions which is way higher than the corrosion rate of steel. Due to the high corrosion rate of aluminium and

the thin plate approximation, the aluminium components will corrode completely in one year, so separate corrosion modelling is not needed. It is conservatively assumed that all the activity of aluminium is released upon contact with water.

The activity from activated concrete is assumed to be released immediately, even though the activity is expected to be released gradually. This assumption is conservative but also practical because the release process of the concrete waste is unknown. Because the Fluental moderator was specifically made for VTT, there is no data how it reacts under disposal conditions.

The most important radionuclides in Fluental are H-3 and C-14. Materials similar to Fluental are actually used for long-term storage of tritium [55], [56], which concludes that its release rate from Fluental is low. Due to the unknown behaviour of Fluental, an immediate release of radionuclides is assumed, even though this may not apply to tritium. However, the activity of H-3 in Fluental is not too high and due to its low half-life, it is not a significant radionuclide from the perspective of the long-term safety. The other materials mentioned in table **??** contain a variety of different materials, which are assumed to release their activity immediately upon contact with water.

4.6 Radionuclide transport in near-field

The modelling of the wastes is similar as described in [15]. The transport of radionuclides released from the waste are governed by: advection, aqueous solubility and speciation, degradation, diffusion, metal corrosion, sorption and desorption and radioactive decay. The processes are explained in-depth in [15].

The inputs needed in the near-field modelling are presented in figure 19. The most important inputs are the evolution of the concrete barriers, waste packages and groundwater flow. The release to the bedrock is the main output of the model.

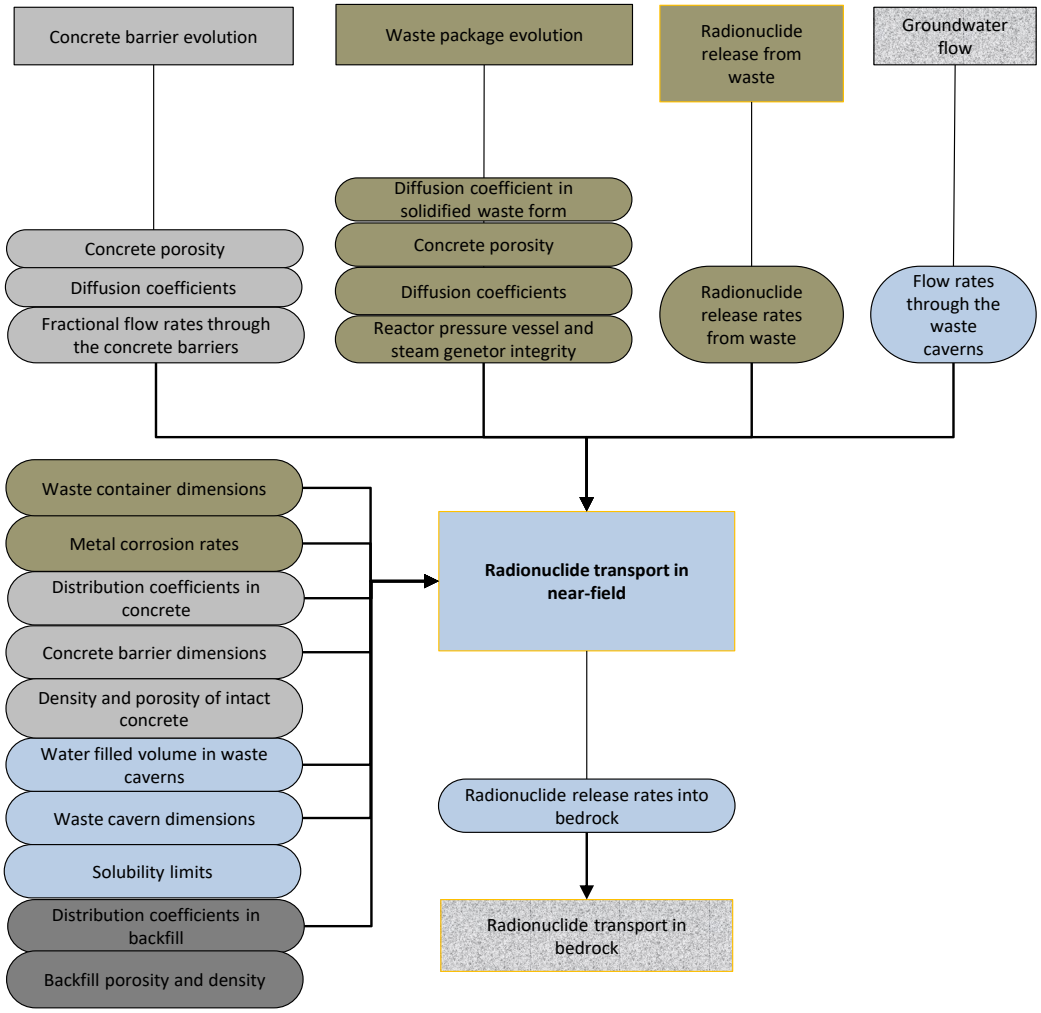

Figure 19. The flow chart for the radionuclide transport in the near-field. The figure is taken from [15].

4.6.1 Modelling of the concrete packages

Most of the decommissioning wastes are placed inside concrete container. The equation governing the diffusion from the inside to the wall of the box can be derived from equation (32) by dividing the equation with a new dimensionless variable 1-α, where α (m^3/m^3) is the filling factor i.e. the fraction how much space is inside the compartment is occupied. The equation is

$$\frac{dN}{dt} = -\frac{2DA}{d}\ \frac{N}{(1-\alpha)V}. \tag{44}$$

The value of α used in the modelling is 0.57, which is defined with the concrete waste of FiR 1 while taking into account the package weight limit. The filling factor is calculated with the concrete waste due to the fact, that such waste packages cannot be filled completely. Partially empty waste packages leave room for free water, which increases the diffusion rate. The same filling factor is assumed for all the concrete packages, which makes it a conservative choice. The equation is multiplied with two due to the fact, that the diffusion length one half of the package wall thickness.

Diffusion does not only occur from inside out, but also in the opposite way. The diffusion from the wall of the packages to the waste inside can also be derived from equation (32), which has the following expression

$$\frac{dN}{dt} = -\frac{2DA}{d}\ \frac{N}{\varepsilon R_w V}, \tag{45}$$

where ε is the porosity factor. The waste drums and metal boxes will not be modelled at all, as they are not thick enough to be considered as an engineered barrier. The activity from the waste drums is assumed to be released immediately upon contact with water. The steel boxes are also too thin to considerably retard the release of radionuclides even when packaged inside the concrete boxes. According to the appendix 1 in [28] the steel boxes contain holes which accelerates the release of radionuclides. In the model it is assumed that there are no steel boxes.

4.6.2 Modelling of the special concrete container

The special concrete container is cylindrical and contains five tubes in the middle, designed to hold filters. The total volume of the five tubes is V_{tubes} =0.158 m^3. Normally the concrete containers does not have tubes in them, but are filled with concrete and liquid waste such that the total volume is V_{spcpkg} =1 m^3.

The special concrete container for OK3 metal samples is modelled similarly to the concrete packages, but the fact that the container contains the tubes and is filled with concrete must be taken into account. The diffusion from the inside of the special concrete container can be derived from equation (44)

$$\frac{dN}{dt} = -\frac{2DA}{d}\,\frac{N}{\varepsilon R_w V(1-\alpha) + V_{tubes}(1-\alpha')}, \tag{46}$$

where the value of $\alpha = V_{tubes}/V_{spc.package}$= 0.158 is the ratio how much space the tubes occupy in the total volume of the special concrete container, and the $\alpha' = V_{samples}/V_{tubes}$= 0.35 is the ratio how much space the metal samples occupy in the tubes. The total volume of the samples is $V_{samples}$ = 0.055 m^3.

The first term in the denominator of the concentration takes into account the volume of water in the concrete structure of the package minus the volume that the tubes occupy, and that the structure retards the release of radionuclides. The second term is added, as there is also assumed to be water inside the tubes, excluding the volume which the metal samples occupy. Equation (45) also describes the diffusion into the container in this case and does not require any modification. The special concrete container is assumed to degrade at the same rate as the concrete packages.

4.6.3 Maintenance waste hall 2 (MWH2)

The maintenance waste hall is assumed to be immediately filled with water shortly after the closure of the repository, which causes most of the activity in the waste drums to be released into the water almost immediately. The rest of the waste will be packed in concrete boxes which will delay the release of radionuclides significantly until they fail completely. Some wastes in the packages are assumed release their activity immediately upon the contact with water e.g. aluminium, activated concrete and Fluental. Metal components in the concrete boxes release their activity via corrosion, which starts immediately after the closure. The compartment structure and the radionuclide transport processes are shown in figure 20. The model assumes

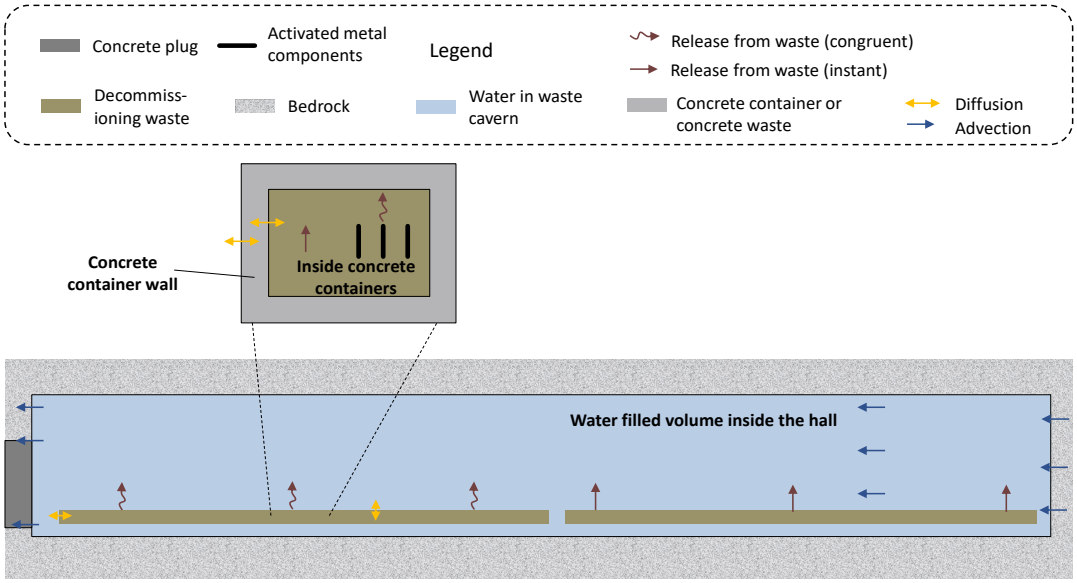

Figure 20. An illustration of the compartment in maintenance waste hall 2 and processes transporting the activity from the waste hall. The figure is edited from [36].

that the waste hall does not contain any operational waste from Loviisa NPP.

The lack of engineered barriers in the hall allows the radionuclides to flow freely without resistance due to the groundwater flow in the hall. The equation describing the movement of the radionuclides out of MWH2 is simply

$$\frac{dN_i}{dt} = -\frac{N_i}{V_i} Q_i, \tag{47}$$

where (N_i is the unbound activity in the hall, V_i is the water filled volume of the hall and Q_i is the groundwater flow through the hall.

4.6.4 Decommissioning waste hall 1 (DWH1)

The decommissioning waste hall is designed to hold part of the decommissioning wastes of Loviisa NPP. The most important difference between DWH1 and MWH2 is that DWH1 contains a concrete basin enclosing the waste packages. The compartment structure and the radionuclide transport processes are shown in figure 21.

The released activity from the waste will first diffuse into the concrete basin and then to the crushed rock filling. From this point onwards the activity will be transported by diffusion and advection into the basin wall and to the crushed rock

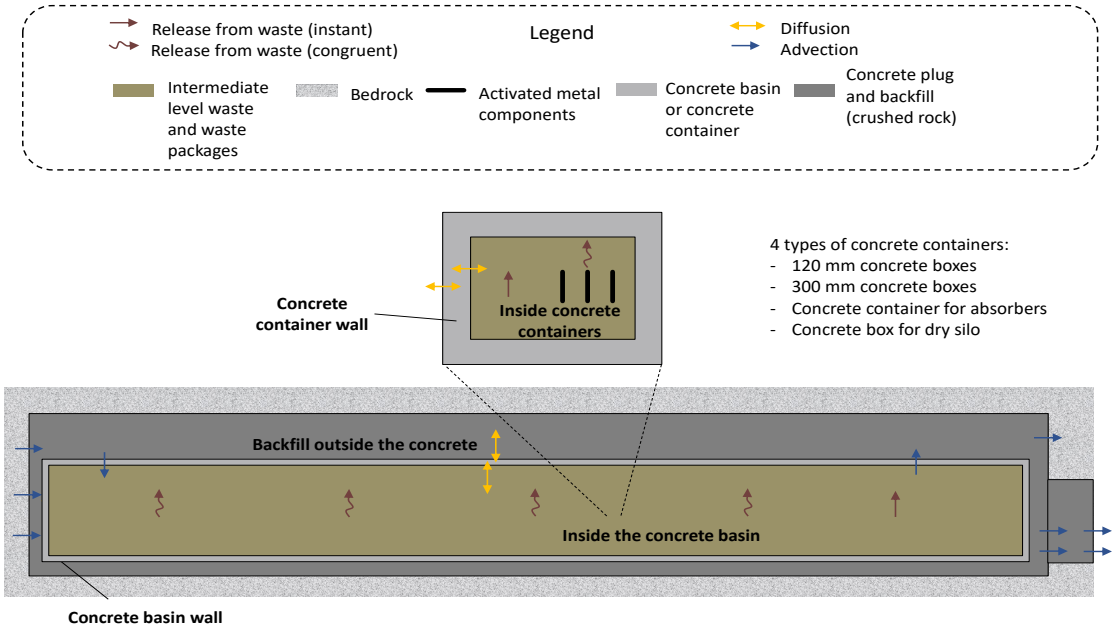

Figure 21. An illustration of the compartment in decommissioning waste hall 1 and processes transporting the activity from the waste hall. The figure is edited from [36].

surrounding the basin. The groundwater flow will transfer the activity from the crushed rock surrounding the basin to the bedrock.

The diffusion from a concrete container into the container wall is governed by equations (44) and (45) governs the diffusion from the container wall back into the concrete container and into the crushed rock filling inside the concrete basin. The equation for diffusion from the crushed rock filling back into the concrete container can derived by combining equations (21) and (32),

$$\frac{dN_i}{dt} = -\frac{2DA}{d(V_{water,i} + Kd_i m_i)} N_i, \tag{48}$$

where $V_{water,i}$ is the total volume of water in the basin, Kd_i is the distribution coefficient of concrete and m_i is the total mass of the concrete waste in the basin. The equation governing the flow of radionuclides through DWH1 is similar to equation (47)

$$\frac{dN_i}{dt} = -\frac{N_i}{\varepsilon_i R_{s,i} V_i} Q_i. \tag{49}$$

4.7 Radionuclide transport in bedrock

The transportation of radionuclides through the bedrock is possible due to the fractures in the bedrock. The process is retarded by matrix diffusion and sorption in the rock matrix. The most important processes, events and features in the modelling are: dispersion, groundwater flow, matrix diffusion, sorption and desorption and radioactive decay, which are explained in-depth in the Analysis of releases and doses -report [15]. Figure 22 contains a flow chart which describes the inputs for the modelling radionuclide transport in bedrock and its relation to other models. The main idea of the modelling is to estimate the flow times through the bedrock due to the groundwater flow.

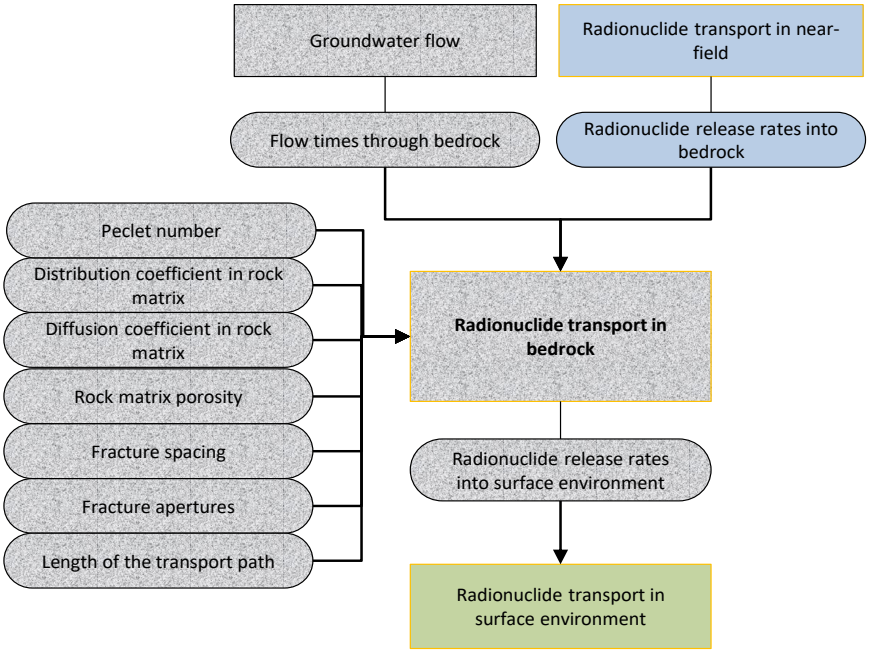

Figure 22. The modelling chain for the radionuclide transport in bedrock. The common legend of the figure is presented in Figure 9. The figure is taken from [15].

The retention mainly takes place before the solute reaches fracture zone R1, which is located above the repository (see figure 23). The model considers only transport between waste cavern and the fracture zone R1, and no retention in the connection tunnel have been considered. The transport path from the waste cavern to the fracture zone R1 is assumed to be identical for all waste caverns, in order to reduce computational cost. [15] The used matrix diffusion model is based on

two-dimensional model made by SKB [57]. The fracture is divided into homogenous compartments of equal size, and the rock matrix is divided into compartments which extends perpendicularly from the fracture into the rock. [15]

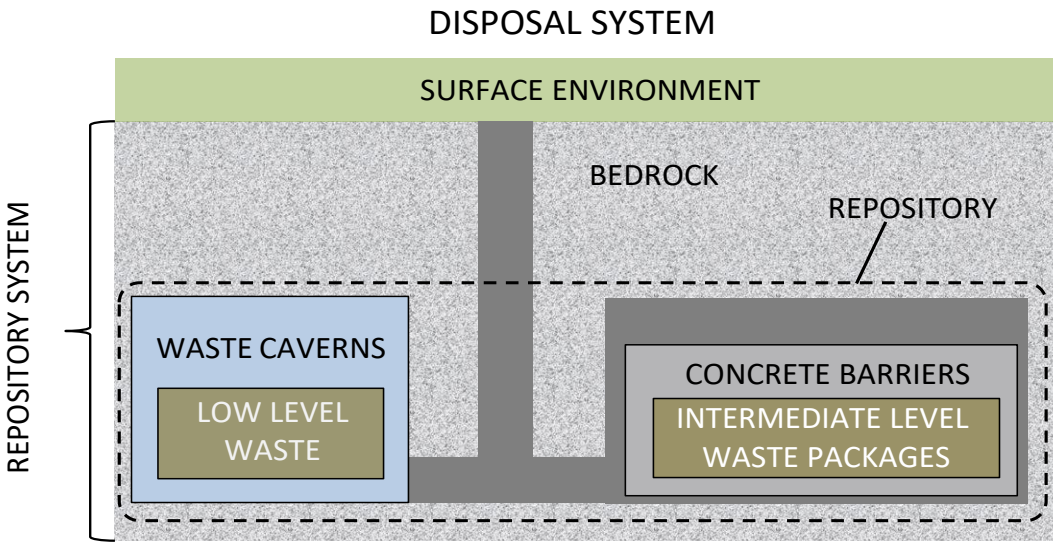

Figure 23. Schematic illustration of the radionuclide transport in the bedrock. The common legend of the figure is presented in Figure 9. The figure is taken from [15].

4.8 Radionuclide transport in surface environment

The model created for the safety case is based on a similar concept used by Posiva in [58]. Using compartment modelling for biosphere transport models is practical since the biosphere is generally easy to divide into smaller objects, and further into compartments. The area chosen for the modelling is the western side of the current Hästholmen island, which is the expected location of the release of activity. The model is limited by landforms and narrow distances over open water on the western and eastern side of the island. The modelling of the southern extent of the island is assumed to be sufficient to cover a lake that forms in the Hudöfjärden bay and possible integration from the lake. The biosphere model is covered in-depth in the Analysis of release and doses -report [15].

The modelling area is divided into 14 biosphere objects (the numbers is figure 24). In addition to the biosphere objects, there are three separate river objects. The biosphere objects can be considered as areas relevant for the radionuclide

transport in the surface environment and dose calculations. They were chosen with an assumption that they are homogenous enough for modelling purposes considering their development history. The biosphere objects change over time as a result of land uplift, sea level change, land use etc. Each biosphere object may contain several ecosystems e.g. lake, sea, cropland etc. [15]

Radionuclides are transported to biosphere from bedrock. Event and processes considered in the analysis are: advection, bioturbation, diffusion, drainage, microbiological activity, radioactive decay, sedimentation and resuspension, senescence and water exchange. The most important processes governing the radionuclide transportation between different compartments are schematically shown in figure 25.

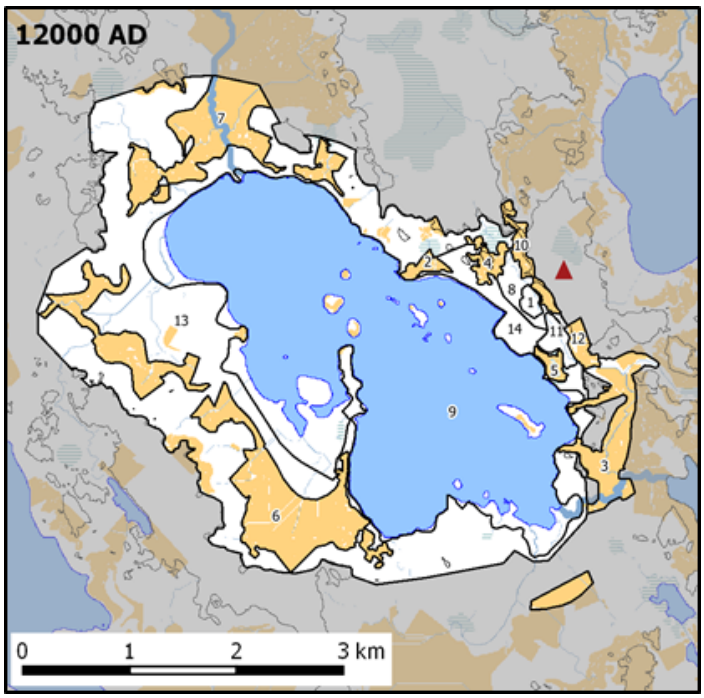

Figure 24. The modelling area with the 14 biosphere objects (numbers). The common legend of the figure is presented in *Figure 12.*. The figure is taken from [15].

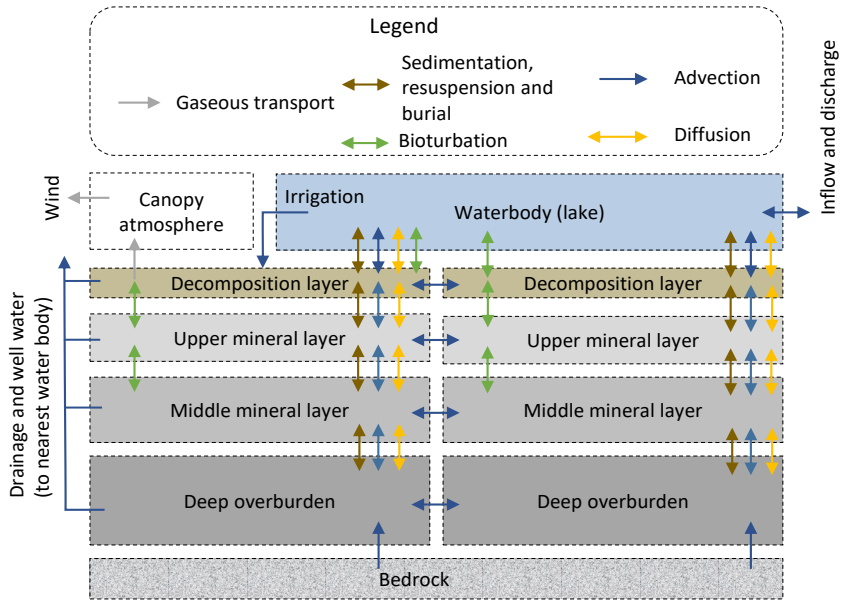

Figure 25. The methods of radionuclide transport between compartments in biosphere. The figure is taken from [15].

4.9 Dose assessment

The dose assessment studies the doses for members of the most exposed group, for larger groups of people and for other biota. However, in this document the dose calculation is only done for the members of the most exposed group due to the fact that the dose rate for larger groups of people and for other biota was insignificant in 2018 safety case [11]. The most exposed group consists of about 10 people who spend all of their time at the contaminated area around the repository which causes inhalation and external radiation dose. The group also utilizes contaminated sources of food and water. The food consumed by the most exposed group consists of meat, milk, vegetables, fruits, berries, roots vegetables, mushrooms and cereals. [15]

According to [59], the four main ways for humans to receive dose are ingestion of food and water, inhalation and external exposure. The total dose rate from a single radionuclide D_{Total} (Sv/a) is a sum of these pathways

$$D_{Total} = D_{ing,water} + D_{ing,food} + D_{inh} + D_{ext}, \tag{50}$$

where $D_{ing,water}$ (Sv/a) is the dose rate from ingestion of water, $D_{ing,food}$ (Sv/a) is the dose rate from ingestion of food, D_{inh} (Sv/a) is the dose rate from inhalation and D_{ext} (Sv/a) is the dose rate from external radiation. Some of the radionuclides

such as organic C-14 and H-3 are released as gaseous form, but dose caused by such releases are assumed to be negligible. The more detailed presentation of the exposure pathways is in figure 26. The calculation of the terms in equation (50) is explained in depth in [15] and will not be covered in this document.

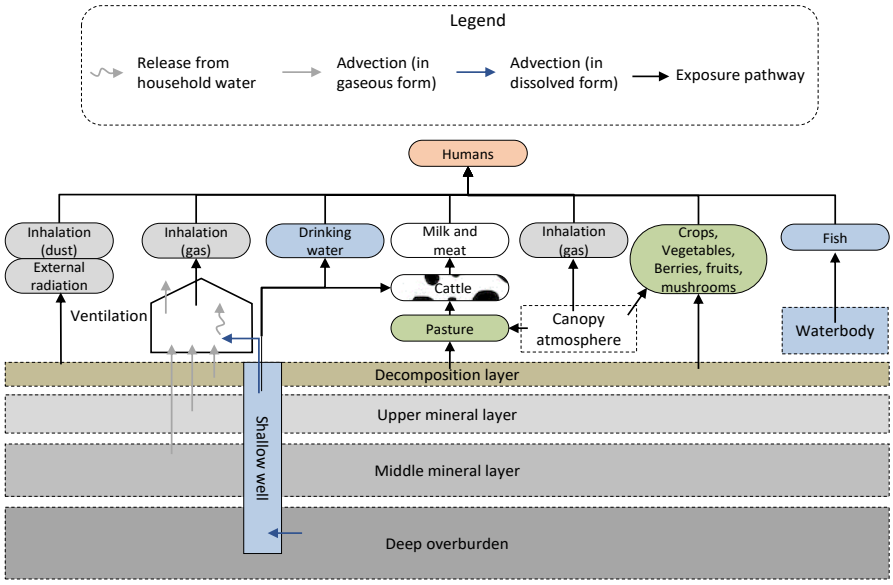

Figure 26. A conceptual figure of the exposure pathways for human and compartment in the surface environment from which the activity originates. The figure is taken from [15].

5 Modelling of scenarios and calculation cases

5.1 Scenarios

Due to the fact that the evolutions of the repository and surface environment is hard to predict, a scenario analysis is needed. Scenarios are used to study different outcomes of the future and they consider events and conditions beyond those predicted by historical data and their extrapolation with the aim of studying the alternative futures in a larger scope [14]. In STUK's YVL D.5 [10] scenario is defined as "*evolution of the disposal system*". The reference [60] gives guidance in the formation of scenarios. The chosen principles for scenario formation are: plausibility, consistency, small number, distinctness, transparency and traceability. Even more principles can be used e.g. reference [61] lists additional principles like creativity, relevance and completeness, but the scenario formation of 2018 safety case concentrates of the four principles mentioned above.

The scenarios for the Loviisa LILW repository were formulated in [14] and the document addresses the evolution of the disposal system, including the performance of the engineered barriers over the assessment period of 100,000 years. The 2018 safety case [11] uses the following definitions:

- *Scenario* describes a potential evolution of the entire disposal system during the assessment period associated with fulfilment of or deviation from performance targets.

- *Evolution* describes changing of the disposal system or parts thereof over time.

The 2018 safety case includes climate evolutions, evolutions of the surface environment or the evolutions of single barriers. The term scenario specifically describes a single evolution of the entire disposal system, i.e. a combination of the evolutions of all the parts of the disposal system, over the whole assessment period of 100,000 years. Altogether four scenarios were formulated for the present safety case, which are listed in table 23.

This report uses the same definitions and scenarios as the 2018 safety case, whenever they are applicable e.g. the variant scenario with the defective welds will not be considered, because this report assumes that the repository contains only the decommissioning wastes from VTT. The actual modelling of the scenarios is done by varying parameters in the Ecolego model, which stem from alternative conceptual models.

Table 23. Scenario descriptions for the Loviisa LILW repository safety case 2018. The table is edited from [14].

Scenario description (scenario name is underlined)
Base scenario assumes all performance targets to be met. The concrete plugs effectively limit the groundwater flow for tens of thousands of years. Concrete barriers and concrete containers effectively limit the radionuclide transport and maintain alkaline conditions over 10,000 years. Reactor pressure vessels and steam generators typically remain intact for tens of thousands of years.
Variant scenario declined concrete performance assumes that the concrete plugs do not limit the groundwater flow. This increases groundwater flow through the waste caverns and together with concrete quality deviations and reinforcement bar corrosion forming penetrating fractures reduces their ability to limit radionuclide transport. The early loss of alkaline conditions together with microbiological corrosion may result in early failure of the reactor pressure vessels before 10,000 years and steam generators after hundreds of years.
Disturbance scenario large earthquake considers possibility of a large earthquake mechanically damaging the concrete plugs, basins and containers. This leads to an increased groundwater flow and increased radionuclide transport through the concrete barriers and concrete containers. Such earthquakes are likely to be connected to ice sheet retreat phases, but can occur also during the temperate periods, with the rate of $1 \cdot 10^{-6}$ 1/a. However, this requires concrete reinforcement bars to become substantially corroded, which is considered to take at least 6000 years.

5.2 Accelerated concrete degradation

The accelerated concrete degradation scenario considers the impact of reinforcement bar corrosion. The corrosion of the reinforcement bars causes penetrating fractures through concrete, concrete quality deviations and an increase in the groundwater flow due to declined performance of the concrete plugs. The results lead to declined concrete performance during the early stages and accelerate concrete degradation during later phases. The accelerated degradation of concrete affects the leaching depths, hydraulic conductivities, fractional flows through concrete and the effective diffusion coefficients. [14] The evolution of the effective diffusion coefficients of the basin of DWH1 and the 120 mm concrete container are presented in figure 27 and

figure 28 respectively.

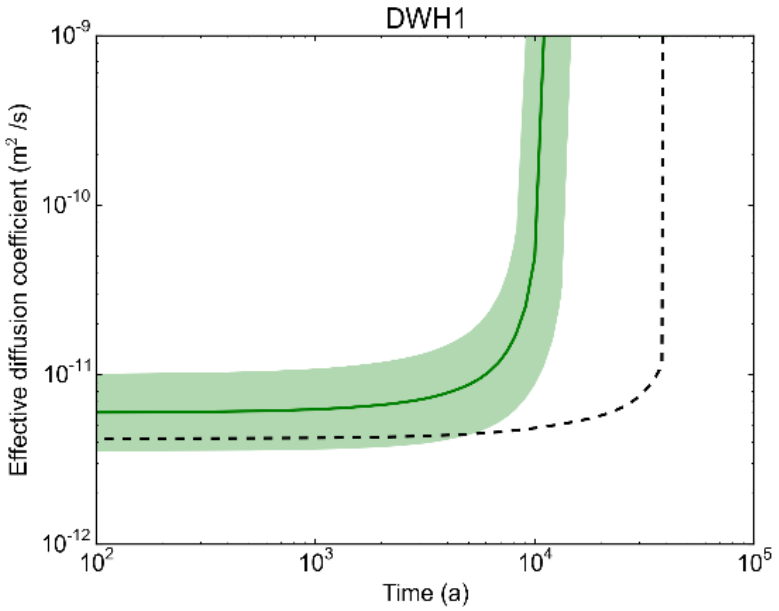

Figure 27. The effective diffusion coefficient in the concrete basin in DWH1 in the accelerated concrete degradation scenario. The green shaded area shows the estimated uncertainty bounds and the solid line is the reference value. The dashed line is the reference value in the reference evolution [14]. The figure is taken from [15].

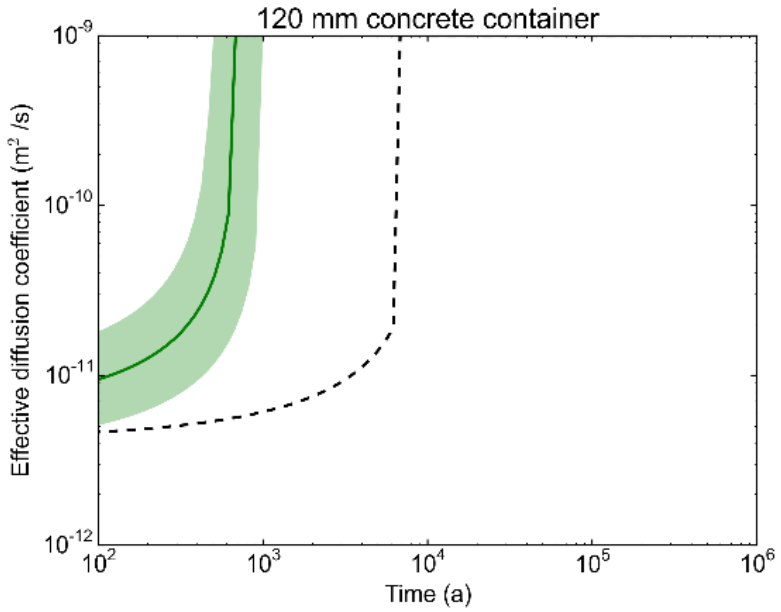

Figure 28. Diffusion coefficient in the concrete containers in the accelerated concrete degradation evolution. The green shaded area shows the estimated uncertainty and the solid line is the reference value. The dashed line is the reference value in the reference evolution [14] The figure is taken from [15].

5.3 Large earthquake

Sensible earthquakes occur very rarely in Finland but weaker ones are measured every year. An earthquake power enough to damage the concrete structures could occurs once in every million years. Thus the probability that such earthquake occurs during the assessment period is 10 %.

The earthquake is assumed to occur 4500 years after closure. This is also the moment in time when the dose rate of Loviisa NPP's waste reach their maximum value. The concrete packages, concrete basin in DWH1 and closure plugs are assumed to be broken completely after the earthquake, which may change the chemical conditions of the waste, depending on the waste cavern. [15]

5.4 Calculation cases

Calculation cases are used to determine the impact of alternative conceptualisations or parameter values on the results. Alternative conceptualisations consider factors having impact on the radiological consequences that is not covered by the model in the reference case. The reference case refers to a deterministic calculation, which utilizes the reference conceptual model and reference parameters values. The alternative parameter values are those indicated to be the most influential in the sensitivity analysis. The aim of these calculations is to demonstrate the impact of most sensitive parameters on the modelling endpoints. [15] The present safety case lists several calculation cases but not all of them are covered in this work. The list of the covered calculation cases are in table 24. The list is based on the factors which have identified to have a potential impact on the release rates or doses. The calculation cases are only applied for the base scenario.

Table 24. A list of calculation cases considered in the base scenario.

Calculation case based on alternative conceptual model	**Calculation cases based on alternative parameter values**
Drilled well	High corrosion rates
Small volumes of maintenance waste walls	Alternate climate evolutions

5.4.1 Drilled well

This calculation case considers the locations of two drilled wells, which are considered to be a rare event (see [10]). Rare events have a low chance of happening, but may significantly reduce the performance of the concrete barriers. A drilled well may have an impact on the dose assessment, as the drilling may damage the waste packages or the concrete basin. Due to the depth of drilled wells, they become a considerable dose path. The different groundwater flow rate has an effect in the performance of the concrete waste packages and the concrete basin of DWH1 but the effect is almost negligible. [14] As an example, the effective diffusion coefficient of the concrete basin in DWH1 is presented in figure 29. The drilled wells are modelled using stylized biosphere model without considering the doses from water bodies. The stylized biosphere is almost identical to the reference case, except the area of the irrigation is smaller.

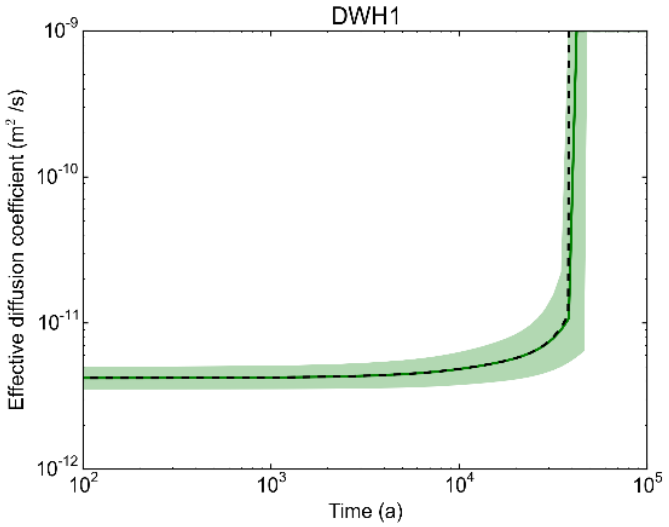

Figure 29. Evolution of effective diffusion coefficient (m^2/s) through the concrete basin in DWH1. The green shaded area shows the estimated uncertainty and the solid green line is the reference value in the groundwater flow evolution drilled wells. The dashed line the reference value in the reference evolution without drilled wells. The figure is taken from [14].

The drilling of the well is assumed to occur at earliest 200 years after the closure of the repository, which is also referred as an administrational control period [10]. The occurrence of a rare event is completely random, which means that it follows the Poisson distribution. The expected value of the dose caused by the drilled wells occurring within 200 years after the closure of the repository is

$$E(t) = \chi(t)(1 - e^{-\lambda(t-200)})\theta(t - 200), \tag{51}$$

where $\chi(t)$ is the dose rate at time t(a), λ(1/a) is the average chance of the event occurring and θ(t) is the Heaviside step function. [15]

5.4.2 High release rates

In this case the corrosion rates are ten times higher than the values given in sections 3.4.4.1 and 3.4.4.2. The new corrosion rates, corrosion end times, gas generation rates and total gas yields are listed in tables 25, 26 and 27. Even if the corrosion rates are increased, the gas generation rates are still insignificant compared to the earlier results of section 3.4.4.3. This calculation case also assumes that the reference parameters of graphite in table 22 are replaced with their upper bounds (table 28),

and that all of the C-14 is released in organic form.

Table 25. The values of the corrosion rates in the high corrosion rates calculation case.

Material	**Release rate in (µm/a) alkaline conditions**	**Release rate in (µm/a) neutral conditions**
Stainless steel	0.5	10
Aluminium	10000	10000

Table 26. Summary of the gas generation rates and the total gas yields with ten times higher corrosion rates in MWH2. The highest overall value indicates the highest gas generation rate of all the components excluding aluminium.

Waste	**Gas generation rate**	**Total gas yield**
Irradiation ring	$\begin{cases} 4.68 \cdot 10^{-5}\ m^3\mathrm{a}^{-1},\ t \leq 9620\ a \\ 9.37 \cdot 10^{-4}\ \mathrm{m}^3\mathrm{a}^{-1}, 9620 \leq\ t \leq 9639\ a \end{cases}$	0.47 m^3
FiR 1 components	$8.29 \cdot 10^{-3}\ m^3\mathrm{a}^{-1},\ t \leq 1001\ a$	8.31 m^3
Aluminium waste	$3167.98\ m^3\mathrm{a}^{-1},\ t = 1\ a$	3167.98 m^3
OK3 components	$0.12 m^3\mathrm{a}^{-1},\ t \leq 1001\ a$	116.21 m^3
Total	**Highest value 1st year:** 3167.98 m^3 **Highest value overall:** 0.12 m^3	3292.97 m^3

Table 27. Summary of the gas generation rates and the total gas yields with ten times higher corrosion rates in DWH1. The highest overall value indicates the highest gas generation rate of all the components excluding aluminium.

Waste	**Gas generation rate**	**Total gas yield**
Irradiation ring	$4.68 \cdot 10^{-5}\ m^3\mathrm{a}^{-1},\ t \leq 10000\ a$	0.47 m^3
FiR 1 components	$8.29 \cdot 10^{-3}\ m^3\mathrm{a}^{-1},\ t \leq 1001\ a$	8.29 m^3
Aluminium waste	$3167.98\ m^3\mathrm{a}^{-1},\ t = 1$	3167.98 m^3
OK3 components	$1.16 \cdot 10^{-1}\ m^3\mathrm{a}^{-1},\ t \leq 1001\ a$	115.63 m^3
Total	**Highest value 1st year**: 3167.98 $\mathrm{m}^3 a^{-1}$ **Highest value overall**: $1.16 \cdot 10^{-1}$ $\mathrm{m}^3 a^{-1}$	3292.37 m^3

Table 28. The parameters of graphite of high release rate calculation case.

Parameter	Value
Fraction of slowly releasable C-14	0.3
Fraction of rapidly releasable C-14	0.002
Release rate of slowly releasable fraction	0.1 1/a
Fraction of organic C-14	1
Fraction of inorganic C-14	0

5.4.3 Smaller volume of MWH2

This calculation case is used to investigate the effect of an inhomogeneous spatial activity distribution in MWH2. The volume of the waste hall is concentrated in a small volume, which leads to higher release rate of activity. The volume of MWH2 is reduced to one tenth of its original value.

5.4.4 Alternate climate evolutions

Posiva has done climate modelling based on four RCPs (Representative Concentration Pathways) which were originally formed in [30]. These different pathways present the possible future climate evolutions where the concentration of greenhouse gases in the atmosphere is different. In-depth explanation of the RCPs can be found in [14] The RCPs used in the 2018 safety case and in this report are presented in figure 9. The main difference between the RPCs is the number of glacial and permafrost periods. RCP4.5 climate evolution is used in the reference case.

6 Modelling results

6.1 Results from the base scenario

This section contains the modelling results of the reference case of the base scenario. The results include release rates, normalized release rates and dose rates, which are presented with graphs as a function of time. STUK's guide YVL D.5 [10] requires that at least the normalized release rates and dose rates must be presented in the safety cases reports, but the release rates in this report are presented as an additional information. The annual dose is a sum which consists of the effective dose caused by external radiation and the committed effective dose due to intake of radioactive substances [10]. The release rate graphs describe, much activity is released into the surface environment during the assessment period of 100,000 years. The normalized release rate is similar to the activity release rate, but its normalized with respect to the corresponding radionuclide constraints, and are only calculated during constraint assessment period (10,000-100,000 years). The dose rates are calculated only during the dose assessment period (0-10,000 years). The term dose rate, annual dose rate or any variant of the term generally refers to the same quantity (the total dose received in one year). The figures contain different colours, which indicate climate conditions (permafrost and glacial period) or whether the discharge locations are under water (submerged). A probabilistic analysis is used to analyse the uncertainty of the main results. Ecolego's probabilistic analysis is similar to a Monte Carlo simulation, and the number of iterations used in the analysis was 1000. The analysis is only done for the dose rates and normalized release rates of the base scenario.

6.1.1 Release rates

In MWH2 the release rates into the biosphere are dominated by Ni-59, H-3, organic C-14, Ca-41 and Cl-36 (figure 30). The most important radionuclides are Ni-59 and organic C-14, as their release continues congruently for tens of thousands of years. Their release rate is reduced by permafrost (colour grey in the figure) and glacial periods (colour blue in the figure) between 30,000 and 65,000 years, as the groundwater flow rate is reduced. The release rates of Ni-59 and organic C-14 reach their peak value at the end of the first glacial period, which is caused by a rapid increase and decrease in the groundwater flow rate. The release rates of H-3, Ca-41 and Cl-36 reach their maximum values 10,000 years after the closure of the repository and are extremely small after that. The submerged period (the light blue colour in the figure) does not have effect on the release rates, but indicates that the discharge locations are located under water during that period. The time in the x-axis indicates years after the closure of the repository.

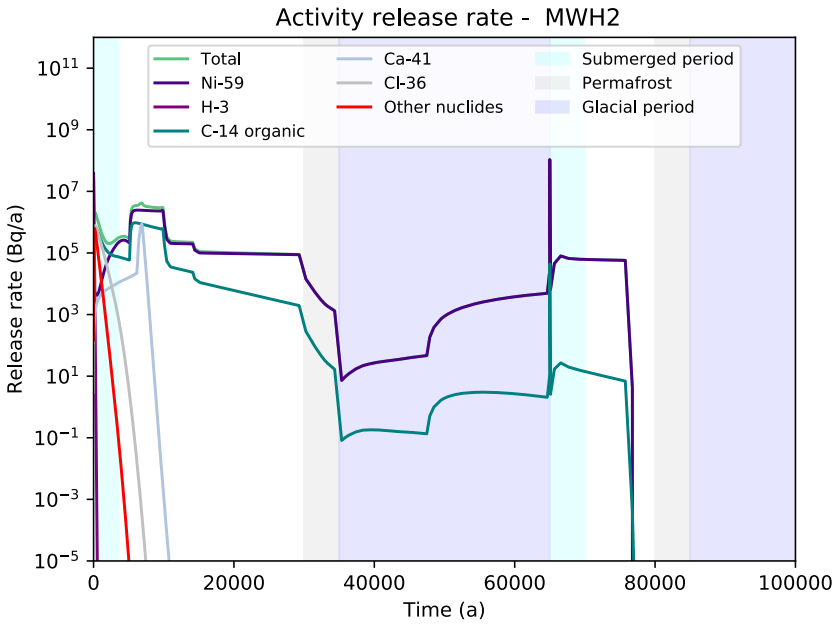

Figure 30. The activity release rate into the surface environment during the assessment period with the decommissioning wastes disposed to MWH2. The x-axis indicates years after the closure of the repository.

The waste specific release rates to surface environment are presented in figure 31. The release rate from the decommissioning waste of FiR 1 is higher in the

beginning due to the fact, that some of the waste is packaged in waste drums which are assumed to release their activity immediately. Most of the decommissioning waste of OK3 is also packaged in waste drums but their activity is quite low compared to activated metal samples. After that, all the release from OK3 decommissioning wastes originate from the activated metal samples. After approximately 7500 years the concrete container holding the activated metal samples breaks and increases the release rate. The metal samples corrode congruently, which causes approximately a constant release rate. The metal samples corrode completely at approximately 15,000 years, causing the release rate to decrease rapidly. The concrete containers holding FiR 1 decommissioning wastes break approximately at 10,000 years, increasing the release rate. It takes longer for the decommissioning wastes of FiR 1 to deplete their activity because most of it is released via corrosion. The MWH2 curve in figure 31 indicates the release rate caused by the operational waste of Loviisa NPP, which are assumed to exist in MWH2 in 2068. The curve reaches its peak value immediately after the closure and decreases quickly, as the activity from the operational waste is assumed to be released immediately upon contact with water.

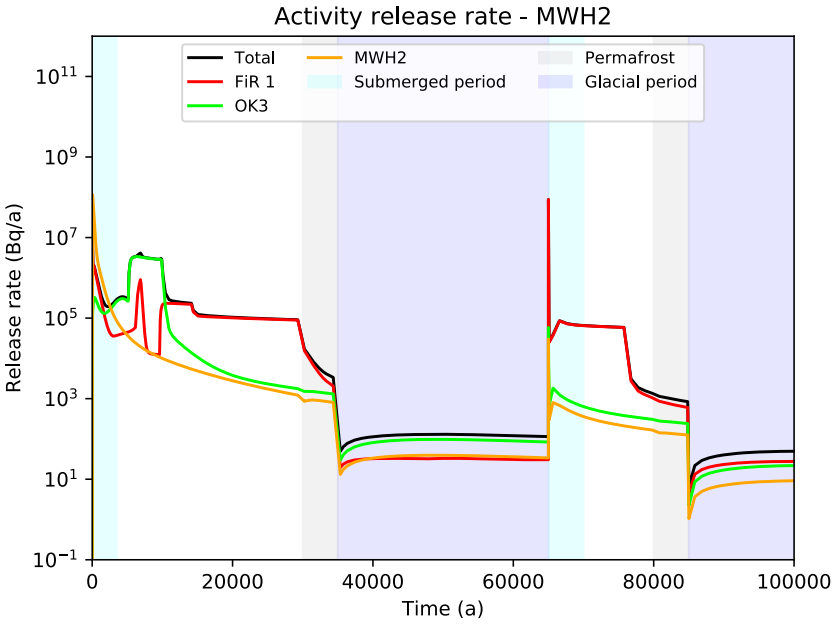

Figure 31. The activity release rate during the assessment period when the decommissioning wastes disposed to MWH2. The MWH2 curve indicates the release rate from the waste of Loviisa NPP assumed to be disposed to MWH2. The x-axis indicates years after the closure of the repository.

The highest release rate from DWH1 is caused by Ni-59, Ca-41 and Cl-36 (figure 32). The release rate of Cl-36 is at its highest during the first 8000 years. The release rate of Ni-59 increases after the closure, and the release of organic C-14 decreases steadily. The release rate of Ca-41 is almost constant during the first 30,000 years. The release rates of all radionuclides decrease during the permafrost and glacial periods. During the glacial period the release rates of Ni-59, organic C-14 and Ca-41 increase due to the change in the chemical conditions in DWH1. The concrete basin breaks down, which changes the chemical conditions from alkaline to neutral, increasing the corrosion rate and the solubilities of Ni and Ca, and changing the Kd-values in the waste hall. After the glacial period ends approximately at 65,000 years, the increasing groundwater flow in the repository causes a sudden increase in the release rates. The contribution of the other nuclides (red curve) to the release rate is minimal. Figure 33 presents the waste specific activity release rates to the surface environment.

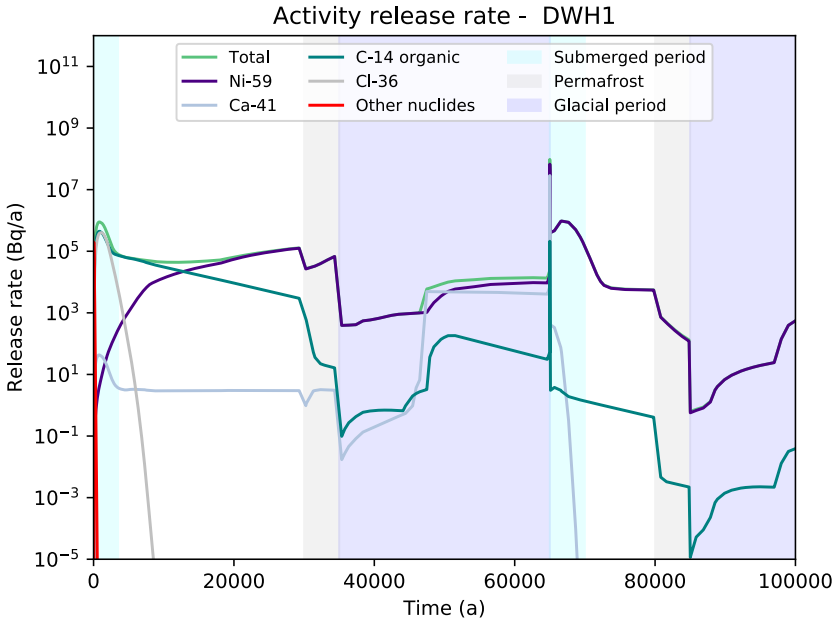

Figure 32. The activity release rate into the surface environment during the assessment period when the decommissioning wastes disposed to DWH1. The x-axis indicates years after the closure of the repository.

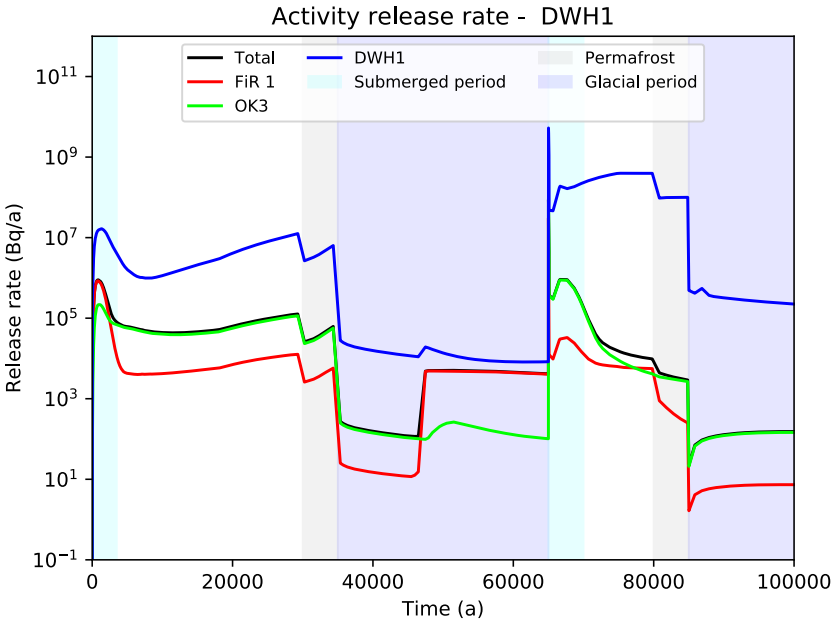

Figure 33. The activity release rate during the assessment period when the decommissioning wastes disposed to DWH1. The DWH1 curve indicates the release rate from the waste of Loviisa NPP assumed to be disposed to DWH1. The x-axis indicates years after the closure of the repository.

6.1.2 Release constraint period

The normalized release rates provide additional information about the radiological effects of the releases, and are presented only during the release constraint period. The normalized release rates emerging from MWH2 are presented in figure 34 and figure 35. According to figure 34 the most important radionuclides are organic C-14, Nb-94 and Ni-59, of which C-14 and Nb-94 are not presented in figure 30. The normalized release rates are only calculated for long-lived radionuclides (half-life over 1000 years), thus the radionuclides in the figures are different. The highest normalized release rate is caused by organic C-14 and the maxima is located at 10,000 years. The normalized release rates of all nuclides decrease during the permafrost and glacial periods, and after that the release rate of Ni-59 reaches its maximum value. The observations about the shapes of the curves made in section 6.1.1 also apply in the figures in this section. The waste specific normalized release rates for MWH2 are presented in figure 35.

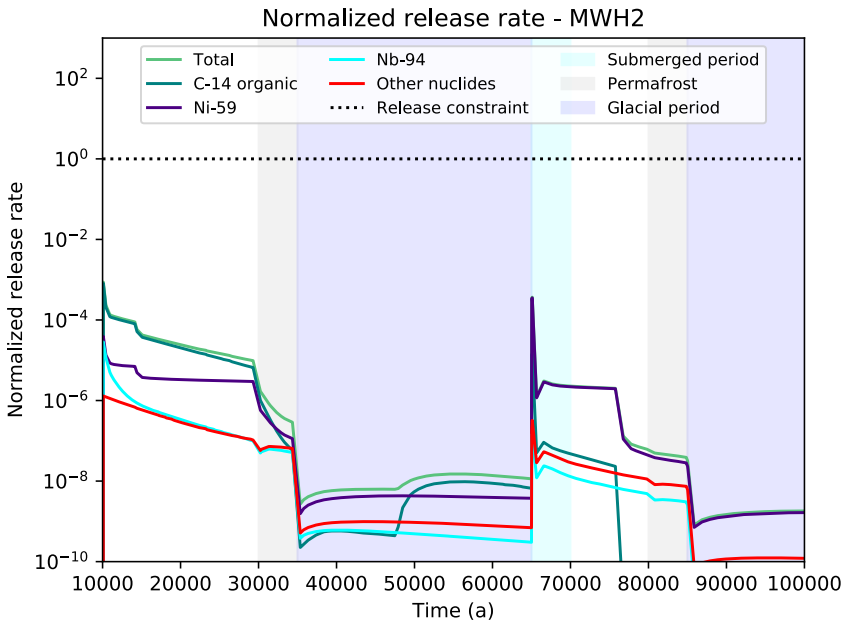

Figure 34. The normalized release rate into the surface environment during the assessment period when the decommissioning wastes disposed to MWH2. The x-axis indicates years after the closure of the repository.

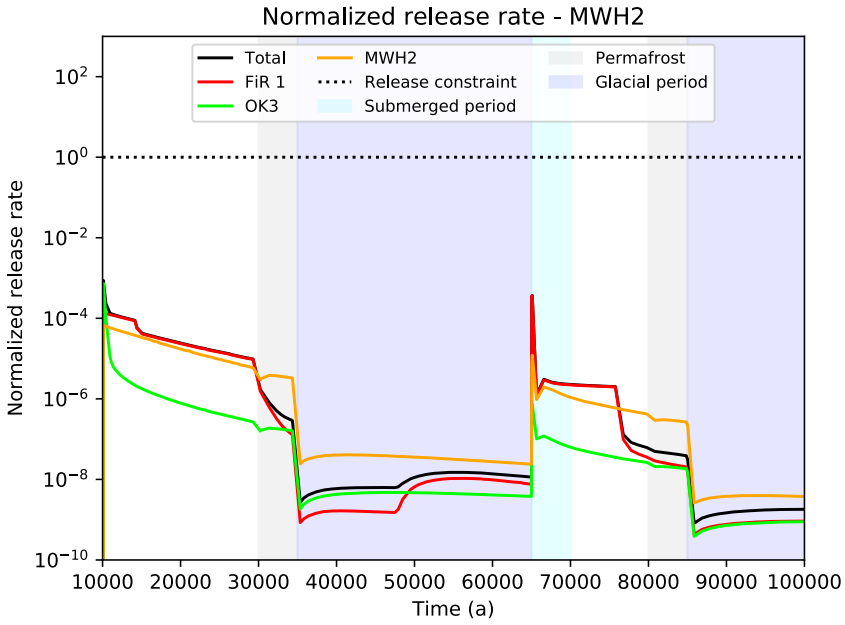

Figure 35. The normalized release rate during the release constraint period when the decommissioning wastes are disposed to MWH2. The MWH2 curve indicates the release rate from the waste of Loviisa NPP assumed to be disposed in MWH2. The x-axis indicates years after the closure of the repository.

For DWH1 the most important radionuclides causing the normalized release rate are Ni-59, Ca-41 and organic C-14 (figure 36). Before the first permafrost period, the release rate is dominated by organic C-14 due to its low Kd-value. The normalized release rate of Ni-59 increases linearly in the beginning due to corrosion of the metal components, but the normalized release rate of Ca-41 stays constant due to the its limited solubility in alkaline conditions. The alkaline conditions change to neutral approximately in the middle of the first permafrost period, which increases the solubility of all radionuclides.

At the end of the first glacial period the release rates reach their maximum values for a short period of time due to the increased groundwater flow rate. The release rate of Ni-59 has the highest value at this point, and the release rates of Ca-41 and organic C-14 decrease rapidly. The waste specific normalized release rates for DWH1 are presented in figure 37.

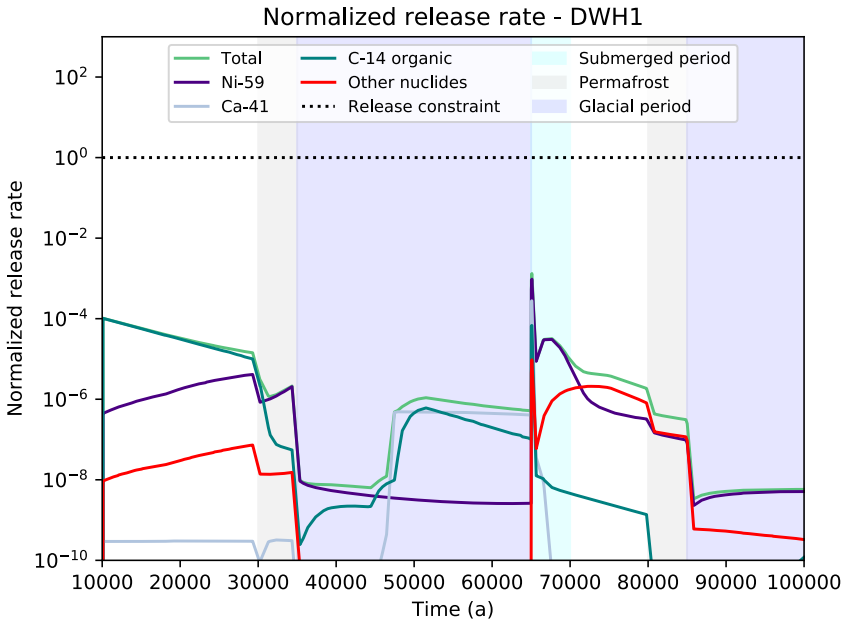

Figure 36. The normalized release rate during the release constraint period when the decommissioning wastes are disposed to DWH1. The x-axis indicates years after the closure of the repository.

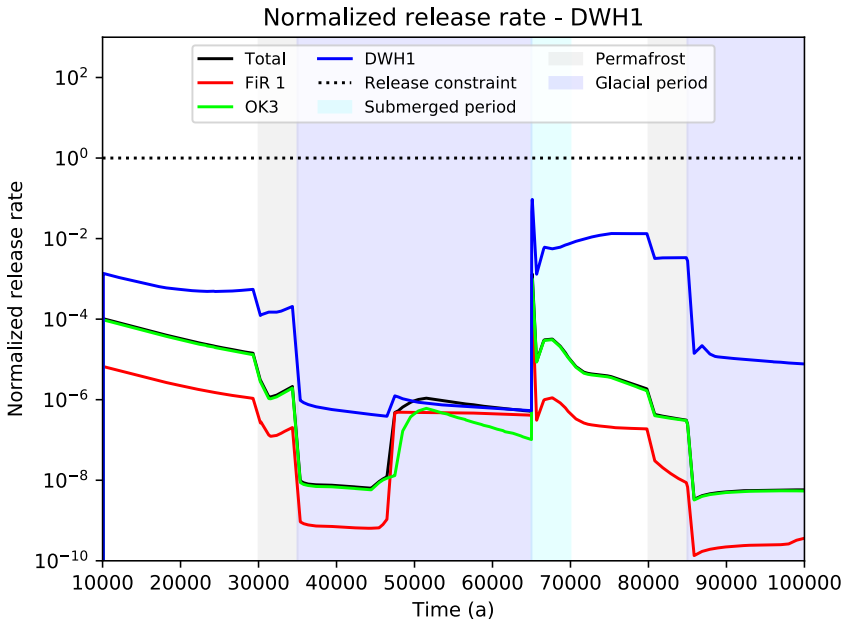

Figure 37. The normalized release rate during the release constraint period when the decommissioning wastes are disposed to DWH1. The DWH1 curve indicates the release rate from the waste of Loviisa NPP assumed to be disposed in DWH1. The x-axis indicates years after the closure of the repository.

6.1.3 Dose assessment period

The annual dose rates are presented in figure 38 and figure 39. These figures present the total dose rate and the most important dose paths, of which the total dose rate consists of. For MWH2 (figure 38), the most dose is gained from consumption of fish, well water and milk. The annual dose rate is at its maximum at approximately 4500 years. At that point the discharge location starts to turn into terrestrial area due to land uplift which makes the location habitable for people. The new land makes it possible to build farms on the discharge location which explains the possible dose rates from the consumption of well water and milk.

Approximately at 5500 years two small lakes will form on the discharge location of the repository (see figure 11 and figure 24). The dose rate caused by consumption of fish increases sharply due to the low volume of water and slow flow rate in the lakes, which causes a higher activity concentration compared to other water bodies. Only one of the lakes is large enough to provide enough fish for consumption. The dose gained from consumption of drops quickly at approximately 9500 years due to the fact, that one of the lakes disappears. A sudden increases in the dose rate between approximately at 5000-6500 years is caused by the breakage of the concrete containers which increases the release rate of activity. The decrease is caused by the changes in the conditions of the repository. For DWH1, similar trends can be seen in figure 39.

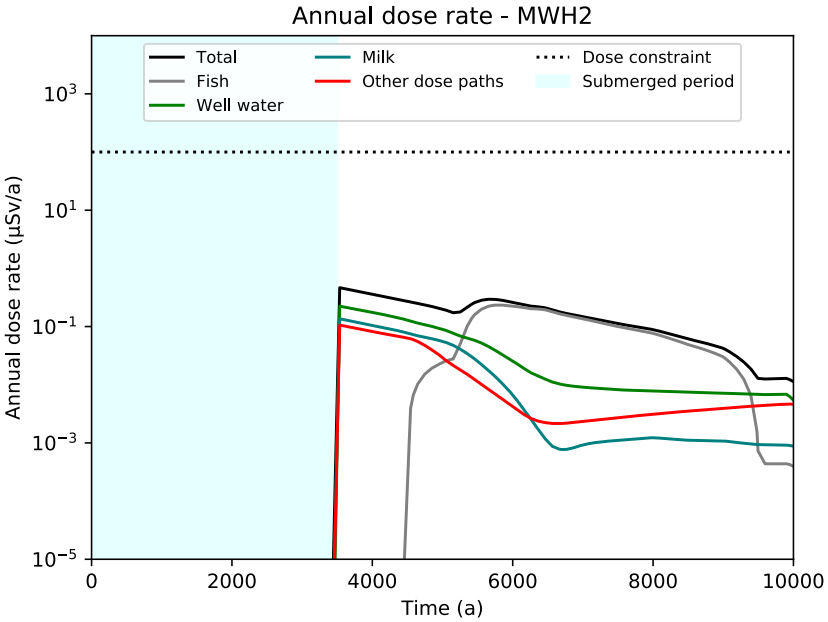

Figure 38. The dose rates during the dose assessment period when the decommissioning wastes are disposed to MWH2. The x-axis indicates years after the closure of the repository.

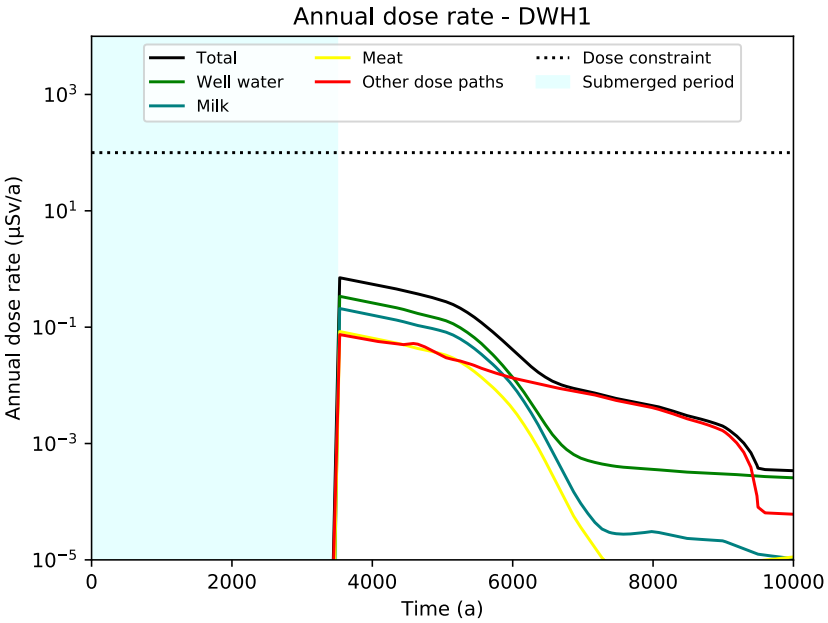

Figure 39. The dose rates during the dose assessment period when the decommissioning wastes are to DWH1. The x-axis indicates years after the closure of the repository.

The most important radionuclides, of which the total dose rate consists of are presented in figure 40 and figure 41. The most important radionuclides for MWH2 are organic and inorganic C-14 and Cl-36, and the contribution of other nuclides is small. C-14 is the most contributing nuclide to the dose rate due to its high release rate, low distribution coefficient soil, and the fact that carbon is easily taken up by organisms. The release rate of Cl-36 is also high due to similar reasons. [15].

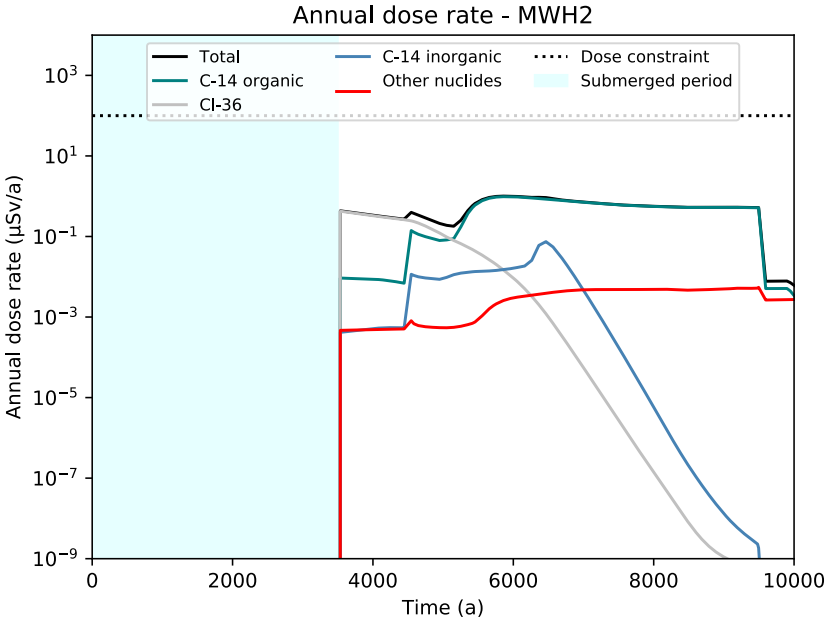

Figure 40. The dose rates during the dose assessment period when the decommissioning wastes are disposed to MWH2. The x-axis indicates years after the closure of the repository.

The total dose rate curve in both figure 38 and figure 39 can also be presented as a sum of the total rate received from FiR 1 and OK3 decommissioning wastes. This presentation allows to study how the wastes affect the shape of the total dose rate curve and gives a possibility to interpret it.

From figure 42 it can be verified that the bump in the total dose rate is indeed caused by the breakage of the special concrete container used for OK3 steel samples. The dose rate caused by FiR 1 decommissioning wastes in the beginning is much higher due to the fact that practically all of the OK3 activity is contained in the metal samples (see table 12). In the beginning the OK3 dose rate curve is caused by the waste disposed in waste drums, as their activity is released immediately.

The shape of the total dose rate curve is similar in figure 43 and it contains an

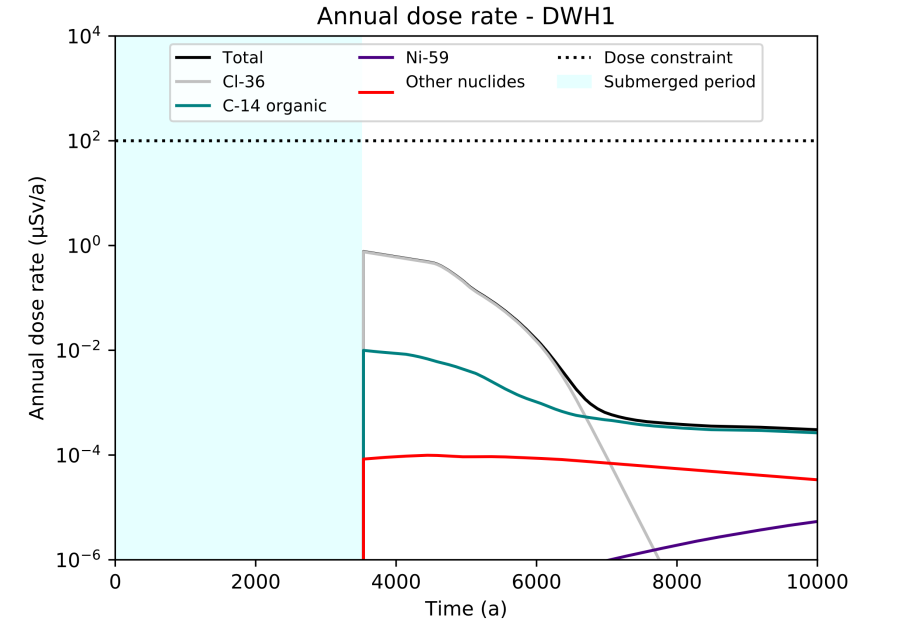

Figure 41. The dose rates during the dose assessment period when the decommissioning wastes are disposed to DWH1. The x-axis indicates years after the closure of the repository.

extremely small bump approximately between 5300 – 6000 years, which is caused by the breakage special concrete container as it can be seen from OK3 dose rate curve. The activity is released faster from DWH1 even though it contains a concrete basin enclosing the waste packages. The higher dose rate is caused by Cl-36 (figure 41), which is not significantly retarded by the concrete.

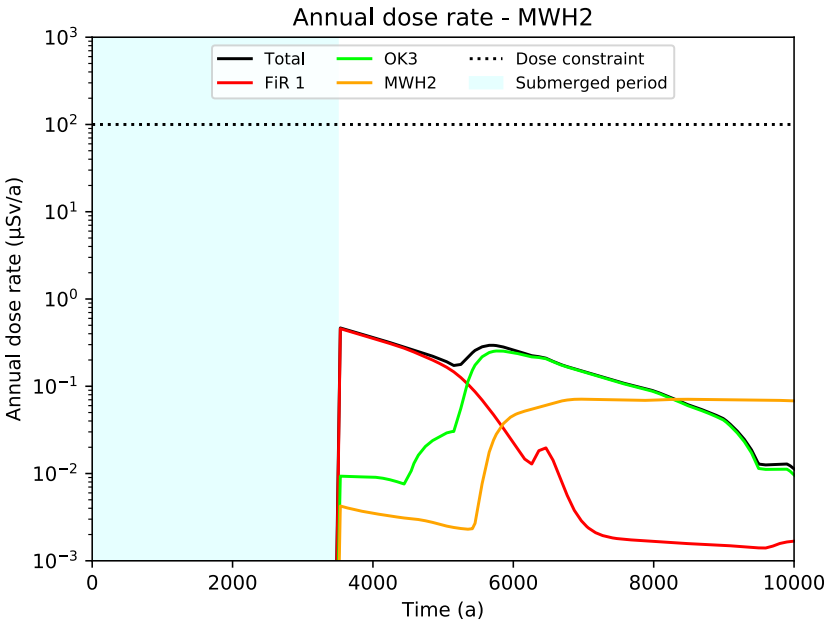

Figure 42. The waste-wise dose rates during the dose assessment period when the decommissioning wastes are disposed to MWH2. MWH2 curve indicates the dose rate caused by the waste of Loviisa NPP. The x-axis indicates years after the closure of the repository.

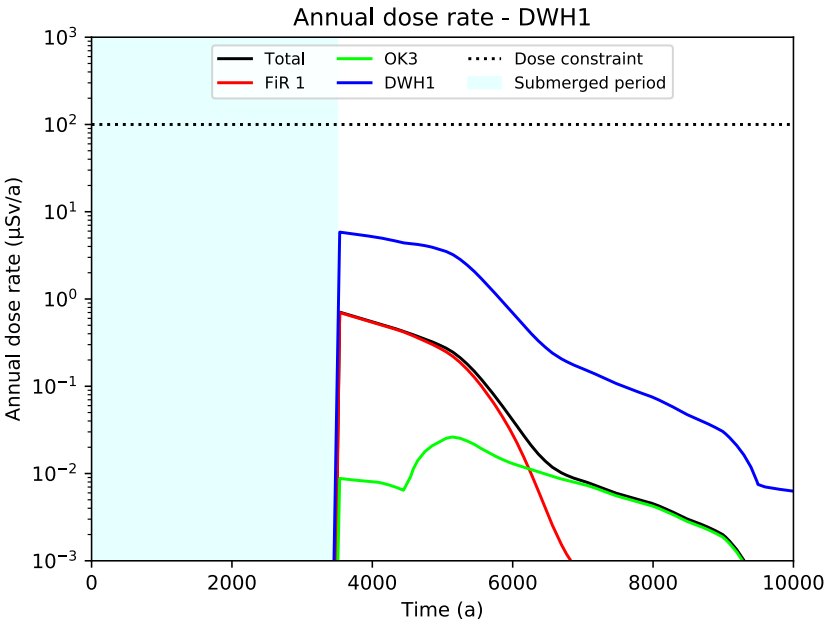

Figure 43. The waste specific dose rates during the dose assessment period when the decommissioning wastes disposed to DWH1. DWH1 curve indicates the dose rate caused by the waste of Loviisa NPP. The x-axis indicates years after the closure of the repository.

6.1.4 Probabilistic analysis

Probabilistic analysis samples parameter values from probability distribution functions and runs the model certain number of times in order to obtain a representative number of model outcomes. Each iteration samples the parameters randomly using Latin Hypercube Sampling (LHS) method. The method is described in [62]. Latin Hypercube Method Divides the probability distribution into parts with equal probabilities. Each part of the probability distribution is chosen randomly in each iteration. A large number of iterations increases the accuracy of the results at the cost of the modelling time. The number of iterations used in the 2018 safety case is 1000, which is a compromise between the time and the computational power, and statistical error of the results. In this document the probabilistic analysis is only carried out for the base scenario. The probabilistic analysis is performed with Ecolego. A schematic flow chart of the uncertainty and sensitive analyses is presented figure 44.

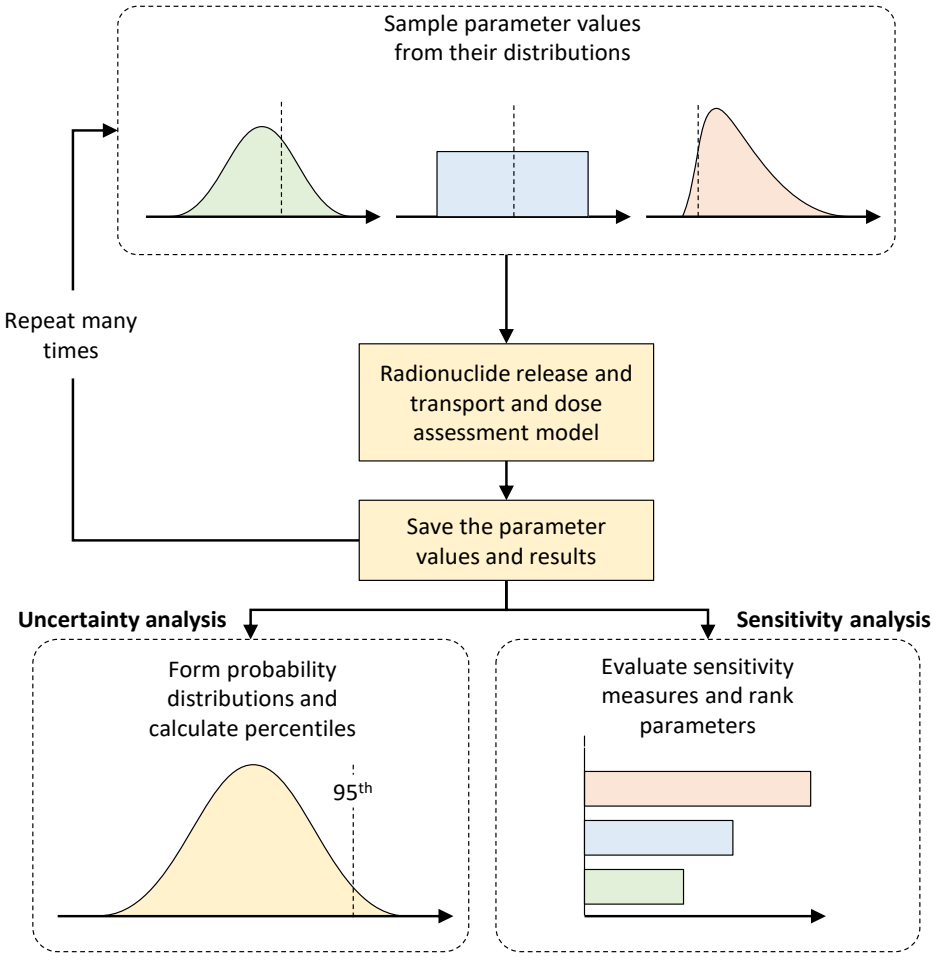

Figure 44. A schematic presentation of probabilistic uncertainty and sensitivity analyses. The figure is taken from [15].

6.1.5 Uncertainty analysis

The probabilistic analysis produces 1000 time-dependent outputs, which are assigned to different parameter values from the probability distribution functions. The results can be analysed statistically in order to calculate the uncertainty. The uncertainty analysis in the 2018 safety case is done using percentiles, which is also planned to be used in Posiva's safety case for the operating license application [63]. Percentiles tell how many percent of the values are below certain value e.g. the value of the 95th percentile tells that 95 % of the iterations are below the calculated value. The 95th percentiles are calculated and compared to the regulatory constraints.

Two methods of calculation are used to calculate the percentiles. The first way is to calculate them from the iterations as a function of time. For example the "total" curve figure 34 contains the reference values of the normalized release rate as a function of time during release constraint period. In this case each data point on the curve contains 1000 possible values, and these data sets are used to calculate the percentile curves as the function of time. These newly calculated curves are plotted in the same figure with the reference case curve. However, this method may cause probability dilution. Such figures can be drawn for the normalized release and dose rates for both MWH2 and DWH1. The results for MWH2 are presented in figure 45 and figure 46. The figures for DWH1 are in APPENDIX A, section A.1.

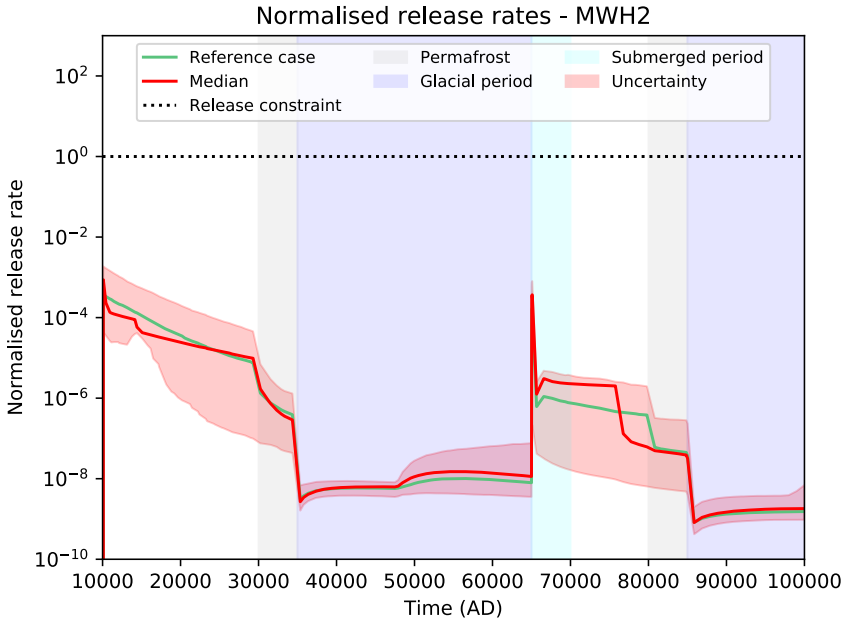

Figure 45. The results for the normalised release rates from the probabilistic analysis. The x-axis indicates years after the closure of the repository. The uncertainty reflects 95th and 5th percentiles.

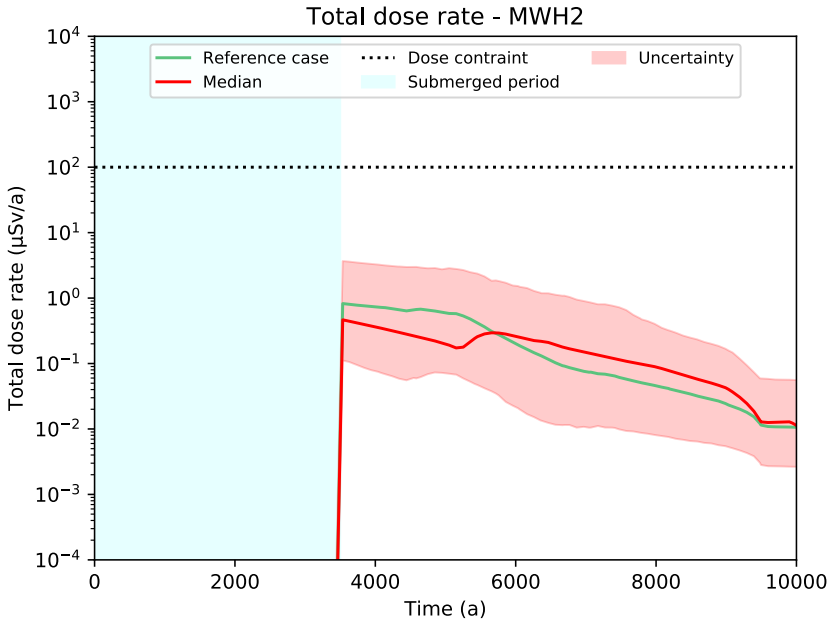

Figure 46. The results for the total dose rates from the probabilistic analysis. The x-axis indicates years after the closure of the repository. The uncertainty reflects 95th and 5th percentiles.

The second way is to find the maximum value from each iteration and use them to calculate the percentiles. The values are plotted as a histogram, which shows their frequency, and the percentiles are marked into the figure. Figure 47 and figure 48 contain the histograms of the normalized release and dose rates for MWH2. Both histograms resemble some kind statistical distribution, but the histogram of the normalized release rate has several outliers. The figures for DWH1 are in appendix A section A.1. The constraint value of 1 for normalized release rate or the constraint value of 100 µSv/a for annual dose are not exceeded in any iteration.

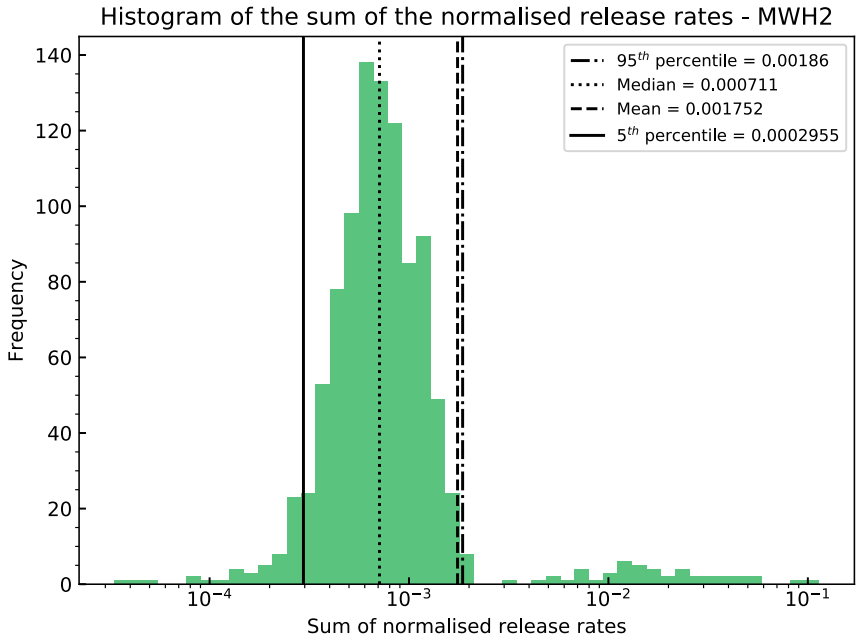

Figure 47. A histogram of the maximum normalised release rates for MWH2.

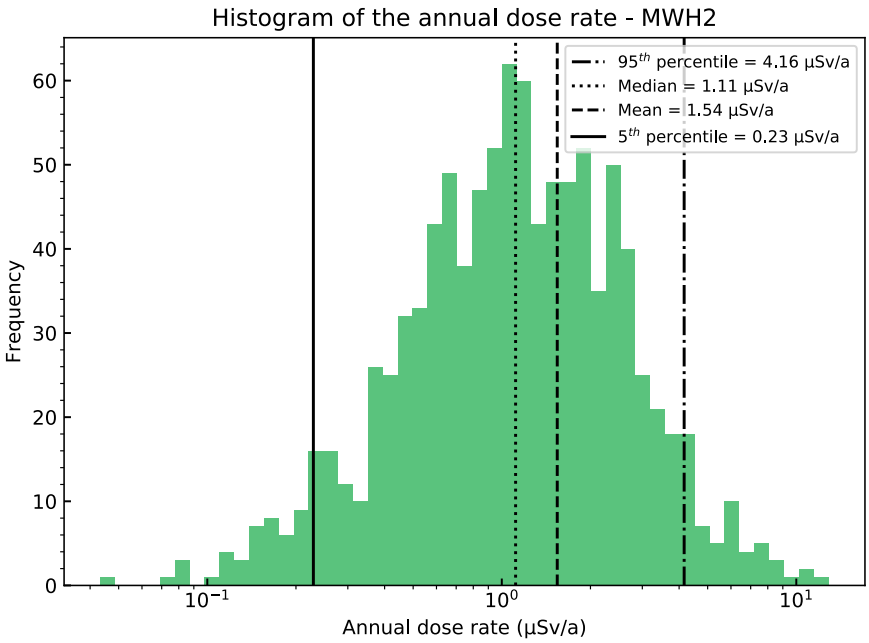

Figure 48. A histogram of the maximum total dose rates for MWH2.

6.2 Results from deterministic calculation cases

6.2.1 Drilled well

The drilled well case assumes that the wells draw all the water flowing through the waste caverns, which leads to earlier doses. For MWH2 the dose rate curve of the drilled wells case has two maxima, one in the beginning and the second at approximately at 7000 years (figure 49). The first maximum is mostly caused by Pu-239 and Pu-240 which originate from OK3 decommissioning wastes. After that the curve decreases, until it raises again at approximately at 5000 years. The increase is caused by Ni-59, Pu-239 and Pu-240. The curve passes the reference case curve, and the last bump is caused by Ca-41, originating from the concrete waste. The highest expected dose rate (a product of dose rate and probability) of the drilled wells case is 0.566 µSv/a, which is slightly higher than the maximum value in the reference case. As it can be seen from figure 49, the dose rate in the drilled wells case is consistently higher, which means that the total dose in the base scenario is lower.

For DWH1 the highest expected dose rate value of the drilled wells case is 0.472 µSv/a, and it does not exceed the maximum value of the reference case (figure 50). The curve decreases exponentially and saturates to when 4000 years has passed

from the closure of the repository, thus the total dose is lower than in the reference case. The normalized release rates figures have little only few differences and are not presented in this section. The figures can be seen in APPENDIX B, section B.1. The submerged period marked in figure 49 and figure 50 does not affect the calculation case due to the fact, that the drilled wells are not located in the discharge locations.

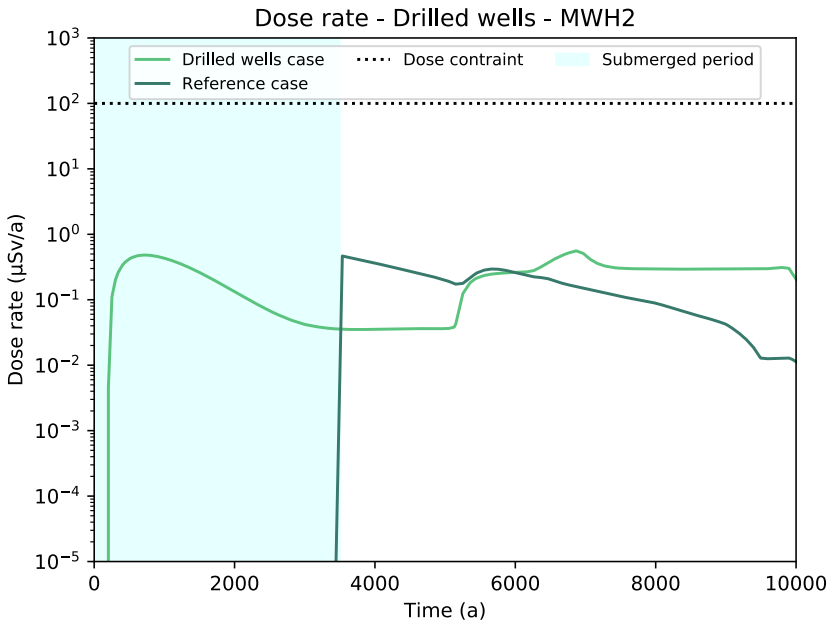

Figure 49. The expected dose rates into the environment in the reference and drilled wells cases during the dose assessment period. The x-axis indicates years after the closure of the repository. The submerged period does not affect the calculation case due to the location of the drilled well.

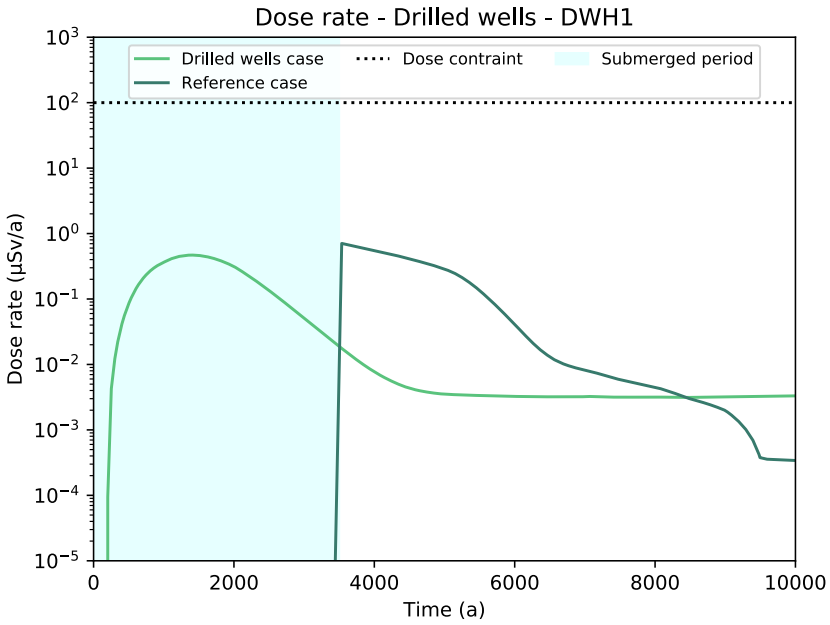

Figure 50. The expected dose rates into the environment in the reference and drilled wells cases during the dose assessment period. The x-axis indicates years after the closure of the repository. The submerged period does not affect the calculation case due to the location of the drilled well.

6.2.2 High release rates

In the high release rates calculation case, the corrosion rates of metals and release rates from graphite are higher. The normalized release rate curves in the high release rates case for MWH2 are presented figure 51. The shape of the high releases case curve differs from the reference case curve mainly in the beginning before the first permafrost and after the first glacial period. Approximately after 13,000 years the curve of the calculation case is consistently lower, due to the fact that more activity has already been released, before the beginning of the release constraint period. The early release is caused by the faster corrosion rate of steel and release rate of graphite, and the fact that the graphite waste consists only of organic C-14, which is easily released. The maximum value of the curve is $6.86 \cdot 10^{-4}$, and does not exceed the maximum value of the reference case. Normalized release rate for DWH1 is presented in figure 52. The high release rates curve reaches its maximum value of $1.00 \cdot 10^{-3}$ approximately at 10,000 years, which is lower than maximum value of the reference case.

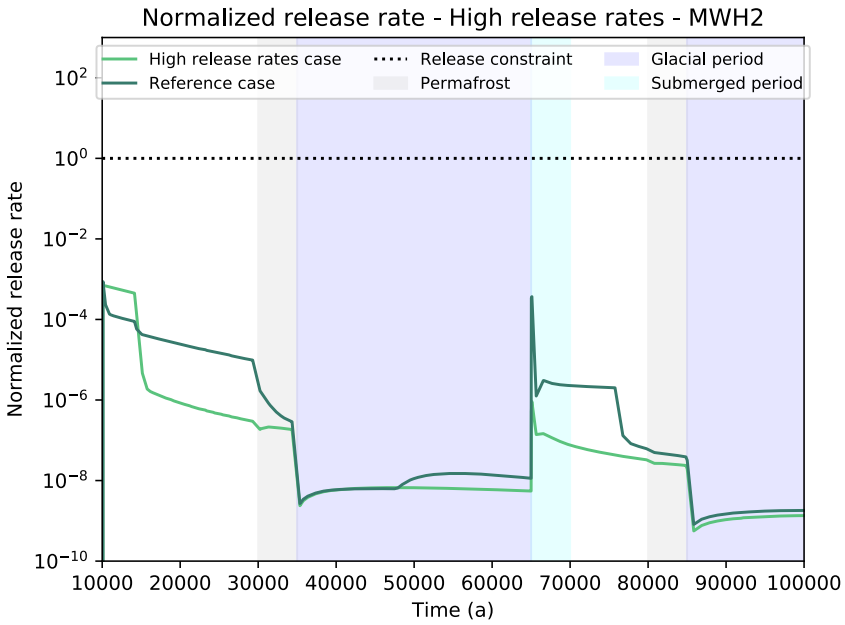

Figure 51. The normalized release rate into the environment in the reference and high release rates cases during the release constraint period. The x-axis indicates years after the closure of the repository.

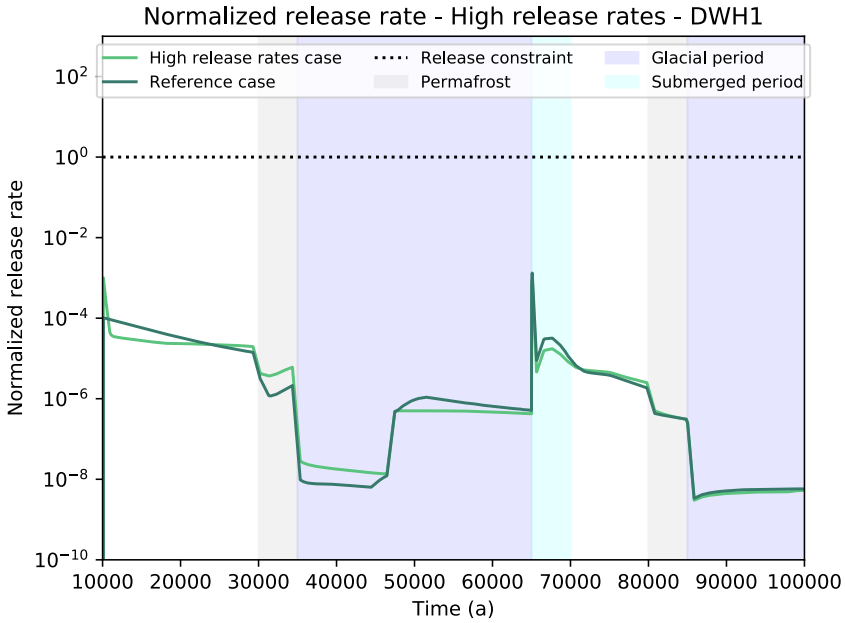

Figure 52. The normalized release rate into the environment in the reference and high release rates cases during the assessment period. The x-axis indicates years after the closure of the repository.

The annual dose rate maximum of the high release rates case is at approximately 5500 years for MWH2 (figure 53), which is caused by the breakage of the special concrete container holding the OK3 metal samples. Actually, the reference case curve also contains a small bump almost in the same exact spot, which is also caused by the breakage of the special concrete container. The bump is larger in the calculation case due to the increased corrosion rate, which also means that the activity release rate is higher. The maximum value is 1.65 µSv/a which is higher than the maximum value of the reference case, but is still much lower than the annual dose rate constraint. After the maximum is reached, the dose rate is lower than in the reference case. For DWH1 the shapes of the curves are similar (figure 54), but after approximately 5500 years the high release rates curve is higher, which is also caused by the faster corrosion of the OK3 metal samples.

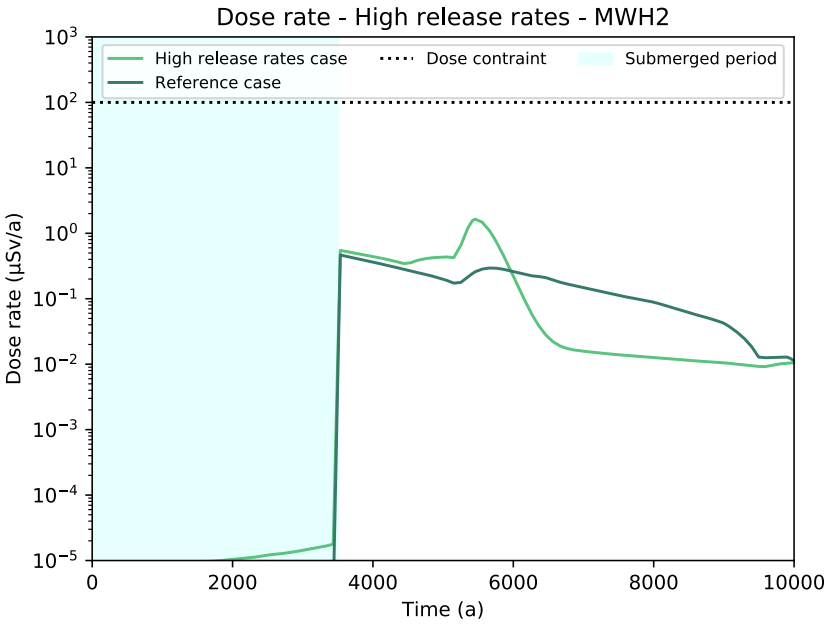

Figure 53. Expected dose rates into the environment in the reference and high release rates cases. The x-axis indicates years after the closure of the repository.

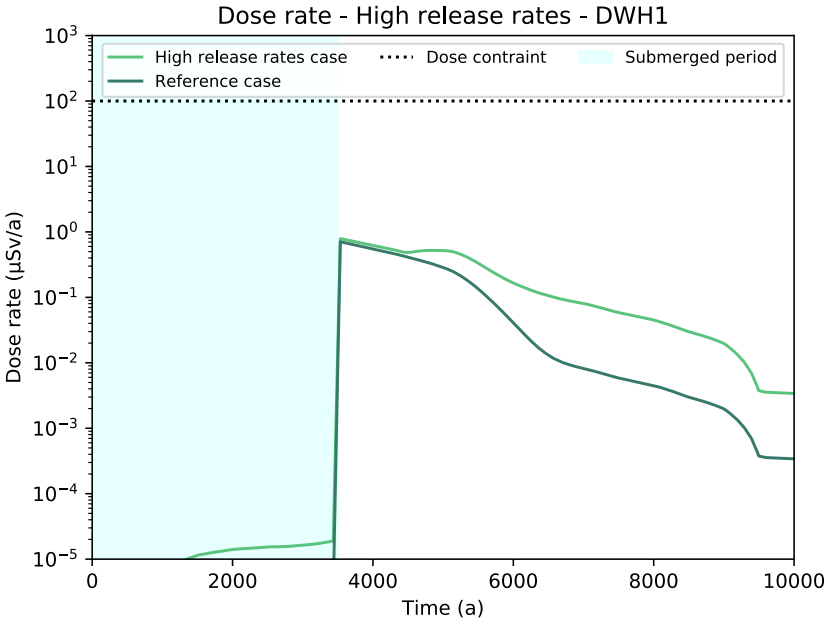

Figure 54. Expected dose rates into the environment in the reference and high release rates cases. The x-axis indicates years after the closure of the repository.

6.2.3 Smaller volume of MWH2

The smaller volume of MWH2 calculation case assumes that the volume of MWH2 is on tenth of the original value. The maximum values of the normalized release rate and dose rate in the small volume of MWH2 are $2.78 \cdot 10^{-4}$ and 0.346 µSv/a respectively. The values are smaller than the maximum values in the reference case. The normalized release and dose rates are presented in figure 55 and figure 56. The general shape of figures is similar but with few exceptions. The normalized release rate curve of the calculation case is higher in the middle of the first glacial period, and the dose rate curve starts lower. The differences can be explained with the higher activity concentration in MWH2. High activity concentration actually leads to high release and dose rate but time is an important factor here. The discharge location will be submerged after the closure, and during that time all the activity released from MWH2 is diluted by the sea. After the land raises from the sea, a significant portion of the activity has already been lost into the sea, which means that the release and dose rates are lower.

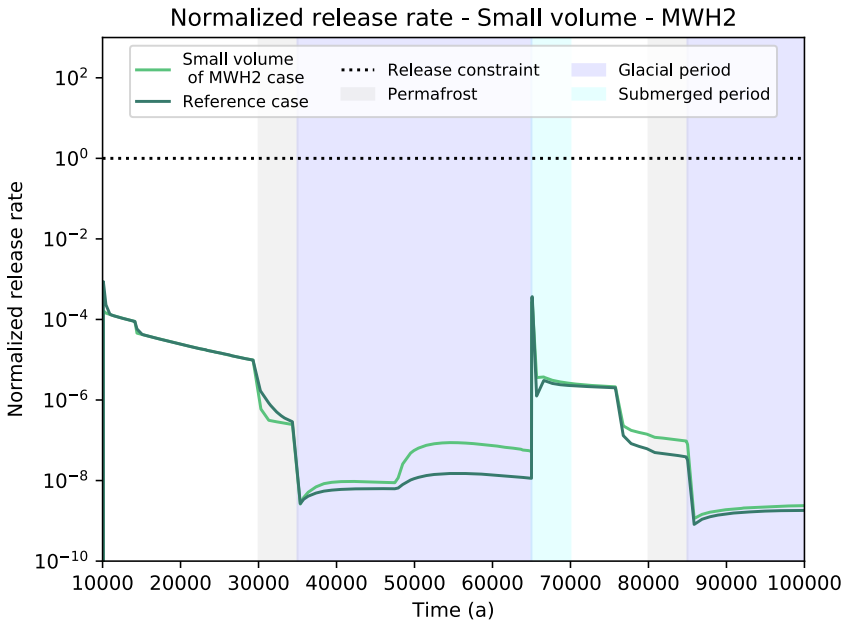

Figure 55. The normalized release rate into the surface environment in the reference and small volume of MWH2 cases during the assessment period. The x-axis indicates years after the closure of the repository.

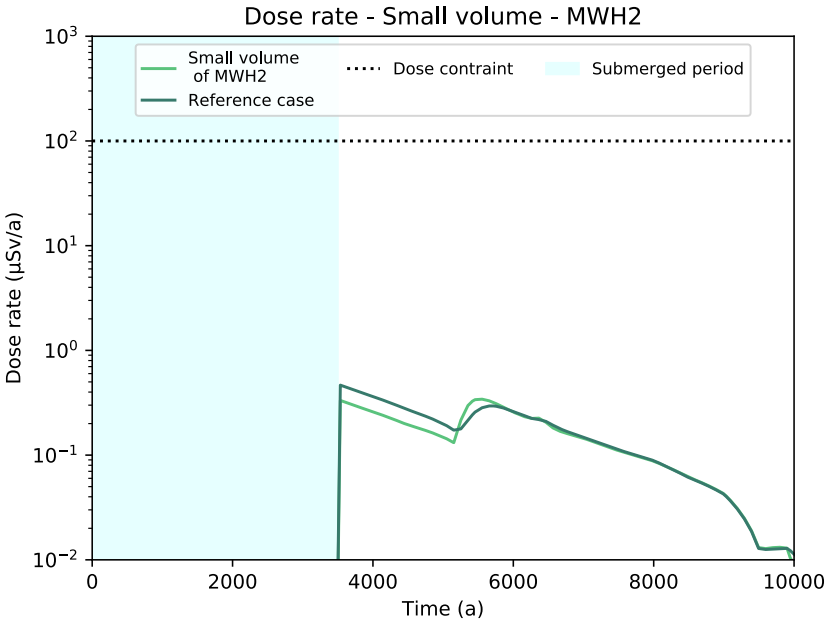

Figure 56. Expected dose rates into the surface environment in the reference and small volume of MWH2 cases. The x-axis indicates years after the closure of the repository.

6.2.4 Alternate climate evolutions

This calculation cases considers the effects of alternate climate evolutions. The release rate curves for MWH2 are presented in figure 57. RCP8.5 curve differs from RCP4.5 and RCP2.6 due to the lack of permafrost and glacial periods, which makes the curve smoother and causes lower normalized release rate. The curve drops at approximately 60,000 years, which is caused by the end of the corrosion of the metal components. The RCP4.5 and RCP2.6 curves are similar, but the normalized release rate of RCP2.6 is $1.30 \cdot 10^3$, which is higher than the value in the reference case.

The results for DWH1 are similar (figure 58), but the curve of RCP8.5 has a bump in the middle of the first glacial period, which is also caused by the same reason as for MWH2. The highest normalized release rate is again caused by the RCP2.6 case with the value of $1.90 \cdot 10^{-3}$, which is higher than the value in the reference case. Dose rates will be omitted due to the fact, that the biosphere objects has not been modelled with RCP2.6 and RCP8.5 climate evolutions thus the results would not be realistic.

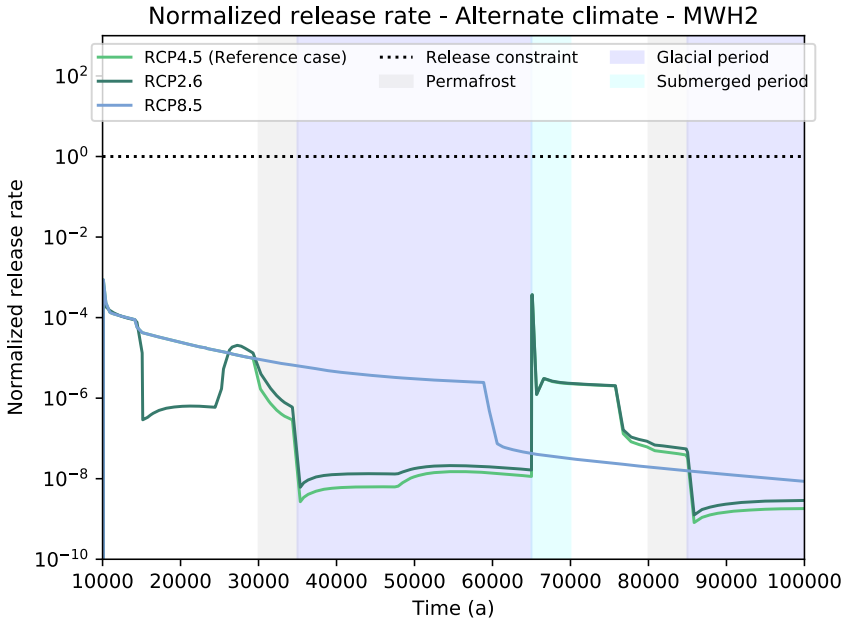

Figure 57. The normalized release rate into the surface environment in the reference and alternate climate cases during the release constraint period. The x-axis indicates years after the closure of the repository.

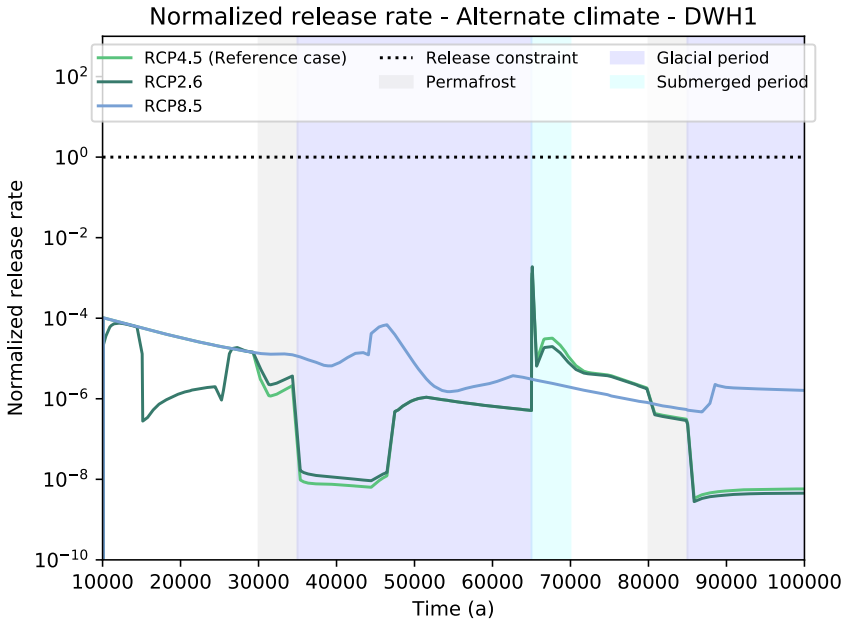

Figure 58. The normalized release rate into the surface environment in the reference and alternate climate cases during the release constraint period. The x-axis indicates years after the closure of the repository.

6.3 Results from other scenarios

6.3.1 Accelerated concrete degradation

This scenario assumes that all the concrete structures (concrete plugs, concrete containers and the basin in DWH1) in the repository degrade faster. Faster concrete degradation leads to a faster release of activity from the concrete packages and decreases the effectiveness of the concrete basin in DWH1. The normalized release curve for the accelerated concrete degradation case is similar to the curve of the base scenario for MWH2 (figure 59). However, in the middle of the first glacial period the normalized release rate of the base scenario is lower, but in the end of the submerged period its larger than the normalized release rate of the declined concrete performance curve. The maximum value of the normalized release rate of the base scenario is not exceeded. The dose rate curves are almost identical, so it will not be covered in this section. The dose rate figure is in APPENDIX C, C.1.

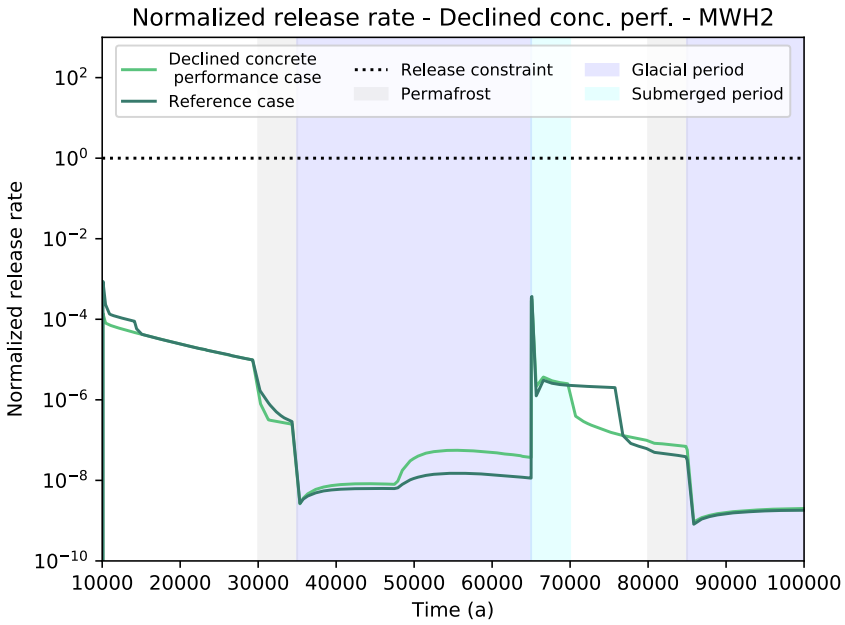

Figure 59. The normalized release rate into the surface environment in the base and accelerated concrete degradation scenarios during the assessment period. The x-axis indicates years after the closure of the repository.

For DWH1 the graph (figure 60) of the and normalized release rates are similar to the one in the reference case with the exception that the maximum values of the

reference case are greater. The accelerated concrete degradation causes an earlier release approximately at 15,000 years, which is also the highest value the curve reaches. The release is caused by corroding metal waste e.g. the irradiation ring. The normalized release rate is also lower in the middle and at the end of the first glacial period compared to the base scenario. The difference is mostly likely caused by the early release i.e. there is less activity to be released after the beginning of the first glacial period. There is no difference between the dose rates of the base and accelerated concrete degradation scenarios. The maximum value of the normalized release rate of the base scenario is not exceeded. The dose rate curves are almost identical, but the curve of the accelerated concrete degradation curve is lower, thus it will not be covered in this section. The figure is in APPENDIX C, C.1.

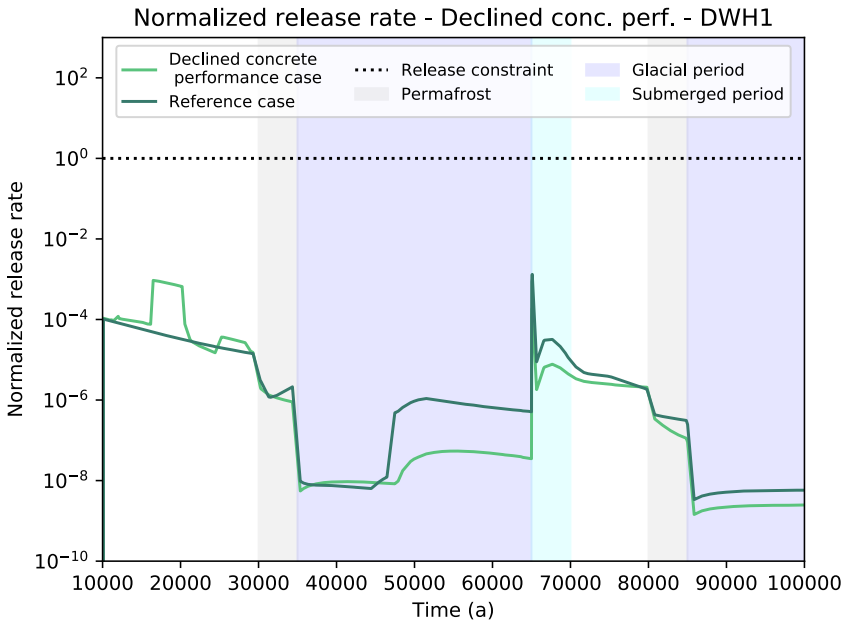

Figure 60. The normalized release rate into the surface environment in the base and accelerated concrete degradation scenarios during the assessment period. The x-axis indicates years after the closure of the repository.

6.3.2 Large earthquake

In this scenario a large earthquake occurs 4500 years after the closure and damages the concrete plugs, concrete barrier and concrete containers, which leads to a higher radionuclide release rate. For both waste caverns, the earthquake had minimal effect on the normalized release rates, thus they will not be covered. The figures can be seen in APPENDIX C, C.2. The effect of the earthquake can be seen in the dose rate figure of MWH2 (figure 61), as it causes a visible increase in the dose rate. The figure of DWH1 has a similar increase, but it is extremely small. The figure is in APPENDIX C, section C.2.

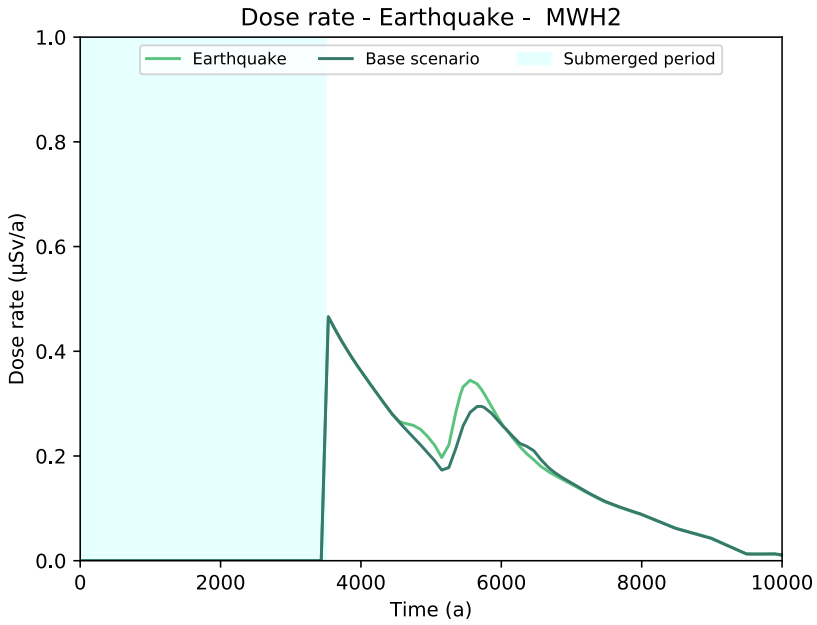

Figure 61. Expected dose rates into the surface environment in the base and earthquake scenarios. The x-axis indicates years after the closure of the repository.

6.4 Results summary

This section summarizes the results from sections 6.1, 6.2 and 6.3. The most important property of the graphs is the maximum value that the curves reach, since they are not allowed to exceed the constraint values at any point in time. The maximum values of all the calculation cases and scenarios are presented in table 29. The maximum dose rate value of the reference case is only exceeded in drilled wells and high release rates calculation cases. The highest dose rate value is 1.65 µSv/a in the drilled wells case for DWH1, however it is only 1.65 % of the constraint value. The maximum normalized release rate value of the reference case is exceeded in drilled wells and alternate climate evolution RCP2.6 calculation cases. The highest normalized release rate value of $1.90 \cdot 10^{-3}$ for DWH1 in the RCP2.6 calculation case. The highest value is only 0.19 % of the constraint value. The fact that the disposal of VTT's decommissioning wastes into DWH1 causes higher dose rate and normalized release rate in the reference case is interesting and contradictory. It should be self-evident that the concrete basin in DWH1 should retard the release of radionuclides, and thus causing lower dose rate and normalized release rate. Due to the fact that the discharge locations are submerged for over 3000 years before the calculation of doses is initiated, a large amount of activity from MWH2 is already lost. The concrete basin of DWH1 prevents the early release of activity, which means that there are more activity left when the calculation of doses is initiated. Nevertheless, all the dose rate and normalized release rate values are small enough, that they don't restrict the choice between MWH2 and DWH1. Both waste caverns are suitable for the disposal of VTT's decommissioning wastes.

Table 29. The summarized results from the scenarios and calculation cases.

Scenario	Calculation case	Max dose rate (µSv/a)		Max normalized release rate	
		MWH2	DWH1	MWH2	DWH1
Base scenario	Reference case	0.471	0.713	$8.69{\cdot}10^{-4}$	$1.32{\cdot}10^{-3}$
	Drilled well	0.566	0.472	$8.52{\cdot}10^{-4}$	$1.36{\cdot}10^{-3}$
	High release rates	1.65	0.796	$6.86{\cdot}10^{-4}$	$1.00{\cdot}10^{-3}$
	Smaller volume of MWH2	0.346	-	$2.78{\cdot}10^{-4}$	-
	RCP2.6	-	-	$1.30{\cdot}10^{-3}$	$1.90{\cdot}10^{-3}$
	RCP8.5	-	-	$8.69{\cdot}10^{-4}$	$1.02{\cdot}10^{-4}$
Accelerated concrete degradation	-	0.372	0.464	$3.13{\cdot}10^{-4}$	$9.35{\cdot}10^{-4}$
Earthquake	-	0.471	0.713	$3.13{\cdot}10^{-4}$	$1.06{\cdot}10^{-3}$

The histograms of normalized release rates (see figure 47 and figure 68) have many outliers and the dose rates have none. The number of outliers change when the model is rerun, which implies that 1000 iterations is not enough not for accurate results. A sensitivity analysis was carried out as a part of the probabilistic analysis, in order to find the most sensitive parameters affecting the results. However due to the fact, that the analysis was not successful, deeper analysis of the results will be omitted. According to results the most important parameter seems to be the corrosion rate of stainless steel in all cases, since that parameter showed up every time when analysis was performed. The R^2 values of the analysis were between 0.3 and 0.6, which suggests that a linear function does not describe the variability around the model's mean. Two mathematical transforms (logarithmic and rank) were performed, but they did not improve the R^2 values much. The sensitivity analysis and the cause of the outliers are something to research in the future. However it is known that the corrosion parameters, have something to do with the outliers in the normalized release rate histograms and low R^2 values due to the fact, that almost all the activity is released via corrosion.

7 Chemical toxicity of VTT's decommissioning wastes

7.1 Regulatory requirements

The chemical toxicity of VTT's decommissioning wastes is investigated even though the it is not required by regulatory body. Since there is no concentration limits for chemically toxic substances for nuclear waste, limits for household water, residual waste and soil are used instead.

The concentrations of different chemicals and elements are regulated in household water and soil in order to protect the people and nature from their harmful effects. Similar limits have also been set for residual waste. The chemical composition of the communal household water is monitored constantly and even small exceedings are always investigated even though they might possess no health hazard. [64] Pollution level of soil is estimated based on many factors e.g. location of the soil, concentration and properties of the toxic chemicals and the possible exposure to humans. If concentration limits of one of more substances is exceeded, the usage of the land may be limited. [65] The concentration of chemical substances in residual waste is regulated in order to minimize the harmful effects of the landfill to people and nature, which closely relates to the limits of the soil. The limits for different chemical and elements for household water, soil and residual waste are listed in references [64], [65] and [66] respectively.

7.2 Waste description

This report considers only the chemical toxicity of FiR 1 decommissioning waste, as the waste inventory of OK3 does not contain any waste types differing from typical waste of Loviisa NPP. The most chemically toxic materials in FiR 1 decommissioning waste are listed in table 30. It is probable that lead and bismuth may be cleared from regulatory control and not disposed into the repository. The bismuth was used as a radiation protection shield in the BNCT station. The lead was also used as a

radiation shield in the BNCT station, and it may be activated. Some samples were taken by VTT, and they were analysed with ISOCS gamma spectrometer. According to the results, the lead may be cleared from regulatory control. [6]

Table 30. The amounts of most toxic materials in FiR 1 decommissioning waste. Based on table 2.

Element	**Amount (t)**
Aluminium	2.2
Fluental	1.3
Lead	2.7
Bismuth	0.8

7.2.1 Aluminium

Aluminium is thermodynamically unstable in water, but the corrosion is limited by a dense oxide layer at neutral or near-neutral pH [37]. The oxide layer will dissolve under high chloride and acid or alkaline conditions, which leads to general aluminium corrosion. In addition, some localized corrosion may exists, which includes pitting, crevice, galvanic and inter-granular corrosions. [67]

Most of the aluminium in the waste exists in its pure metallic form, which may lead to formation of aluminium hydroxide ($Al(OH)_2$) or aluminium oxide (AlO_2) due to corrosion. The solubility of these corrosion products is low at neutral pH, but increases with both increasing and decreasing pH [68]. As an example, aluminium hydroxide can be found in nature as a mineral called gibbsite ($Al(OH)_3$). If gibbsite is dissolved into a solution, hydrolysis products with different solubilities will be formed. The solubilities depend on the pH of the solution (figure 62).

Looking up the values on the Total Al curve, the solubilities of aluminium in alkalic and neutral conditions are approximately to be $1{\cdot}10^{-4}$ mol/l and $1{\cdot}10^{-5}$ mol/l respectively. The boundary between neutral and alkalic is at the pH of 10.5 in the corrosion model used in the 2018 safety case. The figure does not perfectly reflect the corrosion of the aluminium waste, but it is a decent approximation about the solubilities of hydrolysis products of the aluminium waste. The recommended concentration of aluminium in household water is 200 µg/l [64]. The aluminium is assumed to corrode immediately, and that all them aluminium ions are available for chemical reactions. No concentration limits for aluminium in soil or residual waste has been set.

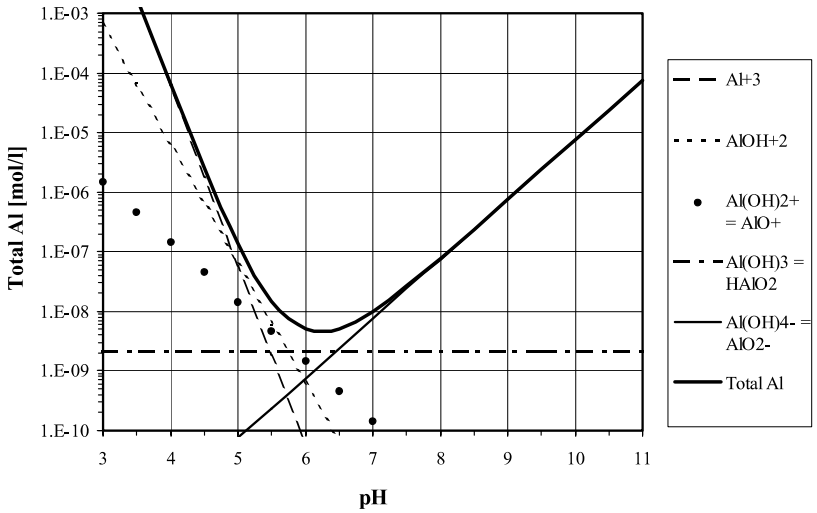

Figure 62. The concentrations of different aluminium hydrolysis products from gibbsite ($Al(OH)_3$) at different pH values. The figure is taken from [68].

7.2.2 Fluental

The decommissioning waste of FiR 1 contains 1.33 tons of Fluental, which was used as a moderator in the BNCT station and which was it was specifically developed and manufactured for VTT. Fluental contains 69 w-% AlF_3, 30 w-% metallic aluminium and 1 w-% LiF [5]. It is unknown how Fluental acts is under the disposal conditions. The Fluental most likely withstands the disposal conditions fairly well, and in the end starts to degrade slowly. In the absence of confirming evidence about Fluental's stability, it is assumed that it disintegrates immediately after the closure. Immediate disintegration means, that all of the radioactivity is released, and all chemical compounds are available for chemical reactions. Since Fluental contains many different elements, they may cause chemical reactions between the elements from other waste, but no such reactions have been recognized. [3]

Aluminium fluoride may form complexes as it reacts, and the toxicity of these complexes is caused by aluminium. The aquatic toxicity of free aluminium ions is much higher than the toxicity of free fluorine ions. [69] The solubility of AlF_3 is 5.59 g/l [70]. Fluental contains approximately 900 kg of aluminium fluoride. The limits of Al and F are applied for AlF_3.

Fluental contains only 13 kg of LiF, and no concentration limit has been set in Finland. The solubility of LiF is 1.34 g/l [70] and the value is assumed to stay constant during the whole assessment period. Exposure to fluorine via drinking

water is not harmful as long as the concentration is below the limit. Many countries add fluorine to household water to prevent tooth cavity. [71] The concentration limits of fluoride are 1.5 mg/l for household water [64] and 10 mg/kg for residual waste [66], but no value for soil has been set.

7.2.3 Lead

Lead is highly toxic metal that affects multiple organs in human body. Lead acts like calcium in human metabolism and accumulates in bones and teeth over time. Lead is especially dangerous to pregnant women since its released into blood during pregnancy and affects the fetus. [72] The concentration limit of lead in household water is 10 µg/l [64].

Water with low alkalinity and pH less than 7 cause lead to corrode. [73] Lead is practically insoluble in water with pH7 and high alkalinity, but some of its compounds are soluble. Some values for solubility in water are given in [74]. The values are calculated at the temperature of 25°C and the pressure of 1 bar. Upper limit for solubility of lead(II) sulphate ($PbSO_4$) is $6.5 \cdot 10^{-5}$ mol/kg and the recommended value for lead carbonate ($PbCO_3$) is $8.8 \cdot 10^{-7}$ mol/kg. Multiplying the upper limit value with the atomic weight of lead (207.2 g/mol [70]) gives a theoretical value of 13.5 mg/l, which is over thousand times higher than the required value in household water. According to [72] all exposure to lead should be avoided, in order to avoid the harmful effects. Thus, it is recommended to clear the lead from regulatory control if possible.

Even though the lead most likely does not corrode significantly in the repository, an immediate release is assumed. The limits for the concentration of lead are 60 mg/kg and 0.5 mg/kg for soil [65] and residual waste [66] respectively.

7.2.4 Bismuth

Bismuth is considered to be a less toxic heavy metal compared to e.g. lead and uranium. It is used in cosmetics and medicine, which causes continuous exposure of people. In medicine bismuth used to treat burns, intestinal disorders, and stomach ulcers, which means that exposure is internal. However, the solubility of bismuth is low which prevents the absorption into human metabolism. Bismuth has been researched as a replacement for lead in many applications. [75]

The concentration of natural bismuth in well water is low, and usually below detection limit. In reference [76], the concentration of bismuth was measured from 1000 wells, and the highest measured concentration was 0.28 µg/l. Even though it seems that the solubility of bismuth in water is low, it cannot be excluded that the concentration would be higher than the natural concentrations in well water. Even though bismuth does not appear to be as toxic as lead, it is still recommended to clear it from regulatory control if possible. The solubility of bismuth is assumed to be practically unlimited in both alkaline and neutral conditions. No concentration limit for bismuth in household water, soil residual waste has been set, and an immediate release is assumed.

7.3 The modelling of the chemical toxicity

A similar approach to the migration of radionuclides was used to model the chemical toxicity of VTT's decommissioning wastes. The same models made with Ecolego for MWH2 and DWH1 were used, but they required minor changes e.g. changing the unit of Bq to moles and changing as the solubility limits. Most of the equations described in chapter 4 still apply but require similar changes. The modelling does not consider the dose or normalized release rates, instead the main concern is the concentrations of the toxic elements in different biosphere objects e.g. wells used to draw drinking water and decomposition layer. The modelling covers only a period of 10,000 years from the closure of the repository due to the fact, that the landscape has not been modelled past that point, and the modelled biosphere objects cease to exist e.g. the glacial period changes the uppermost layer of the soil, which also takes away the chemical substances.

Only the base scenario and the drilled wells calculation case were modelled. The Kd-values of lead were used for aluminium and bismuth, and the Kd-values of AlF_3 and LiF were assumed to be zero, as suitable values for them were not found. These substances are not typically encountered in the long-term safety assessments of the nuclear waste, so no Kd-values have been defined. The assumption adds up to the uncertainty of results. The shapes of the curves will not be analysed in detail due to the fact, that they always depend on three factors: the breakage of the concrete packages, and solubility and the Kd-values of the corresponding element.

7.4 Results from the base scenario

For the base scenario the possible concentrations of different substances were modelled in the decomposition layer and water well. The decomposition layer is the upmost soil layer with the thickness of 30 cm and the water well is deep enough to reach the deep overburden, which makes it at least 7.5 m deep. The soil layers are presented in figure 25. The maximum concentrations of different substances in decomposition layer are presented in figure 63 and figure 64. None of the concentrations exceed the limits set for residual waste and soil, thus they can be considered unimportant.

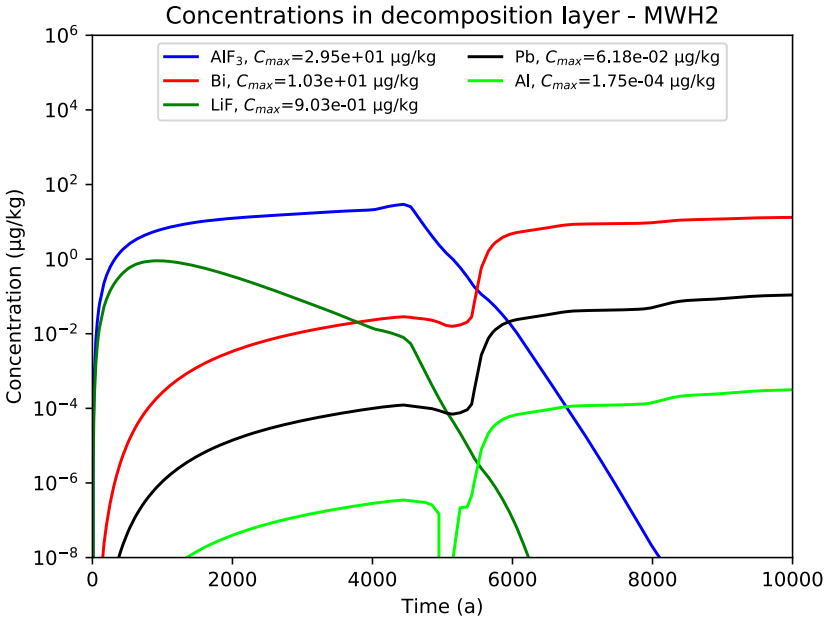

Figure 63. Concentration of different substances in the decomposition layer of the soil 10,000 years after the closure of the repository. The x-axis indicates years after the closure of the repository.

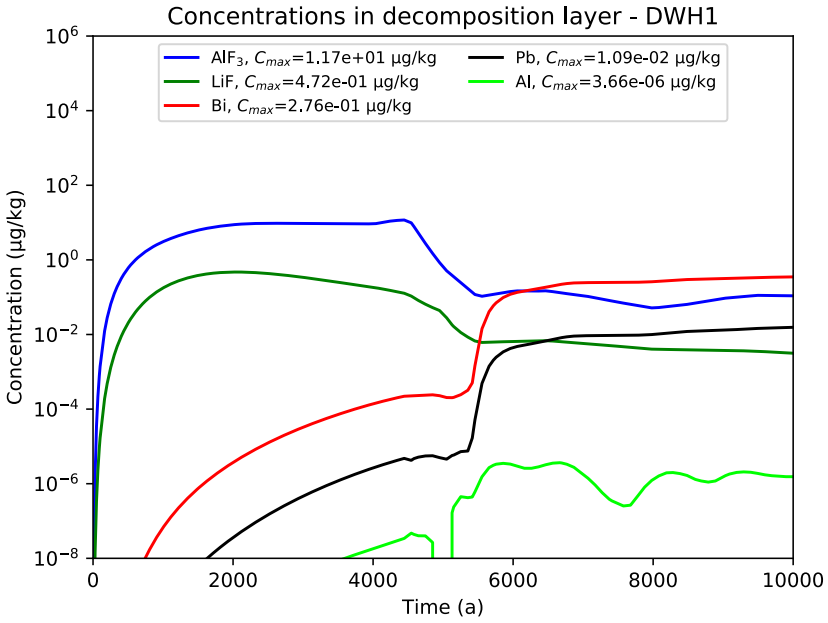

Figure 64. Concentration of different substances in the decomposition layer of the soil 10,000 years after the closure of the repository. The x-axis indicates years after the closure of the repository.

The concentrations of different substances in well water are presented in figure 65 and figure 66. The largest concentration is caused by AlF3. The maximum concentrations of AlF3 are 1300 µg/l and 565 µg/l for MWH2 and DWH1 respectively. Only the recommended maximum concentration for aluminium in household water (200 µg/l) exceeded. The concentration is large due to the large amount of AlF_3 in the waste and its zero Kd-value. The rest of the concentrations are too small to be considered important.

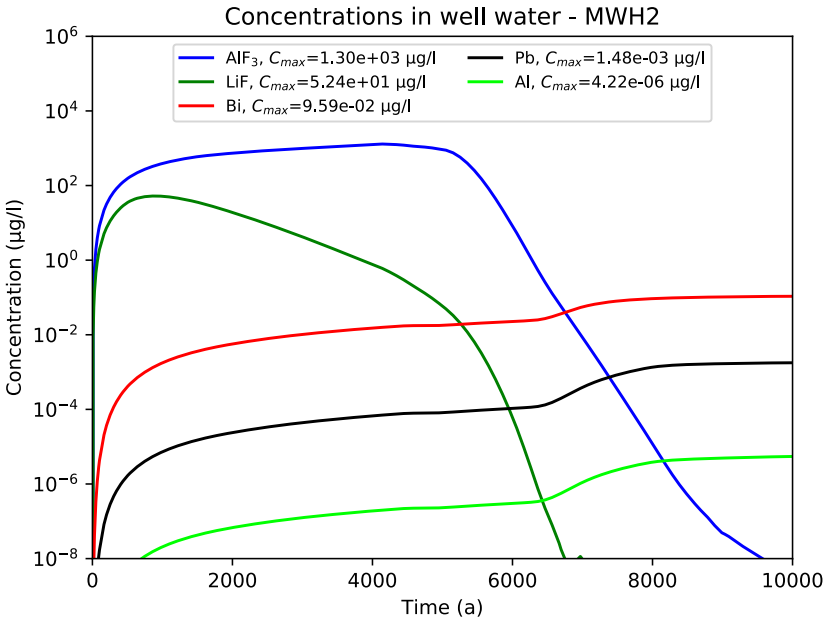

Figure 65. Concentration of different substances in a well water 10,000 years after the closure of the repository. The x-axis indicates years after the closure of the repository.

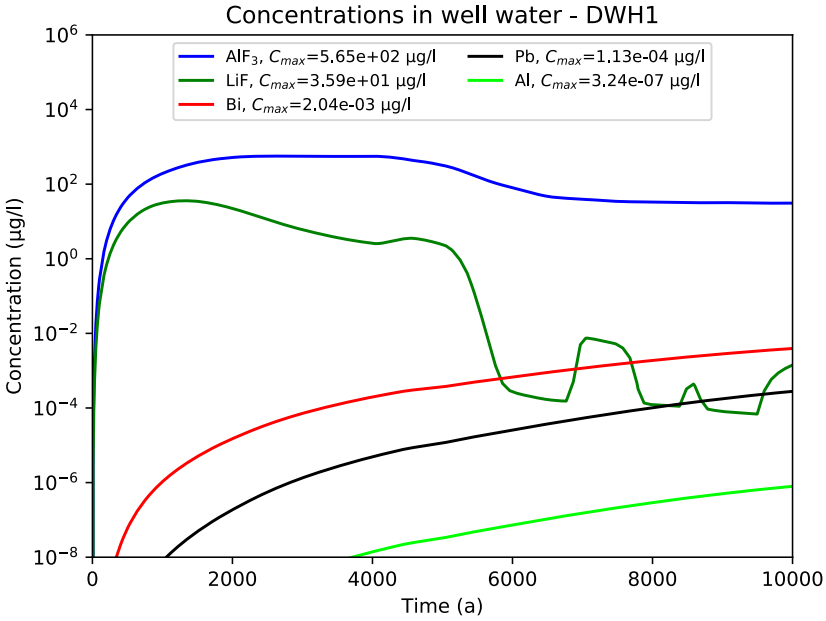

Figure 66. Concentration of different substances in well water 10,000 years after the closure of the repository. The x-axis indicates years after the closure of the repository.

7.5 Results from drilled wells calculation case

Even though the drilled wells calculation case requires the calculation of the expected value and taking into account the administrational control period, they are not applied in this case. Bismuth reaches the highest concentration with the values of 1170 µg/l in the calculation case for MWH2. The value can be considered acceptable due to the reasons explained in section 7.2.4. Aluminium fluoride reaches the second largest concentration with the values of 566 µg/l and 207 µg/l for MWH2 and DWH1 respectively. Like in the base scenario, the maximum recommended concentration for aluminium is exceeded. The limit of lead in household water (10 µg/l) is exceeded in the calculation case for MWH (16.5 µg/l). For DWH1 the concentration is approximately 10 % of the limit. The rest of the concentrations are too small to be considered as a health hazard.

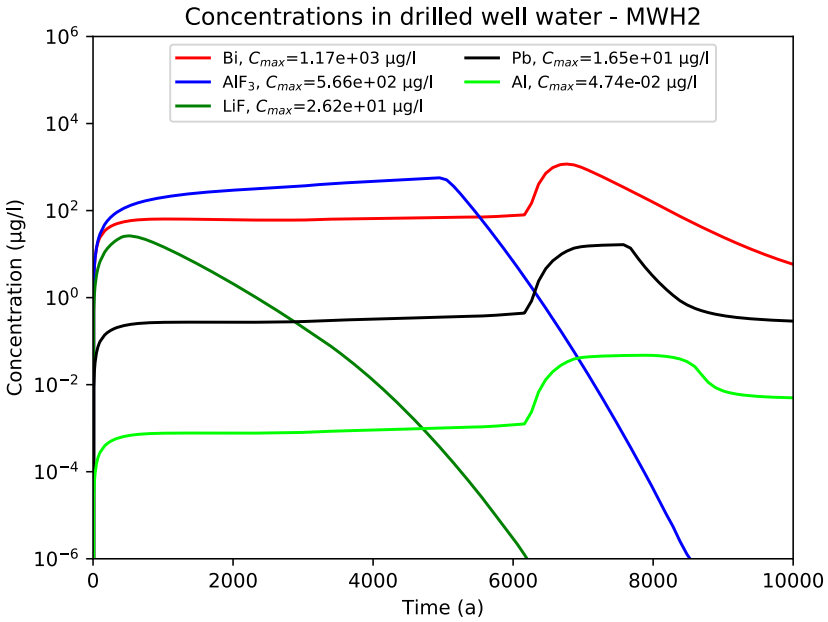

Figure 67. Concentrations of different substances in a drilled wells calculation case 10,000 years after the closure of the repository. The x-axis indicates years after the closure of the repository.

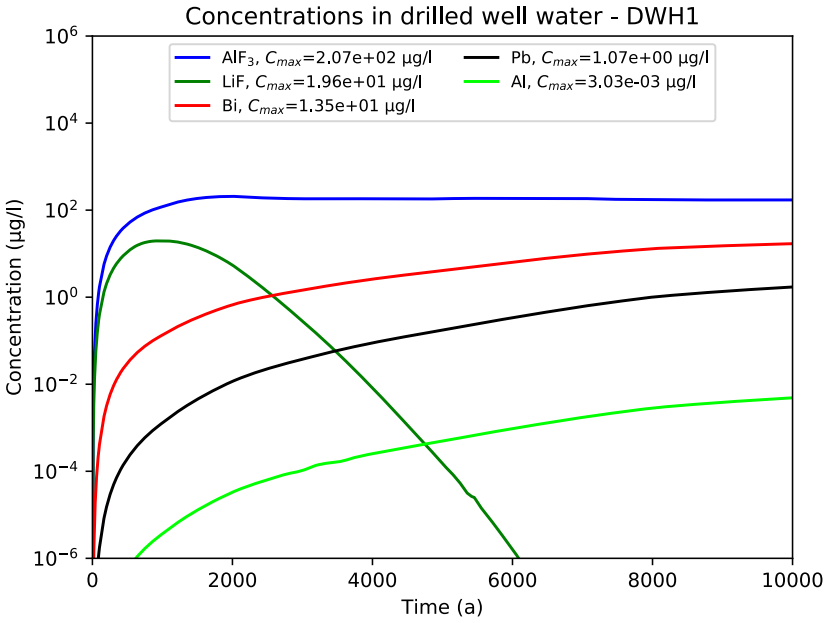

Figure 68. Concentrations of different substances in a drilled wells calculation case 10,000 years after the closure of the repository. The x-axis indicates years after the closure of the repository.

7.6 Results summary

This section summarizes the results of sections 7.4 and 7.5 which are listed in table 31. Considerable concentrations were only observed in water well and drilled well. None of the concentration limits set for soil were exceeded. The most important chemical substance is AlF_3 due to the fact, that it exceeds the recommended maximum concentration of aluminium in household water multiple times. The highest concentration of AlF_3 calculated is 1300 µg/l, which is also close to the limit of F^- in household water (1.5 mg/l). It is not specified in [64] for which molecules of aluminium the recommended concentration is applied.

The concentration limit set for F^- in household water does not perfectly apply to the situation, since the AlF_3 does not behave like pure ion. But due to lack of the known chemical reactions between AlF_3 and the myriad number of different chemical substances present in the repository, such assumption had to be made.

If the AlF_3 molecule is assumed to break down into ions with respect to the molar masses of Al and F, and that the total concentration is the sum of the respective ions, then highest concentration would be a sum of 418 µg/l of Al and 882 µg/l of

F^-. The same principle is used in the value of table 31.

However, it should be noted that assumptions like zero Kd-value and immediate break down of molecules, and the unknown properties of Fluental make the modelling really conservative. However, the recommended maximum concentration of aluminium in household water is based on aesthetical quality of the water, and does not take into account the possible health hazard [73]. More research should be carried out about the chemical toxicity of Fluental.

Table 31. The most considerable concentrations of AlF_3 in the reference case and drilled wells calculation case.

	Limit (µg\l)	Recommended maximum value (µg\l)	Concentration in well water (µg\l)		Concentration in drilled well (µg\l)	
AlF3		200	MWH2	DWH1	MWH2	DWH1
	F^-: 1500	-	418	182	124	67
Pb	10	-	-	-	17	1

The highest concentration of lead is 17 µg/l, which is almost twice the limit in the household water. The concentration of lead in the drilled well case for DWH1 is approximately 1 µg/l, which does not exceed the limit. However, if a probabilistic analysis were performed, the limit might be exceeded. According to [72], all exposure to lead should be avoided, thus it is advisable to clear it from regulatory control.

8 Confidence and Uncertainties

8.1 Activity inventories

The uncertainties of the FiR 1 activity inventory originates from the calculation done with ORIGEN-S and the assumptions made about the waste in the reports provided by VTT. The activity inventory depends on the elemental composition of the reactor structures and the concrete around it. The elemental compositions of the reactor structure materials were assumed to be identical to the construction time specifications. The elemental composition of the concrete structures was determined by taking samples and analysing them. The concrete was assumed to be homogeneous based on the results.

The chlorine content of the graphite was determined from inactive graphite samples with dissolution methods. However, graphite is hard to dissolve, thus different methods were tried. The graphite samples dissolved completely in chlorosulfuric acid ($HClSO_4$), but the trace amounts of chlorine could not be analysed due to the chlorine content of the acid. According to results from preliminary tests, the ratio Cl-36/C-14 = 0.08 [4] is conservative and the results still contain uncertainty. [77]

The activity inventory of OK3 is estimated using a nuclide vector, which was not the final version and is still a work in process. The nuclide vector describes the waste as a whole and it cannot be used to estimate the radionuclide-wise activity of a e.g. single metal sample. The nuclide vector was created with the knowledge of the impurities and the irradiation times of the different steel types handled in the laboratory. The total activity of the samples was estimated by measuring dose rates from the sample storage and assuming, that the dose rate is pure gamma radiation from a point Co-60 source. The total activity of the other waste types of OK3 are conservative approximations, and more accurate values will be calculated as the decommissioning process proceeds.

The radionuclide-wise activities are calculated by multiplying the total activity with the specific radionuclide portion of the nuclide vector. Considering all of these facts, the uncertainty of the activity inventory is quite high and the activities are

overestimated, which is acceptable as it gives a more conservative result. All the C-14 contained in all activated metal is assumed to be organic due to conservatism.

8.2 External processes

Three stylized climate evolutions were formed to cover the uncertainty in the climate evolution, as estimating the changes in the climate over a time period of thousands of years is challenging. Various future human actions may have effect on the repository system, and the most influential actions relate to the drilling of the bedrock for different reasons. The future human actions may depend on the technological and social development of the humanity, which is impossible to predict over long periods of time.

8.3 Surface environment

The terrain and ecosystems modelling is based on the past development of the region since the retreat of the last ice sheet. A model like this has a lot of uncertainties e.g. climate evolution, accumulation and resuspension of sediment, future land use, sea bottom elevation and sediment data. The uncertainty could be reduced with additional research e.g. by studying the accumulation and resuspension of sediment. [14]

8.4 Repository system

The bedrock is considered to be stable over the assessment period of 100,000 years, and the seismic activity at the disposal site is generally low. The main uncertainty relating the bedrock is the stability of the waste caverns after the rock supports are degraded. The degradation of the rock supports could lead to the collapse of the waste cavern.

If the waste cavern were to collapse, it could impact the groundwater flow and the radionuclide transport through bedrock. The effects collapse are most prominent in the waste caverns and tunnels without backfill. The uncertainty could be reduced by analysing the stability of the bedrock and perhaps redesigning the dimensions of those waste caverns that have not yet been excavated.

The groundwater flow in the repository was calculated an equilibrium continuum porous medium approach, which incorporates the small fractures in the bedrock

into homogenized bedrock. The highest uncertainties affecting the groundwater flow relates to the performance of closure plugs limiting the flow rate, the impact of drilled wells and the possible collapse of the waste caverns. Alternate groundwater evolutions were carried out, in order to study the impact of the drilled wells and the reduced performance of closure plugs. [14]

The concrete evolution consists of various degradation processes, of which the leaching of cement hydration products is the most important one. A one-dimensional shrinking core model, which also takes into account the groundwater flow was used to model the concrete evolution. The model was used for concrete plugs, concrete barriers and concrete containers.

The main uncertainties of the model are the formation of penetrating factures through concrete and the impact of quality deviations. The uncertainty considering the concrete plugs is, whether there is a gap between the plug and the wall, which would enhance the hydraulic conductivity. Crushed concrete backfilling around the concrete barriers could improve their durability.

8.5 Radionuclide release

The modelling assumes that radionuclides are released immediately or congruently, and the method depends on the type of the waste. The radionuclides are assumed to be released immediately upon contact with water from contaminated waste materials and other waste types. The properties of some of the waste are unknown from the perspective of the long-term safety e.g. Fluental. The assumption is reasonable, since the activity existing as a contamination is located on the surface of the waste, and is easily removed by the groundwater flow. Also the time scale of this effect is really short compared to the time scale of the safety case.

Radionuclides are assumed to be released congruently from corroding materials such as activate metals and graphite. This assumption however contains multiple uncertainties e.g. the uniform corrosion rate, the geometry of the corroding object and the activity distribution. The corrosion rate is assumed to be constant and dependent on the chemical conditions of the waste caverns. The sources of uncertainty are the corrosion rates and the geometry of the corroding objects e.g. the activated metal components of OK3. The components are of different size and shape, and it is not practical to measure and model every single one of them. With the knowledge of the properties of the metal components i.e. mass, volume etc. can be used to

calculated an area of an thin plate, of which the components could be consist of. The plate must be thin, as this allows to use an assumption, that the corrosion occurs only from above and below the plate, because the area of the upper and lower part of the plate is much larger than the area of the sides. This gives a conservative approximation, as it causes the activity to be released more quickly.

However, this approximation contains its own uncertainties e.g. the area of the plate depends on the properties of the metal components, which are given in VTT's reports. The release of C-14 from the graphite waste was modelled based on the leaching tests. The annual release rate is a percentual fraction of the total activity of the graphite and it does not take into account the geometry of the graphite, which adds to the uncertainty. The activity in the activated components is assumed to be distributed evenly, even though this is not the case as the activity density is higher in the parts closer to the source of the neutron flux.

8.6 Radionuclide transport and dose assessment

In the modelling of the transportation of radionuclides in the near-field it is assumed that the compartments are homogenous. The approximation introduces uncertainty to the model, and its magnitude is hard to estimate without implementing different discretizations and studying their effects on the results. The simplified modelling done in [15] indicates, that a more accurate discretization leads to lower maximum release rates from DWH1. Waste caverns like DWH1 are discretized in more detail than MWH2, as it contains the concrete basin and the activity of the waste is higher.

All concrete barriers in the repository are considered to be homogenous. In reality the concrete degradation and the releases via diffusion proceed at different rates in different waste caverns, concrete packages and concrete barriers. The solubility of radionuclides is also limited by stable nuclides. The existence of the stable nuclides has only been taken into account with calcium. Implementing the stable nuclides to the solubility limits would reduce the releases of certain radionuclide considerably. The solubility of Ca-41 takes into account the amount of stable calcium in concrete waste.

The groundwater flow in the waste caverns is assumed to be homogenous, although it is most likely concentrated in certain parts due to fractures in the bedrocks and engineered barriers. The model used for the transportation of radionuclides through the bedrock was adapted from SKB [57]. The model simplifies certain factors e.g.

the transportation is assumed to take place along a homogeneous fracture and that the matrix diffusion coupled with sorption retards the transport. Finally the SKB's model was used for verification which increases the confidence and discretization of the model. The uncertainty is mainly caused by the properties of the bedrock e.g. the fractures as they are not homogeneous.

The radionuclide transportation in the surface environment contains multiple uncertainties as the surface is evolving constantly. The surface is a subject to unpredictable human activities such as agriculture, and also to the climate change. The amount of radionuclides releasing into the environment contains large uncertainties, and stylized assumptions had to be made in order to create a sufficient model in the modelling.

The dose assessment used in the model is based on the selections made by SKB [78]. Some dose paths are more significant than other, thus some of them are omitted. The highest source of uncertainty has to do with the dietary habits, living conditions and the behaviour of future humans in general, which have been estimated conservatively e.g. all the consumed fish originates from the most contaminated water bodies. The human habits, nutritional needs and metabolism are assumed to be similar to the current, which is allowed by [10]. The radionuclide concentration in the different foodstuff is assumed to be linearly dependent on the radionuclide concentration in soil or water, even though the it depends on the amount of stable nuclides of the same element in the nature [79].

8.7 Chemical toxicity

The largest factors contributing to the uncertainty of chemical toxicity are dissolution, solubility and chemical reactions of the waste materials. The solubility of materials like lead and bismuth in water are known to be poor, and the solubility of Fluental is unknown. The possible chemical reactions, the waste materials may cause are unknown. A conservative assumption was made, that all these materials break down to molecules and ions immediately after closure, and are available for chemical reactions. The possibility of any particular chemical reactions were not considered, but it is known that the complexes formed by AlF_3 are toxic. Solubility or Kd-values for all the materials were not found, due to the insolubility of the materials and the fact that no Kd-values have been determined. The possible water soluble molecules for lead were considered, as it is the most toxic material in the list, and assumption

was made that all the lead consists of lead sulfate ($PbSO_4$). The Kd-values of AlF_3 and LiF are assumed to be zero, and the rest of the materials use the same Kd-values as lead, which means that their actual concentrations would be higher. The uncertainties in the transportation of chemical substances are similar to the ones of the radionuclides, described in section 8.6.

9 Conclusions

The aim of this report was to show that the disposal of VTT's decommissioning wastes into Loviisa LILW repository does not cause a significant increase in the dose rate and normalized release emerging from Loviisa NPP's own waste.

Two of the waste caverns in Loviisa LILW repository are considered to be potential disposal location for VTT's decommissioning waste, which are MWH2 and DWH1. The long-term safety considers the potential radiological effects on humans and environment caused by the waste after the repository has been closed. Disposal of nuclear waste requires an analysis of long-term safety, which demonstrates the safety of the disposal.

The safety case made for Loviisa LILW repository is a report portfolio, which has been used as a reference material in this document. A mathematical model of the repository was created for the 2018 safety case, which was used as a base for calculating dose rates and activity releases into the surface environment caused by VTT's decommissioning wastes.

Both waste caverns with the wastes in them were modelled with Ecolego. The annual dose to a hypothetical most exposed person is not allowed to exceed the value of 100 µSv/a during first 10,000 years after the closure of the repository (dose assessment period). The release of activity into the surface environment is analysed after the dose assessment period. The activity release rates of the long-lived radionuclides are normalized with respect to given radionuclide constraints and summed into a dimensionless value. The sum of normalized release rates is not allowed to exceed the value of 1 during the release constraint period. It is also required that potential scenarios and calculation cases are addressed, which may lead to higher dose or normalized release rates.

The disposal of VTT's decommissioning wastes to DWH1 lead to higher dose rate and normalized release rate in the reference case than in the reference case of MWH2. The values were 0.713 µSv/a and 0.00132 respectively. The results are higher for DWH1 due to the fact, that the concrete basin prevents early release of activity, which means that there is more activity left when the calculation of doses is

initiated. Disposing the wastes to MWH2 causes early release of activity to sea after the closure of the repository.

Slightly higher values resulted from the high release rates and alternate climate RCP2.6 calculation cases, but all the values are less than 2 % of the constraints. The contribution to the dose rate and normalized release rate caused Loviisa NPP's own waste is small, thus the activity inventory of VTT's decommissioning wastes is not a limiting factor for the disposal. Both waste caverns are suitable for the disposal.

However, choosing the right waste cavern is not unambiguous due to number of practical reasons like the schedule of VTT's decommissioning process. The excavation of DWH1 may be postponed even further, which means that the VTT's decommissioning wastes would need a place for interim storage for several years or decades.

The second aim of this report was to address the chemical toxicity of VTT's decommissioning wastes, which was done in a similar way as the modelling of transportation of radionuclides. The two models created for MWH2 and DWH1 were edited to calculate concentrations of chemical substances in decomposition layer, deep overburden and drilled well water. The concentrations were compared to concentration limits set for household water, residual waste and soil. According to results, the most important chemical substances are aluminium fluoride and lead. The highest concentration of AlF_3 calculated in well water was 1300 µg/l, which exceeds the recommended concentration of aluminium set for household water (200 µg/l). The limit is assumed to address all the molecules containing aluminium since it is not specified in the reference [64]. The recommended concentration value for aluminium is based on the aesthetic quality of the water, which does not take into account the possible health hazard. There is evidence thought to suggest that aluminium in drinking water and Alzheimer's disease may have a connection [73].

Disposing Fluental to DWH1 causes lower AlF_3 concentrations, which means that it could be a better choice than MWH2. The highest calculated concentration of lead was calculated in the drilled wells calculation case, which has the value of 16.5 µg/l, and it exceeds the limit set for lead in household water (10 µg/l). The exposure to lead should be kept as low as possible [72], thus it is advised to clear it out of regulatory control.

Even though the dose rates and normalized release rates caused by VTT's decommissioning waste are small and both waste caverns are suitable options, more

research about the waste should be done before their disposal to Loviisa LILW repository can be considered a feasible option. This work did not address the possibility that VTT's decommissioning wastes could jeopardize the long-term safety of Loviisa NPP's own waste.

Gas generation caused by aluminium is one of the detrimental reactions, thus it would be best if the aluminium waste and Fluental are not disposed. Some of the aluminium could be cleared from regulatory control, if all the aluminium containing components are measured individually. Clearing the Fluental from regulatory control is not a feasible option due to the fact, that the clearance value for tritium is 100 Bq/g [24] and it would take over 150 years for the tritium activity to decay to that level. The possibility that Fluental could be sold and reused has been discussed.

Fluental is a good material due to the fact, that it has a good mechanical strength and high resistance to irradiation, which allows it to last under very demanding conditions [80]. Considering the fact that the material has been exposed to neutrons for a long time, its activity is not too high. If the Fluental is disposed, it should be disposed in DWH1 and more research about its chemical toxicity should be done.

References

[1] M. Ek and E. Mayer. *VTT FIR1-Reaktori, Selvitys purkujätteen loppusijoituksesta Loviisan voimalaitoksen loppusijoitustiloihin.* Tech. rep. NUCL-2465, Version 1.0. Espoo, Finland: Fortum Nuclear Services Oy, 2004.

[2] T. Eurajoki and P. Kelokaski. *VTT FiR1 Reactor, Decommissioning Waste, Final Disposal in the Loviisa Low and Intermediate Level Waste Repository.* Tech. rep. Espoo, Finland: Fortum Nuclear Services Oy, 2006.

[3] O. Nummi. *Preliminary safety assesment for the FiR 1 decommissioning waste.* Tech. rep. NUCL-3608, Version 2.0. Espoo, Finland: Fortum Power and Heat Oy, 2017.

[4] P. Kotiluoto and A. Räty. *FiR 1 activity inventories for decommissioning, research report.* Tech. rep. VTT-R-03599-16. Espoo, Finland: VTT Technical Research Centre of Finland Ltd, 2016.

[5] T. Carlsson et al. *Chemical aspects on the final disposal of irradiated graphite and aluminium, a literature survey.* Tech. rep. VTT Technology 156, 2014.

[6] M. Airila et al. *FiR 1 -reaktorin käytöstäpoistosuunnitelma.* Tech. rep. FiR 1-A13, Version 3.0. Espoo, Finland: Teknologian Tutkimuskeskus VTT Oy, 2017.

[7] *Nuclear Energy Act.* Tech. rep. 990/1987.

[8] *Nuclear Energy Decree.* Tech. rep. 161/1988.

[9] STUK. *Regulation on the Safety of Disposal of Nuclear Waste.* Tech. rep. Regulation Y/4/2018. Helsinki, Finland: Radiation and Nuclear Safety Authority, 2018.

[10] STUK. *Disposal of nuclear waste.* Tech. rep. Guide YVL D.5. Helsinki, Finland: Radiation and Nuclear Safety Authority, 2018.

[11] O. Nummi. *Safety case for Loviisa LILW repository 2018 - Main report.* Tech. rep. LO1-T3552-00023, Version 1.0. Espoo, Finland: Fortum Power and Heat Oy, 2018.

[12] M. Kaisanlahti et al. *Decommissioning of the Loviisa NPP*. Tech. rep. TJATE-G12-145. Espoo, Finland: Fortum Power and Heat Oy, 2012.

[13] O. Nummi. *Safety case for Loviisa LILW repository 2018 - Description of the disposal system and design basis*. Tech. rep. LO1-T3552-00020, Version 1.1. Espoo, Finland: Fortum Power and Heat Oy, 2019.

[14] O. Nummi. *Safety case for Loviisa LILW repository 2018 - Performance assessment and formulation of scenarios*. LO1-T3552-00021, Version 1.1. Espoo, Finland, 2019.

[15] F. Jansson, O. Nummi, and J. Mäki. *Safety case for Loviisa LILW repository 2018 - Analysis of releases and doses*. Tech. rep. LO1-T3552-00022, Version 2.0. Espoo, Finland: Fortum Power and Heat Oy, 2018.

[16] J. Väinölä. *Säteilytysrengas ja komponentit*. Tech. rep. VTT Internal memorandum. 2014.

[17] *Specimen ring assembly rotary rack*. Tech. rep. TOS614R130. San Diego 12, California: General Dynamics General Atomics Division, 1959.

[18] A. Räty. *FiR1-tutkimusreaktorin ja OK3-laboratorion aktiivisuusinventaarit loppusijoituksen safety case -laskentaan*. Tech. rep. VTT-R-00739-19. Espoo, Finland: Teknologian Tutkimuskeskus VTT Oy, 2019.

[19] A. Räty. *Otakaari 3 laboratorion nuklidivektori*. Tech. rep. VTT-R-00881-19. Espoo, Finland: Teknologian Tutkimuskeskus VTT Oy, 2019.

[20] V. Kämäräinen. *Pilot plant -hallin kontaminaatio, 8.-10.4.1986, Reaktorilaboratorion muistio, 24.6.1986*. Tech. rep. Valtion Teknillinen Tutkimuskeskus, 1986.

[21] T. Shinonaga et al. "Production and Characterization of Plutonium Dioxide Particles as a Quality Control Material for Safeguards Purposes". In: *Analytical Chemistry* 84 (2012), pp. 2638–2646.

[22] Y. Y. Fialkov. *Primenenie izotopov v khimii i khimicheskoy promyshlennosti*. Kiyev: «Tekhnika», 1975.

[23] *Exemption of radiation use from safety licensing*. Tech. rep. ST 1.5. Helsinki, Finland: Radiation and Nuclear Safety Authority, 2013.

[24] *Predisposal management of low and intermediate level nuclear waste and decommissioning of a nuclear facility*. Tech. rep. Guide YVL D.4. Helsinki, Finland: Radiation and Nuclear Safety Authority, 2014.

[25] E. Ruokola. *FiR 1 Decommissioning plan: Clearance of radioactive materials and structures*. Tech. rep. Espoo, Finland: VTT Technical Research Centre of Finland Ltd, 2016.

[26] Cyclife. *Cyclife Sweden, Nykoeping facility*. 2019. URL: `https://www.cyclife-edf.com/en/cyclife/governance/cyclife-sweden` (visited on 07/20/2019).

[27] *Dismantling and Waste Management Planning of Decommissioning of FiR 1, TRIGA Mk II, Cutting scheme activated concrete around beam tubes*. Tech. rep. Germany: Babcock Noell GmbH, 2016.

[28] M. Kaisanlahti. *FIR 1 -tutkimusreaktorin ja Otakaari 3 -tutkimuslaboratorion käytöstäpoistojätteen pakkaussuunnitelma*. Tech. rep. LO1-T354-00011, Version 1.0. Espoo, Finland: Fortum Power and Heat Oy, 2019.

[29] P. Kupiainen, T. Eurajoki, and O. Nummi. *Safety case for Loviisa LILW repository 2018 - Activity inventory*. Tech. rep. LO1-T3552-00012, Version 1.0. Espoo, Finland: Fortum Power and Heat Oy, 2019.

[30] D. van Vuuren et al. *The representative concentration pathways: an overview*. Tech. rep. Climatic Change vol. 109, 2011.

[31] *Safety analysis for SRF Long-term safety, main report for the safety assessment SR-PSU*. Tech. rep. TR-41-01. Stockholm, Sweden: Svensk Kärnbränslehantering AB (SKB), 2015.

[32] *Climate and climate-related issues for the safety assessment SR-PSU*. Tech. rep. TR-13-05. Stockholm, Sweden: Svensk Kärnbränslehantering AB (SKB), 2014.

[33] M. Gunia, K. Tegel, and G. K. *Safety Case for Loviisa LILW repository 2018 - Terrain and ecosystems modelling*. Tech. rep. LO1-T3552-00014, Version 1.1. Espoo, Finland: Fortum Power and Heat Oy, 2018.

[34] T. Rämä. *Safety case for Loviisa LILW repository 2018 - Groundwater flow modelling*. Tech. rep. LO1-T3552-00018, Version 1.0. Espoo, Finland: Fortum Power and Heat Oy, 2018.

[35] T. Lahtinen and T. Eurajoki. *Olkiluoto VLJ Repository, Effects of gas generation*. Tech. rep. NUCL-3455. Espoo, Finland: Fortum Nuclear Services, 2006.

[36] F. Jansson and T. Rämä. *Safety case for Loviisa LILW repository 2018 - Gas generation and transport*. Tech. rep. LO1-T3552-00019, Version 1.2. Espoo, Finland: Fortum Power and Heat Oy, 2018.

[37] L. Moreno and I. Neretnieks. *Impact of gas generation on radionuclide release, comparison between results for new and old data*. Tech. rep. SKB P-13-40. Stockholm, Sweden: Svensk Kärnbränslehantering AB (SKB), 2013.

[38] A. Hoch et al. *A Survey of Reactive Metal Corrosion Data for Use in the SMOGG Gas Generation Model*. Tech. rep. Serco Assurance Report SA/ENV-0895. 2010.

[39] N. Diomidis. *Scientific basis for the production of gas due to corrosion in a deep geological repository*. Tech. rep. NAB-14-21. Nagra, 2014.

[40] *Data report for the safety assessment SR-PSU*. Tech. rep. TR-14-10. Stockholm, Sweden: Svensk Kärnbränslehantering AB (SKB), 2014.

[41] *Ideal Gas Law*. Hyper Physics. 2017. URL: `http://hyperphysics.phy-astr.gsu.edu/hbase/Kinetic/idegas.html` (visited on 06/23/2019).

[42] R. Lidin, M. V.A, and L. Andreyeva. *Reaktsii neorganicheskikh veshchestv*. Moskva, Rossiya: OOO «Drofa», 2007.

[43] N. Platts, D. J. Blackwood, and C. C. Naish. *Anaerobic oxidation of carbon steel in granitic groundwaters: A review of the relevant literature*. Tech. rep. SKB Technical Report 94-01. Stockholm, Sweden: Svensk Kärnbränslehantering AB (SKB), 1994.

[44] P. Kelokaski and M. Paloneva. *Performance assessment for decommissioning waste of Loviisa nuclear power plant, calculation models, release of activity and doses*. Tech. rep. TJATE-G12-107. Espoo, Finland: Fortum Nuclear Services, 2008.

[45] O. Nummi. *Metal Corrosion and Concrete Degradation in the Loviisa Final Disposal facility*. Tech. rep. TJATE-G12-147. Espoo, Finland: Fortum Power and Heat Oy, 2012.

[46] *Ecolego User Guide*. Tech. rep. AB, Facilia, 2015.

[47] H. Mehrer. *Diffusion in Solids - Fundamentals, Methods, Materials, Diffusion-Controlled Processes*. Springer-Verlag Berlin Heidelberg, 2007.

[48] E. Crespo et al. "Significance of graphite occurrences in the Aracena Metamorphic Belt". In: *Geological Magazine* 141.6 (2004), pp. 687–697.

[49] S. Norris. *WP5 Review of Current Understanding of Inventory and Release of C14 from Irradiated Graphite (D5.5)*. Tech. rep. CAST (Carbon-14 Source Term), 2015.

[50] B. Swift et al. *Carbon-14 Project Phase 2: Irradiated Graphite Wastes*. AMEC/200047/004 Issue 2. Amec, 2016.

[51] V. Vendé. "Comportement des déchets graphite en situation de stockage: Relâchement et répartition des espèces organiques et inogarniques du carbone 14 et du tritium en milieu alcalin". PhD thesis. l'Université Nantes Angers Le Mans, 2012.

[52] C. Bucur, C. Ichim, and I. Florea. "C-14 release from TRIGA irradiated graphite". In: *Radiocarbon* 60.6 (2018), pp. 1819–1829.

[53] *Processing of Irradiated Graphite to Meet Acceptance Criteria for Waste Disposal*. Tech. rep. IAEA-TECDOC-1790. Vienna, Austria: International Atomic Energy Agency (IAEA), 2016.

[54] A. Wareing et al. *Final Publishable CARBOWASTE Report*. Tech. rep. Deliverable D-0.3.12. 2013.

[55] E. Roth, J. Abassin, and F. Botter. "Irradiation of lithium aluminate and tritium extraction". In: *Journal of Nuclear Materials* 133-134 (1985), pp. 238–241.

[56] K. Shiraishi and R. Nagasaki. "Behaviour of Tritium in Aluminium-Lithium Alloys". In: *Nuclear Science and Technology* 2 (1965), pp. 499–505.

[57] *Radionuclide transport and dose calculations for the safety assessment SR-PSU*. Tech. rep. Technical Report TR-14-09. Svensk Kärnbränslehantering AB (SKB), 2015.

[58] *Safety Case for the Disposal of Spent Nuclear Fuel at Olkiluoto - Radionuclide Transport and Dose Assessment for Humans in the Biosphere Assessment*. Tech. rep. Posiva Report 2012-31. Eurajoki, Finland, 2014.

[59] P. Saetre et al. *The Biosphere model for radionuclide transport and dose assessment in SR-PSU*. Tech. rep. R-13-46. Svensk Kärnbränslehantering AB (SKB), 2013.

[60] H. Kosow and R. Gaßer. *Methods of Future and Scenario Analysis - Overview, assessment, and selection criteria*. Studies 39. Bonn, Germanny: Deutsches Institut für Entwicklungspolitik (DIE), 2008.

[61] M. Amer, D. T. U., and A. Jetter. "A review of scenario planning". In: *Futures* 46 (2013).

[62] M. D. McKay, R. J. Beckman, and W. J. Conover. "A Comparison of Three Methods for Selecting Values of Input Variables in the Analysis of Output from a Computer Code". In: *Technometrics* (1979).

[63] O. Nummi. *Uncertainty assessment in the safety case for operating licence application*. Tech. rep. Posiva 2018-02. Eurajoki, Finland: Posiva Oy, 2019.

[64] *Sosiaali- ja terveysministeriön asetus talousveden laatuvaatimuksista ja valvontatutkimuksista annetun sosiaali- ja terveysministeriön asetuksen muuttamisesta*. Tech. rep. 683/2017. Finlex, 2017.

[65] *Valtioneuvoston asetus maaperän pilaantuneisuuden ja puhdistustarpeen arvioinnista*. Tech. rep. 214/2007. Finlex, 2007.

[66] *Valtioneuvoston asetus kaatopaikoista*. Tech. rep. 331/2013. Finlex, 2013.

[67] *Corrosion of research reactor aluminium clad spent fuel in water*. Tech. rep. IAEA TECDOC 1637. Vienna, Austria: International Atomic Energy Agency (IAEA), 2009.

[68] W. Hummel et al. *Nagra / PSI Chemical Thermodynamic Data Base 01/01*. Tech. rep. Nagra Technical Report 02-16. Nagra, 2002.

[69] *Aluminum fluoride - Summary risk assessment report*. Tech. rep. Final report. European Chemicals Agency, 2008.

[70] D. R. Lide. *CRC Handbook of Chemistry and Physics*. Boca Raton, FL: CRC Press, 2005.

[71] *Fluoridi*. Terveyden ja hyvinvoinnin laitos. 2019. URL: `https://thl.fi/fi/web/ymparistoterveys/vesi/talousvesi/kaivovesi/kaivoveden-kemialliset-epapuhtaudet/fluoridi` (visited on 11/12/2019).

[72] *Lead poisoning and health*. World Health Organization (WHO). 2019. URL: https://www.who.int/news-room/fact-sheets/detail/lead-poisoning-and-health (visited on 06/12/2019).

[73] M. Johnson, D. D. Ratnayaka, and M. J. Brandt. *TWORT's Water Supply*. 6th. Elsevier Ltd., 2009.

[74] U. Berner. *Solubility of Radionuclides in a Bentonite Environment for Provisional Safety Analyses for SGT-E2*. Tech. rep. Nagra Technical report 14-06. Wettingen, Switzerland: Nagra, 2014.

[75] *Bismuth Statistics and Information*. National Minerals Information Center. 2019. URL: https://www.usgs.gov/centers/nmic/bismuth-statistics-and-information (visited on 06/12/2019).

[76] M. Keinänen-Toivola, M. Ahonen, and T. Kaunisto. *Talousveden laatu Suomessa vuosina 1984-2006 - Vesi-Instituutin julkaisuja 2*. Tech. rep. Vesi-Instituutti/Prizztech Oy, 2007.

[77] A. Räty et al. "Characterisation measurements of Fluental and graphite in FiR1 TRIGA research reactor decommissioning waste". In: *Nuclear Engineering* 353 (2019).

[78] *Handling of biosphere FEPs and recommendations for model development in SR-PSU*. Tech. rep. R-14-02. Stockholm, Sweden: Svensk Kärnbränslehantering AB (SKB), 2015.

[79] T. Tuovinen et al. "Transfer of Cs-137 from water to fish is not linear in two northern lakes". In: *Hydrobiologia* 700 (2013).

[80] I. Auterinen. *Properties of Fluental*. Tech. rep. Espoo, Finland: VTT Technical Research Centre of Finland Ltd, 2006.

A Results from probabilistic analysis - figures

A.1 Uncertainty analysis

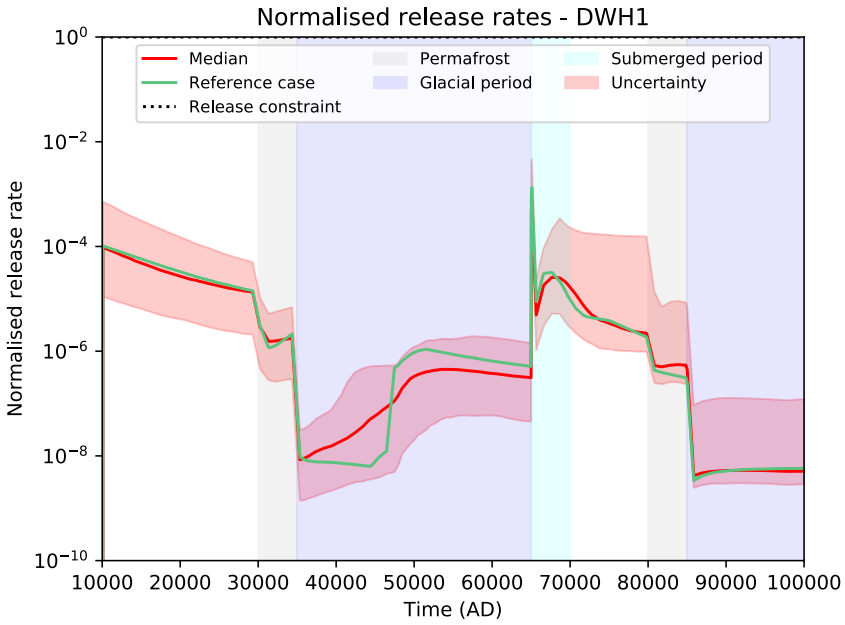

Figure 69. The results for the normalised release rates from the probabilistic analysis for DWH1. The x-axis indicates years after the closure of the repository. The uncertainty reflects 95th and 5th percentiles.

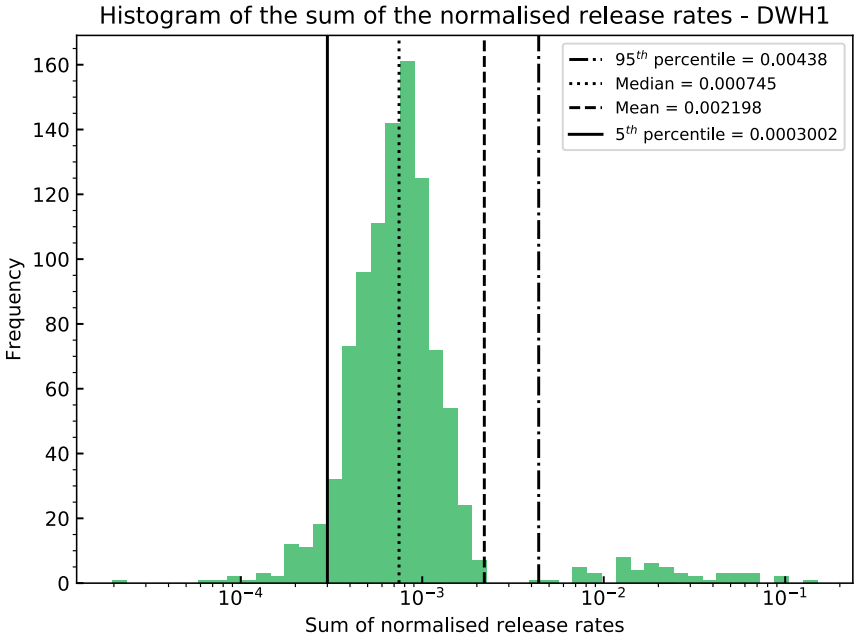

Figure 70. A histogram of the maximum normalised release rates for DWH1.

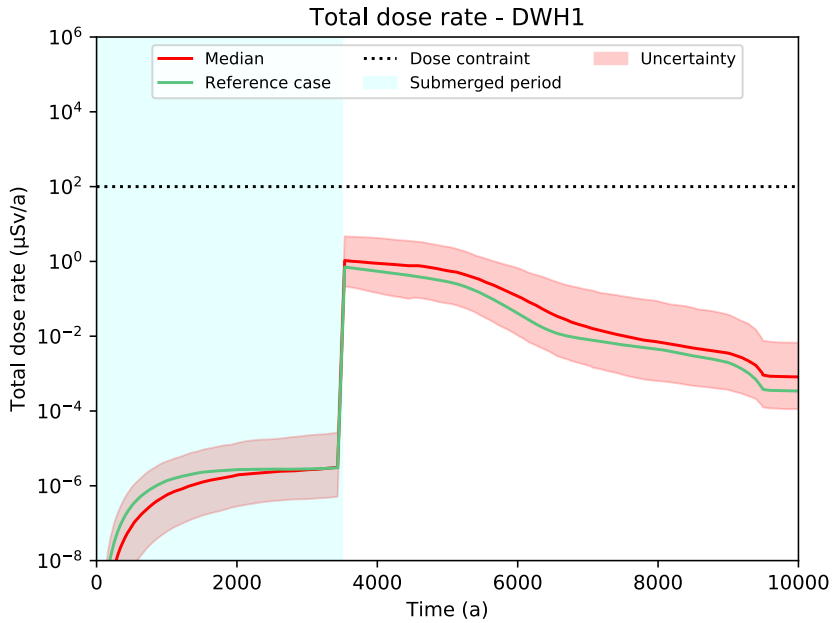

Figure 71. The results for the total dose rates from the probabilistic analysis for DWH1. The x-axis indicates years after the closure of the repository. The uncertainty is estimated with 95th and 5th percentiles.

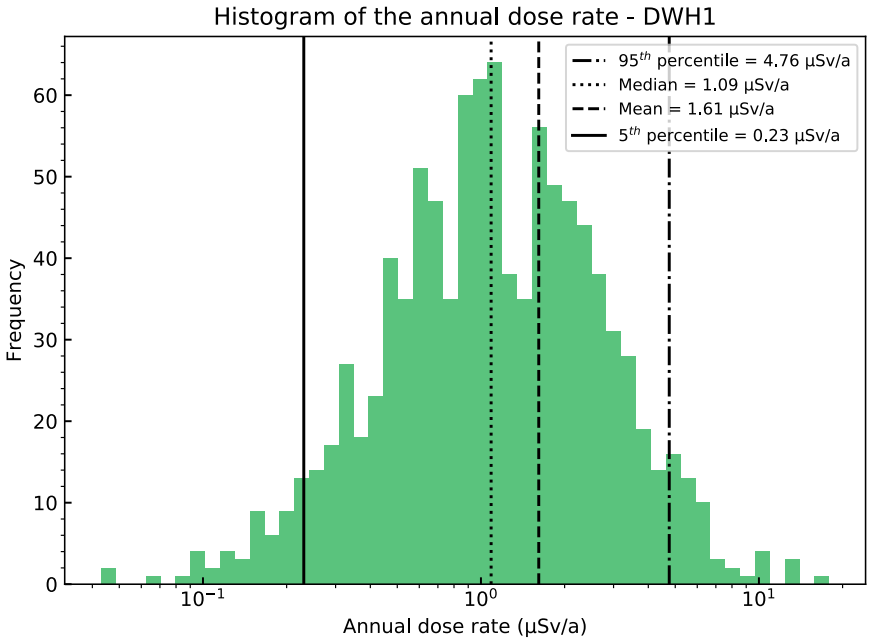

Figure 72. A histogram of the maximum total dose rates for DWH1.

B Results from calculation cases - figures

B.1 Drilled wells

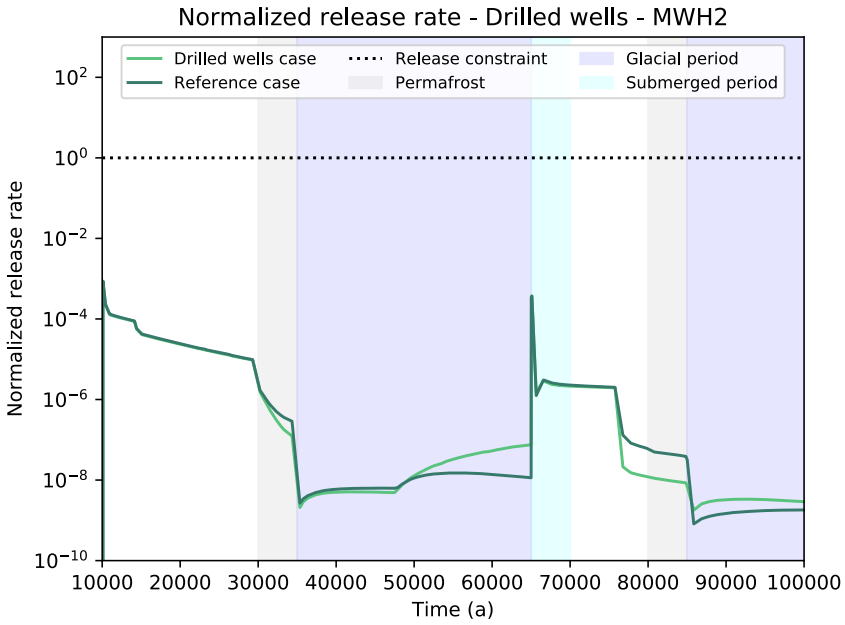

Figure 73. The expected dose rates into the environment in the reference and drilled wells cases during the dose assessment period. The x-axis indicates years after the closure of the repository.

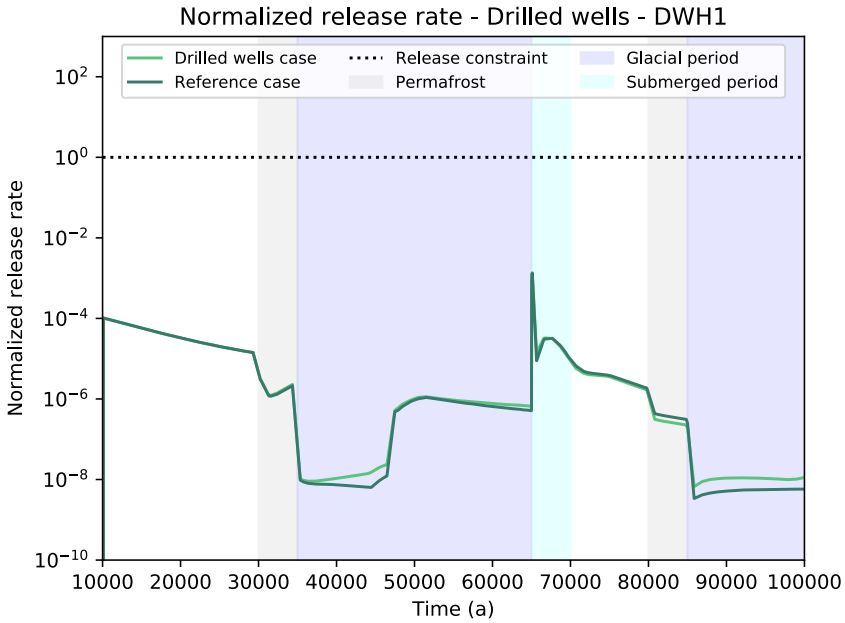

Figure 74. The expected dose rates into the environment in the reference and drilled wells cases during the dose assessment period. The x-axis indicates years after the closure of the repository.

C Results from scenarios - figures

C.1 Accelerated concrete degradation

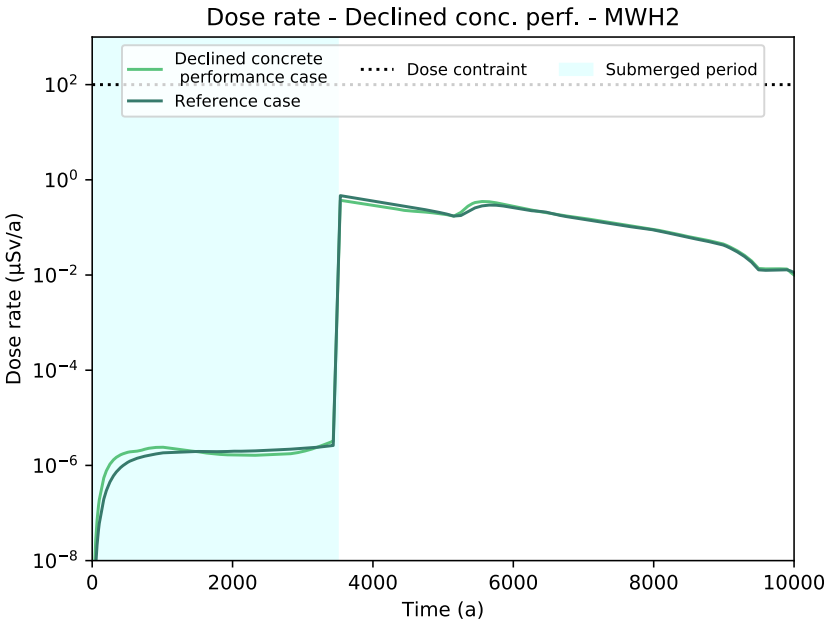

Figure 75. The expected dose rates into the environment in the reference and drilled wells cases during the dose assessment period. The x-axis indicates years after the closure of the repository.

C.2 Large earthquake

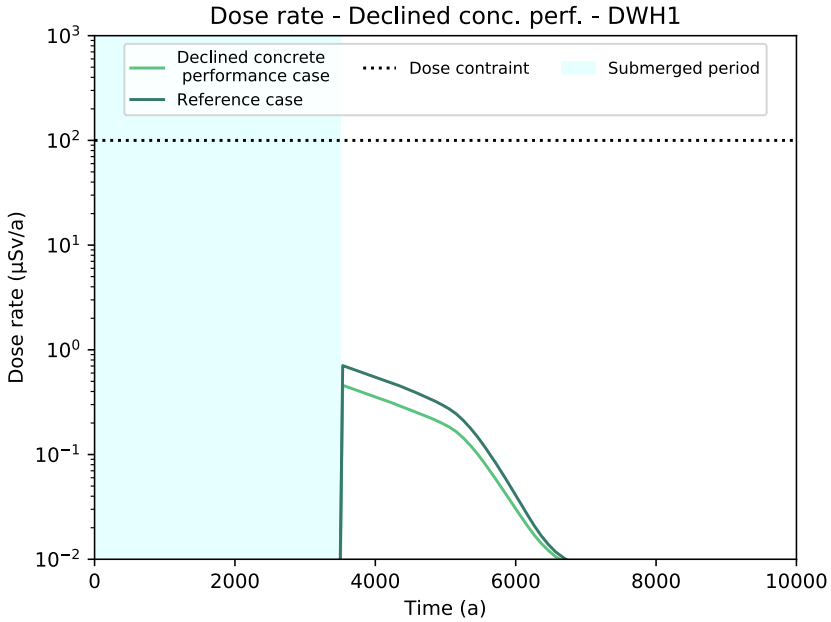

Figure 76. The expected dose rates into the environment in the reference and drilled wells cases during the dose assessment period. The x-axis indicates years after the closure of the repository.

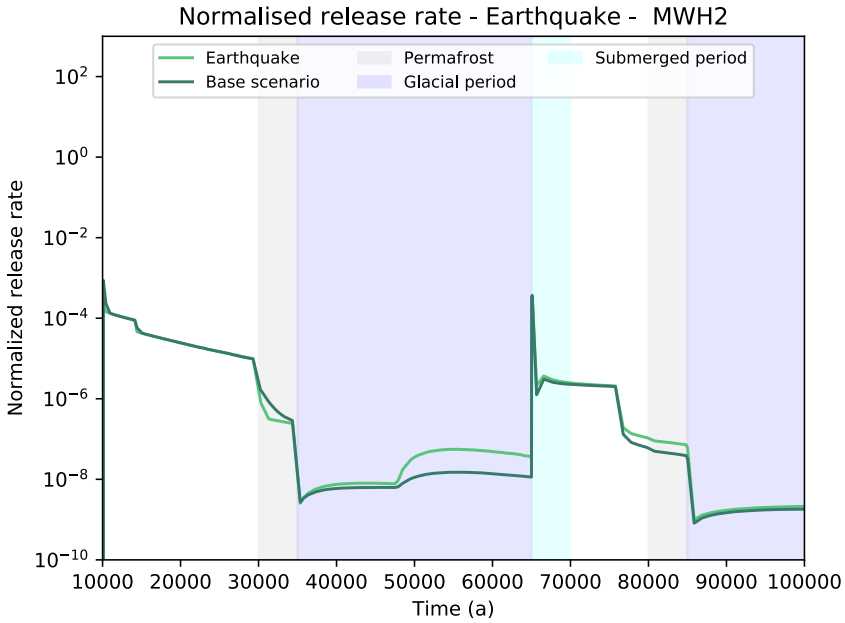

Figure 77. The expected dose rates into the environment in the reference and drilled wells cases during the dose assessment period. The x-axis indicates years after the closure of the repository.

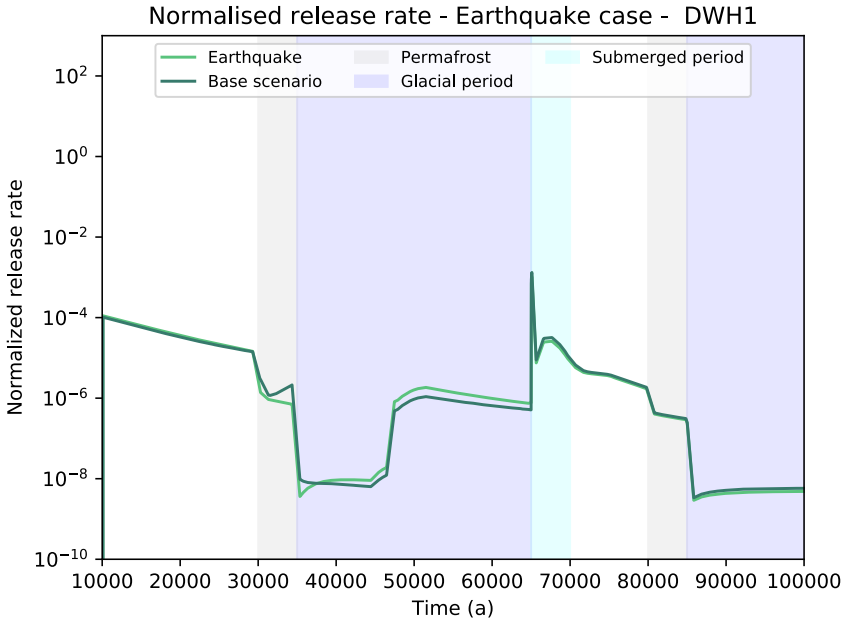

Figure 78. The expected dose rates into the environment in the reference and drilled wells cases during the dose assessment period. The x-axis indicates years after the closure of the repository.

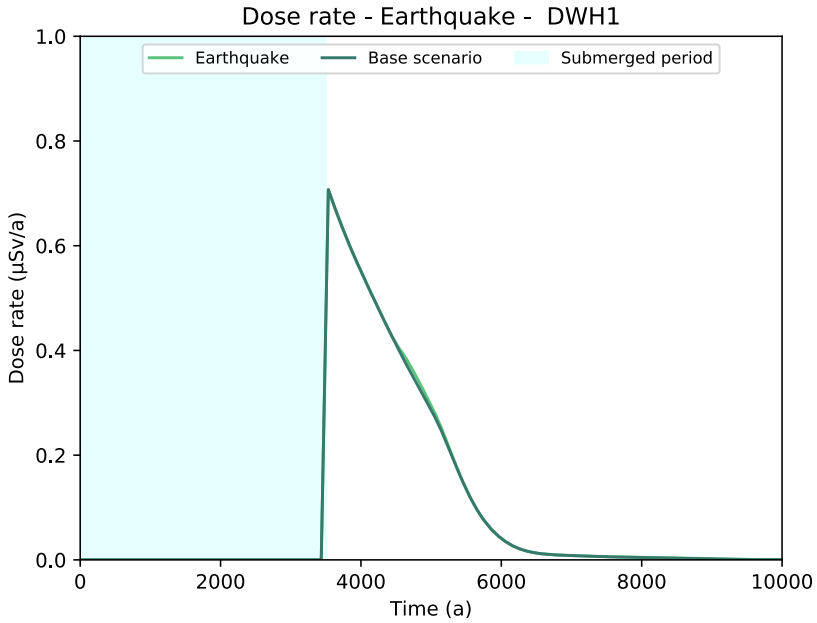

Figure 79. The expected dose rates into the environment in the reference and drilled wells cases during the dose assessment period. The x-axis indicates years after the closure of the repository.